Transient Scattering of Electromagnetic Waves by Circular Cylinders

by

Jinxi Ma

A dissertation
presented to the University of Manitoba
in partial fulfillment of the
requirements for the degree of
Doctor of Philosophy
in
Electrical Engineering

Winnipeg, Manitoba, 1991

ISBN 0-315-77980-2

TRANSIENT SCATTERING OF ELECTROMAGNETIC WAVES BY CIRCULAR CYLINDERS

BY

JINXI MA

A Thesis submitted to the Faculty of Graduate Studies of the University of Manitoba in partial fulfillment of the requirements for the degree of

DOCTOR OF PHILOSOPHY

I hereby declare that I am the sole author of this dissertation.

I authorize the University of Manitoba to lend this dissertation to other institutions or individuals for the purpose of scholarly research.

Jinxi Ma

I further authorize the University of Manitoba to reproduce this dissertation by photocopying or by other means, in total or in part, at the request of other institutions or individuals for the purpose of scholarly research.

The University of Manitoba requires the signatures of all persons using or photocopying this dissertation.

Jinxi Ma

TO MY PARENTS

ABSTRACT

An analytical study of the transient response of a perfectly conducting circular cylinder to cylindrical electromagnetic waves has been carried out. The time dependent expressions of the induced current density on the surface of the cylinder are derived for both the shadow and illuminated regions and for both the early and late times. The analysis is based on the frequency domain eigenfunction solution of the induced current density on the cylinder surface. For the early-time solution, the Watson transformation is employed to transform the eigenfunction solution to an integral. The integral is then evaluated for large values of the Laplace transform variable, in the shadow region by a residue series, and in the illuminated region by the saddle point method. For the late-time solution, the inverse Laplace transform is computed by evaluating the corresponding contour integral. A single expression which is valid for both the shadow and the illuminated regions is derived and the range of validity of the expression is discussed. It covers all the time ranges in the shadow region, the late time range in the illuminated region and part of the early and intermediate time ranges for large angles in the illuminated region. In the analysis of the early-time solution, alternate approaches are also presented and the corresponding results are compared. The current response to an impulsive plane wave is derived as a special case. A similar analysis is applied to obtain the transient current response of a circular cylinder to an electromagnetic pulse of a double exponential type. The transient field response is studied for a perfectly conducting cylinder and an analytical expression is also derived for the transient field response of a dielectric cylinder.

ACKNOWLEDGEMENTS

I am indebted to the members of my advisory committee, which consisted of Professors I. R. Ciric, L. Shafai and P. N. Shivakumar, for their guidance and direction in my post-graduate study program.

In particular, innumerable hours of consultation and discussion with Dr. I. R. Ciric, who supervised the dissertation and suggested the topic, have provided inspiration for this work. His frank and constructive criticism of the research, which proved to be invaluable, is gratefully acknowledged.

I wish to acknowledge my gratitude to Dr. A. Tijhuis of Department of Electrical Engineering, Delft University of Technology, The Netherlands, for providing his specialized computer programs and other related information.

I wish to express my appreciation for the financial support from the University of Manitoba in the form of a University Graduate Fellowship and from the Natural Science and Engineering Research Council of Canada in the form of a research assistantship, without which it would have been impossible to complete this work.

I also wish to thank Dr. F. P. Dawalibi and Safe Engineering Services & Technologies Ltd. for providing necessary facilities during the completion of this thesis.

Finally, I wish to express my deep appreciation to my wife Cheng Huang Tay for her blessings and support during my study.

TABLE OF CONTENTS

LIST OF FIGURES

CHAPTER 1

INTRODUCTION

1.1 Electromagnetic Transients

The subject of time domain electromagnetic scattering has received considerable attention in the last two decades [1]-[4]. This is mainly due to the very useful and interesting properties of the time domain scattering solution, one of which being that the time domain signature of a scatterer is very closely related to its physical shape parameters [5].

Different techniques have been developed for solving transient scattering problems, which include: a) numerical inverse Fourier transform of frequency domain solutions; b) space-time integral-equation technique; c) Singularity Expansion Method; d) finite difference time domain solutions; and e) closed form transient solutions for special geometries.

Even though most of the scattering problems have to be solved using numerical methods, there are some special types of geometries which admit exact analytical solutions. For example, the scattering of a plane wave by a perfectly conducting sphere [6], by a perfectly conducting cylinder [7], and by a perfectly conducting wedge [1,ch.1] have all been treated analytically and explicit solutions have been obtained. Study of these special geometries is of great theoretical importance.

Out of all the two-dimensional structures, the circular cylinder has the simplest

shape and, has been studied most intensively in both the frequency and time domains. It has, in particular, been extremely valuable as a basic model for the development of different techniques applicable to more general shapes. The study of this simple model enables us to gain more physical insight into the transient scattering process and the results for this benchmark can be used as a test case for numerical methods applicable to a variety of complex geometries.

1.2 Literature Review

Transient response of a perfectly conducting circular cylinder to both the TE (transverse electric) and TM (transverse magnetic) polarized plane electromagnetic waves has been already exhaustively studied by analytical and numerical methods. For the case of TE polarization, the incident magnetic field is parallel to the axis of the cylinder, while for TM polarization the incident electric field is parallel to the axis of the cylinder.

In 1959, Wait and Conda [8] considered the transient scattering of plane electromagnetic waves by a perfectly conducting circular cylinder. In their paper the exact eigenfunction infinite series for the time-harmonic current density has been replaced by an approximate integral expression which is valid for large values of the Laplace transform variable s. The exponential part in the integrand has then been represented by its power series expansion to facilitate the inverse Laplace transform. By employing the Laplace transform pair

$$\frac{1}{s^{\lambda}} <-> \frac{t^{\lambda-1}}{\Gamma(\lambda)} u(t) \tag{1.1}$$

for values of λ such that $\mathrm{Re}(\lambda) \leq 0$, where $\Gamma(\lambda)$ and $u(t)$ are the gamma function and the unit-step function, respectively, the time dependent solution has finally been obtained. Numerical results have been calculated by retaining the first ten terms in the series solution. The authors of [8] claim that when the time parameter is larger than 1 the maximum error is about 1% and that when it is smaller than 1 the results are probably not valid. There are some doubts about their results. Firstly, since an approximation has been made under the condition that the Laplace transform variable s is large, which corresponds to the time domain solution for the small values of time variable, it is unreasonable to obtain results that are more accurate for large values of the time variable than for small ones. Secondly, since the series expansion of the exponential part in the integrand is slowly convergent for large and moderate values of s, only the first ten terms cannot give a very good accuracy. Thirdly, the Laplace transform pair utilized in the paper is not an appropriate one. In the theory of Laplace transform developed for classical functions, the Laplace transform pair (1.1) is valid only for $\mathrm{Re}(\lambda) \geq 0$. When the theory is extended to distributions, it is also valid for $\mathrm{Re}(\lambda) < 0$ provided that λ is not an integer and that $t^{\lambda-1} u(t)$ is replaced by the pseudofunction $Pf[t^{\lambda-1} u(t)]$ [9]. When λ is a negative integer, however, it is not valid and the correct formula is [9]

$$s^m <-> \delta^{(m)}(t) \quad m = 1, 2, 3, \cdots \tag{1.2}$$

where $\delta^{(m)}(t)$ is the m-th derivative of the Dirac delta function $\delta(t)$. The complex frequency domain solution given in [8] is of the form

$$F(s) = e^{-As} \sum_{n=0}^{\infty} B_n s^{n/3} \tag{1.3}$$

where there are indeed terms containing s^m with m being a positive integer, which makes

the use of (1.1) with λ a negative integer obviously incorrect. Hence, although the approximation of Wait and Conda is compact and convenient, inherently it is not an accurate representation for either large or small values of the time parameter. In a later paper [10] Wait reexamined this problem and restricted his results to the early-time solution in the penumbral region.

The field response of a perfectly conducting circular cylinder to a unit-step plane electromagnetic wave was considered by Chen [11] in 1964. His solution is restricted to the time range when the incident wavefront has completely passed the cylinder. Starting with the eigenfunction representation of the electric field in the frequency domain, he made approximations suitable for small values of s/a so that upon inversion he obtained a large-time asymptotic approximation. Unfortunately, there are some mathematical errors in his work which affect some of his formulas. For instance, in the case of TM polarization the time domain expression he obtained is complex which is not physically realizable since the fields which result from a real transient excitation must themselves be real. Chen did not present any numerical data in his paper.

In 1965, Barakat [12] investigated the current density induced on a circular cylinder by a TE incident plane wave with unit-step time dependence. Essentially, he began with the convergent infinite eigenfunction series for the time-harmonic current density induced on the cylinder surface. Next, the transient current density was expressed as the inverse Laplace transform in the form of a contour integral. Barakat did not complete the evaluation of the integral nor did he give numerical results for the induced current density. Instead he integrated the current density multiplied by $\cos\phi$ from 0 to 2π and claimed that this is "a more interesting quantity". But due to the orthogonality property,

$$\int_0^{2\pi} \cos\phi \cos n\phi \, d\phi = \begin{cases} 1 & n=1 \\ 0 & n\neq 1 \end{cases} \tag{1.4}$$

the above step is equivalent to dropping all the terms in the original infinite series eigenfunction expansion except the one which has a $\cos\phi$ dependence. The quantity obtained here does not appear to be useful for calculating the scattered fields since it is not dependent upon the specific shape of the scatterer.

The problem of an infinitely long, acoustically soft, circular cylinder illuminated by an impulsive plane wavefront was considered by Uberall *et al.* [13] in 1965. This problem corresponds to the electromagnetic impulse problem and the results these authors have obtained represent the early-time solution. Their analysis began with the steady state eigenfunction solution which was converted from its infinite series form into an integral form by means of the Watson transformation. In the shadow region the original integral was approximated by a residue series. In the illuminated region the integral was decomposed into a sum of two integrals individually corresponding to the contributions associated with the reflected wave and the creeping waves. The integral corresponding to the reflected wave contribution was evaluated by the saddle point method.

In 1967, Schafer [14] made a great effort to complete the analysis of the transient scattering of plane electromagnetic waves by a conducting circular cylinder and eight years later he published his results [7]. In [14], he studied the transient current density induced on a perfectly conducting circular cylinder illuminated by an impulsive and a unit-step plane electromagnetic wave, and obtained analytical expressions for both the illuminated and shadow regions and for all the time ranges. For the early-time solution in the illuminated region, he used the frequency domain Luneberg-Kline expansion solution, which gave a simple expression. He also used the method of steepest descent to

evaluate the integral which had been obtained from the frequency domain eigenfunction solution by means of the Watson transformation. But the final results obtained are too complicated to be put into a single expression. For the early-time solution in the shadow region, he evaluated the corresponding integral by a residue series, and for the late-time solution, the inverse Laplace transform of the eigenfunction solution was represented by a contour integral. By employing approximate expressions of Hankel functions for s small, he finally obtained the analytical expressions of the time domain induced current density. He then derived the expressions for the intermediate time by means of a functional interpolation scheme between the early- and late-time solutions.

In 1970, Bennet and Weeks [15] calculated the transient response of conducting cylinders by means of a numerical solution of the time domain integral equation. In 1973, Lee *et al.* [16] derived an asymptotic series which is suitable for the evaluation of the early-time response in transient problems and presented some results for the early-time currents induced on a cylinder illuminated by a TM polarized plane wave with a unit-step time dependence.

In 1985, Chung *et al.* [17] calculated the late-time field response of a conducting circular cylinder to an impulsive plane wave by the Singularity Expansion Method. What they actually did was evaluating the inverse Laplace transform by a contour integral to obtain the forward-scattered far field. In principle, the results can be obtained by integrating the induced current density on the cylinder surface, which has been derived in [7].

The field response of a lossy dielectric circular cylinder illuminated by a plane electromagnetic wave has also been analyzed using the Singularity Expansion Method by Tijhuis and Weiden 1986 [18,19].

Less work has been done in the transient scattering of cylindrical waves. Even though plane wave incidence is of practical interest, it is a special case of the more general case of cylindrical wave incidence. In 1954, Frieldlander [20] studied the diffraction of acoustic pulses by a circular cylinder, which corresponds to the problem of the early-time field response of a conducting cylinder to TE polarized cylindrical electromagnetic waves. By extending the range of the angular coordinate from $(0, 2\pi)$ to $(-\infty, +\infty)$, he applied the Laplace transform with respect to time and the Fourier transform with respect to the angular coordinate to the wave equation. After obtaining the solution of the transformed wave equation, he evaluated the inverse Fourier transform for large values of the Laplace transform variable. The time dependent expression was then derived which corresponds to the early-time solution. In 1959, Gilbert and Knopoff [21] considered the scattering of cylindrical elastic waves by a rigid cylinder using the same method as in [20] and obtained the early-time solution. Their problem, however, does not correspond to the problem of scattering of either TE polarized or TM polarized electromagnetic waves, due to the difference in the boundary conditions.

In 1983, Heyman and Felsen [22] studied the relationships between creeping waves and resonances for a perfectly conducting circular cylinder with a parallel magnetic line source located on the cylinder surface. Since the field points are also chosen on the surface of the cylinder, the results are only applicable to the shadow region. In 1986, they extended their study to acoustic scattering [23]. Both the source and field points are off the cylinder in the analysis and a hybrid formula which consists of geometrical optics solution, creeping waves and resonances has been developed.

1.3 Objectives of the Study

As seen from above, although the transient response of a circular cylinder to plane waves has been thoroughly studied, the problem of transient response to cylindrical waves has received relatively less attention. To the best of the author's knowledge, the complete analytical expressions of the transient response of a circular cylinder to both the TE and TM polarized cylindrical waves have not been available in the literature. One objective of the present study is to determine the current response of a conducting cylinder to cylindrical electromagnetic waves generated from a line current. Different analytical approaches will be presented and discussed in the analysis.

It is also noticed that the transient response usually has two parts: the early-time solution and the late-time solution. In the analysis of the early-time response, the local time which is counted from the arrival of the wavefront at the point under consideration, is generally used, while in the analysis of the late-time response, the global time is used, which is usually counted from the time when the initial wavefront reaches the scatterer. Generally, the early-time solutions are valid for small local times, with the late-time solutions being valid only after the incident wavefront has completely passed the scatterer. It can be seen that the early-time and the late-time solutions are not complementary in the sense that in the deep shadow zone they can have an overlap while in other regions there is a gap between the time ranges in which they are valid. One way to eliminate this gap is to develop a solution for the intermediate time ranges by elaborate interpolation of the early- and late-time solutions, as demonstrated in [14]. An ultimate solution to this problem would be to extend the range of validity of the early-time and/or the late-time solutions. This is another objective of this study. The application of various new analytical

approaches will also be demonstrated by analyzing the field responses of conducting and dielectric cylinders excited by a line current and the current response of a conducting cylinder to an electromagnetic pulse.

1.4 General Methods and Techniques

The primary purpose of this investigation is to study the transient surface current density induced on an infinitely long, perfectly conducting circular cylinder, illuminated by a cylindrical electromagnetic wave, generated from a parallel filament carrying a current with unit-step time dependence. The geometry of the problem is shown in Fig. 1.1, where a is the radius of the cylinder, r_0 the distance from the line current to the cylinder axis and ϕ the angular coordinate of the polar coordinate system (r, ϕ). Outside the cylinder and the line source, the medium is the unbounded free space.

The line current is represented by

$$J_l = \frac{1}{r}\delta(r - r_0)\,\delta(\phi)\,u(t) \tag{1.5}$$

where $\delta(z)$ is the Dirac delta function of argument z defined by

$$\delta(z) = 0 \quad \text{for } z \neq 0 \tag{1.6}$$

and

$$\int_{-\infty}^{+\infty} \delta(z)dz = 1 \tag{1.7}$$

and $u(t)$ the unit-step function defined by

$$u(t) = \begin{cases} 0 & t \leq 0 \\ 1 & t > 0 \end{cases}. \tag{1.8}$$

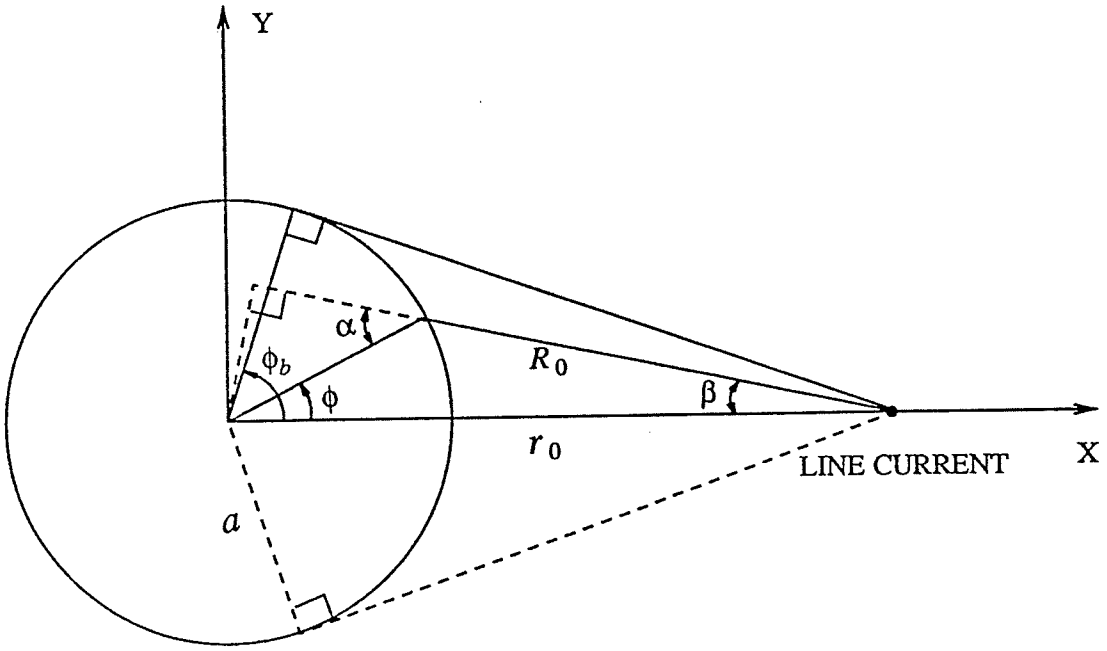

Fig. 1.1. Cross section of the conducting cylinder to line current configuration.

The basic problem considered is to determine the current density induced everywhere on the cylinder surface as a function of the position and time. We start from the frequency domain eigenfunction solution of the fields and the induced current density. Since it is impossible to obtain a single expression of the transient response which is numerically useful for all the time ranges, we have to consider the early-time solution and the late-time solution separately.

The early-time solution of the induced current density in the shadow region is obtained in Chapter 2 by using a Watson transformation approach and also a double Laplace transform approach. The Watson transformation approach consists in replacing

the frequency domain eigenfunction series solution of the induced current into a Cauchy integral and then expressing this integral by a residue series which converges rapidly for large values of the Laplace transform variable s, and therefore yielding the early-time results. The second approach consists in applying a double Laplace transform to the wave equation for the vector potential with respect to time and to angle variable. The transformed current density induced on the surface of the cylinder is derived from the solution of the ordinary differential equation satisfied by the transformed vector potential. To obtain the time domain surface current density we perform the inversion of the angle transform for large values of the time transform variable by using the theorem of residues. A second inverse Laplace transform yields the time dependent early-time solution. The current response to an impulsive plane wave is derived as a special case.

In Chapter 3, the early-time solution of the induced current density in the illuminated region is obtained by using a Watson transformation approach and a Luneberg-Kline expansion approach. In the latter, we assume the frequency domain solution of the scattered electric field to be in the form of an asymptotic series expansion ($s \to \infty$). By satisfying the wave equation and the boundary conditions, the unknown functions in the assumed asymptotic series can be determined. The asymptotic form of the frequency domain induced current density can then be derived from the field quantities and the time domain solution can be readily obtained. Again, the current response to an impulsive plane wave is derived as a special case.

The late-time solution for the induced current density is given In Chapter 4. The frequency domain eigenfunction series solution for the induced current density is slowly convergent for large values of s and rapidly convergent for small values of s. This

implies that we can directly apply the inverse Laplace transform to the eigenfunction series solution to obtain the corresponding time domain expression which is valid for large values of the time variable. To evaluate the resultant inverse Laplace transform integral, we choose appropriate contours, evaluate the branch cut integrals and residue contributions, and finally obtain the late-time solution of the induced current density. A different solution is also obtained by considering separately the incident and scattered magnetic fields on the cylinder surface. The relation between the two solutions and their ranges of validity are discussed.

The methodology used in Chapter 4 is applied in Chapter 5 to obtain the transient current response of a conducting circular cylinder to a plane electromagnetic pulse of a double exponential type. The field response of a conducting cylinder is obtained in Chapter 6 by using the double Laplace transform approach. Analytical expressions of the field response of a dielectric cylinder are derived in Chapter 7 without presenting numerical results.

Chapter 8 concludes the dissertation with suggestions for future research.

CHAPTER 2

EARLY-TIME CURRENTS INDUCED BY A CYLINDRICAL WAVE IN THE SHADOW REGION

2.1 The Watson Transformation Solution

For the geometry of the problem shown in Fig. 1.1, the Laplace transform of the induced current density on the cylinder surface can be derived as (Appendix A)

$$J_z(\phi, s) = -\frac{1}{2\pi as} \sum_{n=-\infty}^{\infty} \frac{H_n^{(1)}(\frac{jsr_0}{c})}{H_n^{(1)}(\frac{jsa}{c})} e^{jn\phi} \tag{2.1}$$

where $j \equiv \sqrt{-1}$, c is the speed of light, s the Laplace transform variable, and $H_n^{(1)}$ the Hankel function of the first kind and order n. The exact series solution given by (2.1), is not useful for the early-time response analysis since it requires more and more terms for a given accuracy as $|s|$ becomes larger and larger. To overcome this difficulty, we apply the Watson transformation [24] to express the above infinite series in terms of a Cauchy integral,

$$\sum_{n=-\infty}^{+\infty} f(n) = \frac{j}{2} \int_C \frac{f(\nu)}{\sin\pi\nu} e^{-j\pi\nu} d\nu \tag{2.2}$$

where the closed path C consists of two infinitely long straight lines, the first one just below the real axis and the second one just above it. Applying (2.2) to (2.1) and

transforming the integral along the first line into an integral along the second line by the substitution $\nu \to -\nu$, with $H_{-\nu}^{(1)}(z) = e^{j\nu\pi} H_{\nu}^{(1)}(z)$, yields finally the integral expression

$$J_z(\phi, s) = -\frac{j}{2\pi as} \int_{j\varepsilon-\infty}^{j\varepsilon+\infty} \frac{H_{\nu}^{(1)}(\frac{jsr_0}{c})}{H_{\nu}^{(1)}(\frac{jsa}{c})} \frac{\cos\nu(\phi-\pi)}{\sin\nu\pi} d\nu \tag{2.3}$$

with the integration performed from $-\infty$ to $+\infty$ just above the real ν-axis.

For the shadow region, the integral in (2.3) can be evaluated as an infinite residue series by considering the zeros of $H_{\nu}^{(1)}(\frac{jsa}{c})$ regarded as a function of ν, in the form

$$J_z(\phi, s) = \frac{1}{as} \sum_{n=1}^{\infty} \frac{H_{\nu_n}^{(1)}(\frac{jsr_0}{c})}{\dot{H}_{\nu_n}^{(1)}(\frac{jsa}{c})} \frac{\cos\nu_n(\phi-\pi)}{\sin\nu_n\pi} \quad . \tag{2.4}$$

With

$$\cos\nu_n(\phi-\pi) = \frac{e^{-j\nu_n\pi}(e^{j\nu_n\phi} + e^{j\nu_n(2\pi-\phi)})}{2} \tag{2.5}$$

and

$$\frac{1}{\sin\nu_n\pi} = -2je^{j\nu_n\pi} \sum_{q=0}^{\infty} e^{j2q\pi\nu_n} \tag{2.6}$$

(2.4) can be written in the form

$$J_z(\phi, s) = -\frac{j}{as} \sum_{i=1}^{2} \sum_{n=1}^{\infty} \sum_{q=0}^{\infty} \frac{H_{\nu_n}^{(1)}(\frac{jsr_0}{c})}{\dot{H}_{\nu_n}^{(1)}(\frac{jsa}{c})} e^{j\nu_n(2q\pi+\phi_i)} \tag{2.7}$$

where $\dot{H}_{\nu_n}^{(1)}$ represents the derivative of $H_{\nu}^{(1)}$ with respect to the order ν for $\nu=\nu_n$, ν_n

being the n-th zero of $H_{\nu}^{(1)}(\frac{jsa}{c})$, and

$$\phi_i = \begin{cases} \phi & \text{for } i=1 \\ 2\pi - \phi & \text{for } i=2 \end{cases} . \tag{2.8}$$

The summation indices in (2.7) have the following interpretation: the two values of i correspond to the two directions of circumferential wave propagation, n is the mode number, and q the number of creeping wave encirclements for a given n and i. For the early-time solution only $q=0$ is needed, since the contributions due to $q=1, 2, 3, \cdots$ in (2.7) are delayed by a time interval of $2q\pi a/c$, which is greater than the time range corresponding to the early-time solution. For large values of $|s|$, the expressions of ν_n and $\dot{H}_{\nu_n}^{(1)}(\frac{jsa}{c})$, when the order and the argument are nearly equal, are (Appendix B)

$$\nu_n = j\left[\frac{sa}{c} + \alpha_n \left(\frac{sa}{2c}\right)^{1/3} + \frac{\alpha_n^2}{60}\left(\frac{sa}{2c}\right)^{-1/3} + \frac{1}{140}\left(1-\frac{\alpha_n^3}{10}\right)\left(\frac{sa}{2c}\right)^{-1} + \cdots\right] \tag{2.9}$$

$$\dot{H}_{\nu_n}^{(1)}\left(\frac{jsa}{c}\right) = 2Ai'(-\alpha_n)\left(\frac{sa}{2c}\right)^{-2/3}\left[1-\frac{\alpha_n}{10}\left(\frac{sa}{2c}\right)^{-2/3} + \frac{37}{2520}\alpha_n^2\left(\frac{sa}{2c}\right)^{-4/3} + \cdots\right] \tag{2.10}$$

where Ai is the Airy function, Ai' its derivative with respect to the argument, and α_n the n-th zero of $Ai(-\alpha)$. The values of α_n and $Ai'(-\alpha_n)$ for $n=1$ through 9 [26] are listed in Table I.

Table I

Values of α_n and $Ai'(-\alpha_n)$

n	α	$Ai'(-\alpha_n)$
1	2.33810741	+0.70121082
2	4.08794944	−0.80311137
3	5.52055983	+0.86520403
4	6.78670809	−0.91085074
5	7.94413359	+0.94733571
6	9.02265085	−0.97792281
7	10.04017434	+1.00437012
8	11.00852430	−1.02773869
9	11.93601556	+1.04872065

Equation (2.7) can now be written as

$$J_z(\phi, s) = -\frac{j}{2as}\left(\frac{sa}{2c}\right)^{2/3} \sum_{i=1}^{2} \sum_{n=1}^{\infty} D_n H_{\nu_n}^{(1)}\left(\frac{jsr_0}{c}\right) e^{j\nu_n \phi_i} \tag{2.11}$$

where

$$D_n = \frac{1}{Ai'(-\alpha_n)}\left[1 + \frac{\alpha_n}{10}\left(\frac{sa}{2c}\right)^{-2/3} - \frac{59\alpha_n^2}{12600}\left(\frac{sa}{2c}\right)^{-4/3} + \cdots\right] . \tag{2.12}$$

The Hankel functions in (2.11) are replaced by their asymptotic expansions when both the argument and the order are complex and large in magnitude [27],

$$H_\nu^{(1)}(z)=\frac{e^{\nu(\tanh\gamma-\gamma)-j\frac{\pi}{4}}}{(-\frac{1}{2}j\pi\nu\tanh\gamma)^{1/2}}\sum_{m=0}^{\infty}\frac{\Gamma(m+\frac{1}{2})}{\Gamma(\frac{1}{2})}\frac{A_m}{(\frac{1}{2}\nu\tanh\gamma)^m} \tag{2.13}$$

where

$$\begin{aligned} A_0&=1\\ A_1&=\frac{1}{8}-\frac{5}{24}\coth^2\gamma \\ A_2&=\frac{3}{128}-\frac{77}{576}\coth^2\gamma+\frac{385}{3456}\coth^4\gamma \\ &\cdots\cdots \end{aligned} \tag{2.14}$$

and

$$\cosh\gamma\equiv\frac{\nu}{z}\ . \tag{2.15}$$

By evaluating the hyperbolic functions for large $|s|$ and retaining only $m=0, 1, 2$ in (2.13), the Laplace transform of the surface current density can finally be written in the form (Appendix C)

$$J_z(\phi,s)=-\frac{1}{2}\frac{\sqrt{\cot\phi_b}}{\sqrt{2\pi acs}}\sum_{i=1}^{2}\sum_{n=1}^{\infty}\sum_{h=1}^{5}\frac{b_{inh}}{Ai'(-\alpha_n)}(\frac{sa}{2c})^{-h/3}\,e^{-t_{0i}s-\beta_{in}(\frac{sa}{2c})^{1/3}} \tag{2.16}$$

where ϕ_b is the angular coordinate corresponding to the shadow boundary, as shown in Fig. 1.1,

$$t_{0i}=\sqrt{r_0^2-a^2}/c+a(\phi_i-\phi_b)/c\ ,\ \ \beta_{in}=\alpha_n(\phi_i-\phi_b) \tag{2.17}$$

and

$$b_{in1}=1$$

$$b_{in2}=A_{in}$$

$$b_{in3}=\frac{1}{2}A_{in}^2+B_n \tag{2.18}$$

$$b_{in4}=\frac{1}{6}A_{in}^3+A_{in}B_n-C+D_{in}$$

$$b_{in5}=\frac{1}{24}A_{in}^4+\frac{1}{2}A_{in}^2B_n-\frac{1}{16}A_{in}C+A_{in}D_{in}+E_n$$

in which

$$A_{in}=\frac{1}{4}\alpha_n^2[\frac{1}{15}(\phi_b-\phi_i)-\cot\phi_b]$$

$$B_n=\frac{1}{10}\alpha_n(1+\frac{5}{2}\cot^2\phi_b)$$

$$C=\frac{1}{16}\cot\phi_b(1+\frac{5}{3}\cot^2\phi_b) \tag{2.19}$$

$$D_{in}=\frac{1}{140}(1-\frac{\alpha_n^3}{10})(\phi_b-\phi_i)+\frac{1}{140}(1-\frac{19}{15}\alpha_n^3)\cot\phi_b+\frac{1}{120}\alpha_n^3\cot^3\phi_b+\frac{1}{8}\alpha_n^3\cot^5\phi_b$$

$$E_n=\frac{1}{8}\alpha_n^2(-\frac{59}{1575}+\frac{11}{15}\cot^2\phi_b+\frac{5}{4}\cot^4\phi_b)\ .$$

Applying the inverse Laplace transform [28] yields

$$J_z(\phi,t)=-\frac{\sqrt{3/2\cot\phi_b}}{4\pi a}\sum_{i=1}^{2}\sum_{n=1}^{\infty}\sum_{h=1}^{5}\frac{b_{inh}}{Ai'(-\alpha_n)}(\frac{6}{\beta_{in}})^{h/2}\tau_i^{(h-1)/2}\,e^{-\xi_{in}}(1-\frac{3h^2+3h-1}{18\xi_{in}})\,u(\tau_i) \tag{2.20}$$

where

$$\xi_{in}=\sqrt{2/\tau_i}\,(\beta_{in}/3)^{3/2}\ ,\quad \tau_i=\frac{c}{a}(t-t_{0i})\ . \tag{2.21}$$

It should be noted that $\tau_i=0$ corresponds to $t=t_{0i}$, which is the time required for the

wave to travel with a velocity c from the current filament to the point under consideration on the cylinder surface, via the two different directions of circumferential propagation (Fig. 2.1). It should also be noted that the expression obtained in (2.20) is valid only for the shadow region since the summation in (2.7), as seen from (2.16), is convergent only for $\phi_i > \phi_b$.

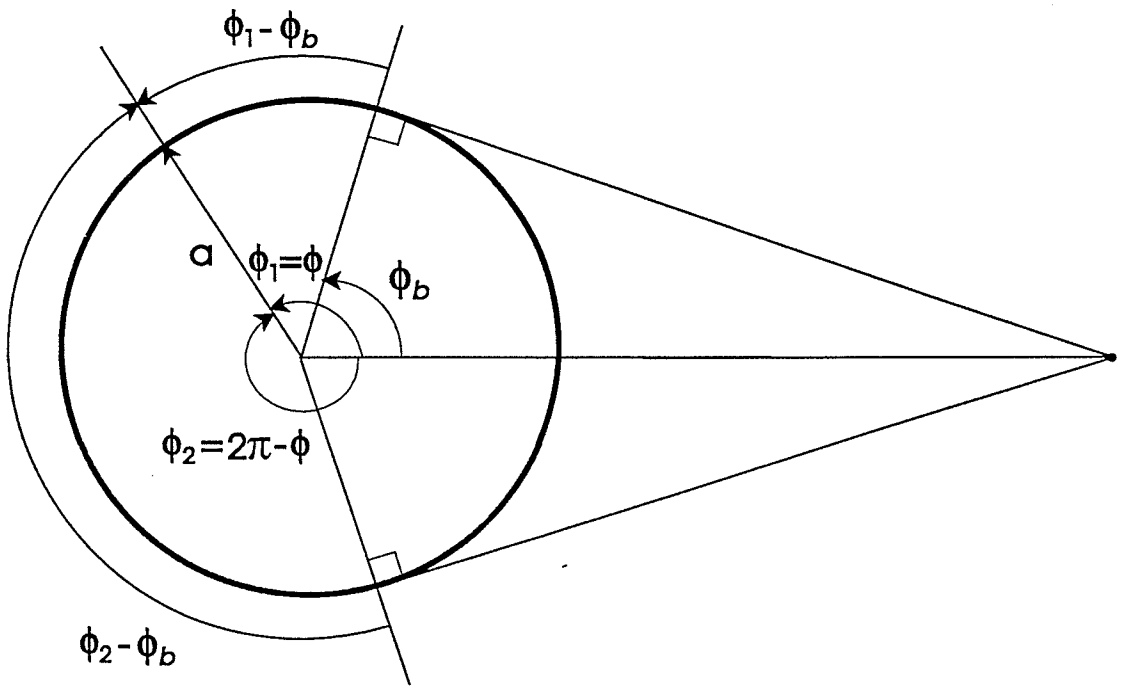

Fig. 2.1. Two directions of circumferential propagation of the creeping waves.

2.2 A Double Laplace Transform Approach

The early-time current response in the shadow region can also be obtained by using a double Laplace transform. For the cylinder to line current configuration shown in Fig. 1.1, the vector potential equation in cylindrical coordinates is

$$\nabla^2 A_z(r,\phi,t) - \frac{1}{c^2}\frac{\partial^2 A_z(r,\phi,t)}{\partial t^2} = -\frac{\mu_0}{r}\delta(r-r_0)\delta(\phi)u(t) \ . \tag{2.22}$$

Taking the Laplace transform with respect to t, we have

$$\nabla^2 \tilde{A}_z(r,\phi,s) - k^2 \tilde{A}_z(r,\phi,s) = -\frac{\mu_0}{kcr}\delta(r-r_0)\delta(\phi) \tag{2.23}$$

where $k=s/c$, with $\tilde{A}_z$ being defined for $-\pi < \phi \le \pi$. For an $\tilde{A}_z$ continued in ϕ $(-\infty,\infty)$ as a periodic function of ϕ, $\delta(\phi)$ in (2.23) has to be continued periodically as $\sum_{m=-\infty}^{\infty} \delta(\phi - 2m\pi) \equiv \sum_{m=-\infty}^{\infty} \delta(\phi_m)$. With $\tilde{A}_z$ in the form

$$\tilde{A}_z(r,\phi,s) = \sum_{m=-\infty}^{\infty} \tilde{A}_{zm}(r,\phi_m,s) \tag{2.24}$$

$\tilde{A}_{zm}$ is defined in ϕ_m $(-\infty, \infty)$ by the equation

$$\nabla^2 \tilde{A}_{zm}(r,\phi_m,s) - k^2 \tilde{A}_{zm}(r,\phi_m,s) = -\frac{\mu_0}{kcr}\delta(r-r_0)\delta(\phi_m) \ . \tag{2.25}$$

Taking the two-sided Laplace transform with respect to ϕ_m, we get

$$\frac{d^2 \mathrm{A}_{zm}(r,p,s)}{dr^2} + \frac{1}{r}\frac{d\mathrm{A}_{zm}(r,p,s)}{dr} - [k^2 + (jp/r)^2]\,\mathrm{A}_{zm}(r,p,s) = -\frac{\mu_0}{kcr}\delta(r-r_0) \tag{2.26}$$

where p is the second transform variable. The surface current density component corresponding to the solution of this equation is obtained in the form

$$\mathrm{J}_{zm}(p,s) = -\frac{1}{kac}\frac{K_{jp}(kr_0)}{K_{jp}(ka)} \tag{2.27}$$

where K_{jp} is the modified Bessel function of the second kind and order jp. The inverse of the two-sided Laplace transform in (2.27) is

$$\tilde{J}_{zm}(\phi_m, s) = -\frac{1}{2\pi j}\int_{\sigma-j\infty}^{\sigma+j\infty} \frac{1}{kac}\frac{K_{jp}(kr_0)}{K_{jp}(ka)} e^{p\phi_m} dp \quad . \tag{2.28}$$

For the early-time solution we consider the behavior of the integrand in (2.28) as the real-valued $s \to \infty$ [9]. In this case it can be shown that the expression in (2.28) can be replaced by the sum of residues of its integrand relative to the poles in the left or right half-plane of p corresponding to the sign of ϕ_m, $\phi_m > 0$ or $\phi_m < 0$, respectively. These poles are given by the zeros of $K_{jp}(ka)$ regarded as a function of p, which occur for real p only, when s is real [29]. Hence, for $\phi_m < 0$, the integral in (2.28) can be evaluated as

$$\tilde{J}_{zm}(\phi_m, s) = \frac{1}{kac}\sum_{n=1}^{\infty} e^{p_n\phi_m}[K_{jp}(kr_0)/\frac{\partial}{\partial p}K_{jp}(ka)]_{p=p_n} \quad . \tag{2.29}$$

The asymptotic expressions for $K_{jp_n}(kr_0)$ and $\frac{\partial}{\partial p}K_{jp}(ka)\,|_{p=p_n}$ are [29], [21]

$$K_{jp_n}(kr_0) \approx (\pi/2)^{1/2}\,(k^2r_0^2 - p_n^2)^{-1/4}\, e^{-(k^2r_0^2-p_n^2)^{1/2} + p_n\cos^{-1}(p_n/kr_0) - p_n\pi/2} \tag{2.30}$$

and

$$\frac{\partial}{\partial p}K_{jp}(ka)\,|_{p=p_n} \approx \frac{2^{1/2}\pi}{3(ka)^{2/3}}\, e^{-p_n\pi/2}\, f'(x_n) \tag{2.31}$$

where

$$f(x) = 3(2^{-1/6})\,Ai(-2^{1/3}x),\ \ p_n \approx ka + x_n(ka)^{1/3},\ \ x_n = 2^{-1/3}\alpha_n \quad . \tag{2.32}$$

From (2.29)-(2.32), we obtain

$$\tilde{J}_{zm}(\phi_m, s) = \frac{3}{2c\pi^{1/2}}\sum_{n=1}^{\infty}\frac{(ka)^{-1/3}}{f'(x_n)}(k^2r_0^2 - p_n^2)^{-1/4} e^{-(k^2r_0^2-p_n^2)^{1/2} + p_n\cos^{-1}(p_n/kr_0) + p_n\phi_m} \quad . \tag{2.33}$$

Since the terms in (2.33) decrease practically exponentially with p_n as n increases, we may retain only the first term. Thus

$$\tilde{J}_{zm}(\phi_m, s) = -\frac{1}{4cAi'(-\alpha_1)} \left(\frac{\cot\phi_b}{\pi}\right)^{1/2} \left(\frac{sa}{2c}\right)^{-5/6} e^{-t_{0m}s - \beta_m \left(\frac{sa}{2c}\right)^{1/3}} \tag{2.34}$$

where

$$\beta_m = \alpha_1(|\phi_m| - \phi_b), \quad t_{0m} = [(r_0^2 - a^2)^{1/2} + a(|\phi_m| - \phi_b)]/c \ . \tag{2.35}$$

To ensure that the summation in (2.33) is convergent for ϕ_m negative, we require that $|\phi_m| > \cos^{-1}(a/r_0)$, which shows that (2.33) is valid only in the region of geometric shadow.

The transformed current density corresponding to $\tilde{A}_z(r, \phi, s)$ is given by

$$\tilde{J}_z(\phi, s) = \sum_{m=-\infty}^{\infty} \tilde{J}_{zm}(\phi_m, s) \ . \tag{2.36}$$

For the early-time response we retain only two terms corresponding to the smallest values of $|\phi_m|$, which for $-\pi \le \phi < -\phi_b$ are

$$|\phi_m| = \begin{cases} |\phi| & \text{for } m=0 \\ 2\pi - |\phi| & \text{for } m=1 \ . \end{cases} \tag{2.37}$$

Thus

$$\tilde{J}_z(\phi, s) = -\frac{1}{4cAi'(-\alpha_1)} \left(\frac{\cos\phi_b}{\pi}\right)^{1/2} \left(\frac{sa}{2c}\right)^{-5/6} \sum_{m=0}^{1} e^{-t_{0m}s - \beta_m \left(\frac{sa}{2c}\right)^{1/3}} \ . \tag{2.38}$$

Due to symmetry, the expression in (2.38) with (2.37), is also valid for $\phi_b < \phi \le \pi$. By using an approximate formula [28], the inverse Laplace transform of this expression can be obtained in the form

$$J_z(\phi, t) = -\frac{3\sqrt{\cot\phi_b}}{4\pi aAi'(-\alpha_1)} \sum_{m=0}^{1} \beta_m^{-1/2} e^{-\xi_m} \left(1 - \frac{5}{18\xi_m}\right) u(\tau_m) \tag{2.39}$$

where

$$\tau_m = \frac{c}{a}[t-(r_0^2-a^2)^{1/2}/c]-(|\phi_m|-\phi_b),\ \xi_m = \sqrt{2/\tau_m}\,(\beta_m/3)^{3/2}\ . \qquad (2.40)$$

2.3 Special Case: Current Response to an Impulsive Plane Wave

The current response of a perfectly conducting circular cylinder to an impulsive or a unit-step plane electromagnetic wave, which is TM polarized, can be determined as a special case from the above results. As an example, consider the case of an impulsive plane wave (Fig. 2.2).

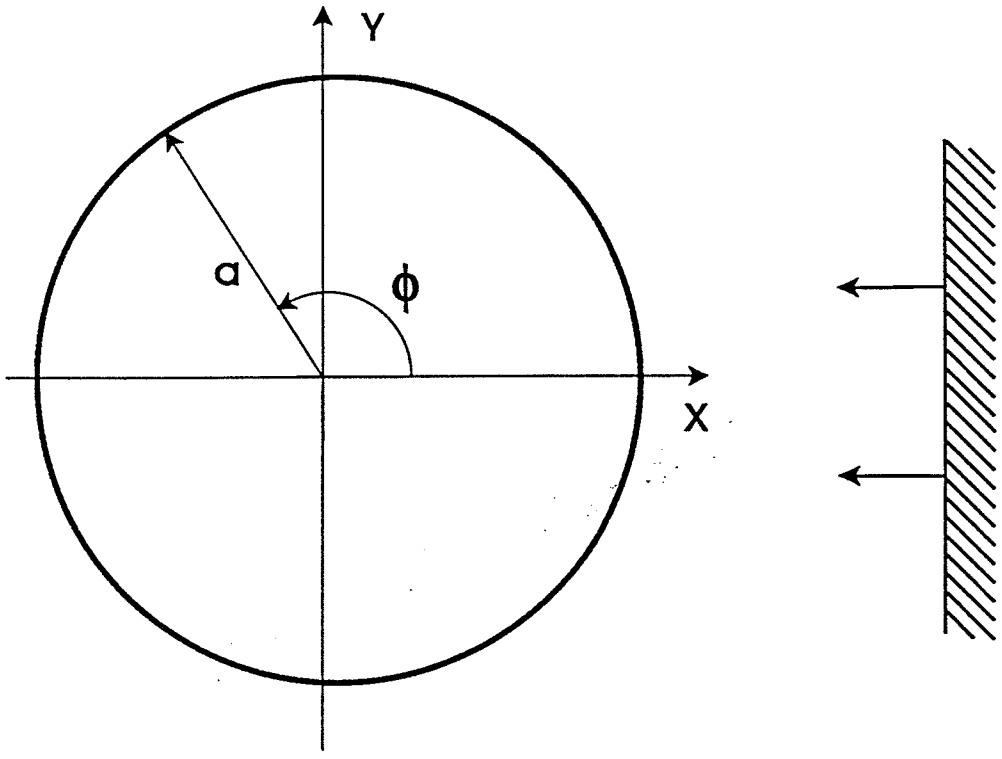

Fig. 2.2. Cross section of the circular cylinder illuminated by an impulsive plane wave.

The incident electric field $E_z^{i,p}(\mathbf{r},t)$ is taken to be

$$E_z^{i,p}(\mathbf{r},t)=\eta_0\,\delta(t+\frac{x}{c}-\frac{a}{c}) \tag{2.41}$$

where η_0 is the intrinsic impedance of free space. Note that at a time $t=0$ the incident plane wavefront is tangential to the cylinder at $r=a$. The Laplace transform of the incident field is

$$E_z^{i,p}(\mathbf{r},s)=\eta_0\,e^{\frac{s}{c}(r\cos\phi-a)}\ . \tag{2.42}$$

On the other hand, the Laplace transform of the electric field intensity produced by the line source carrying a unit-step current in Fig. 1.1 in an unbounded free space of permeability μ_0 is [30]

$$E_z^i(\mathbf{r},s)=-j\frac{\mu_0}{4}H_0^{(1)}(j\frac{s}{c}|\mathbf{r}-\mathbf{r}_0|)\ . \tag{2.43}$$

For large r_0, (2.43) becomes

$$E_z^i(\mathbf{r},s)\approx-\frac{\mu_0}{4}\left[\frac{2}{\pi s r_0/c}\right]^{1/2}e^{-\frac{s}{c}r_0}e^{\frac{s}{c}r\cos\phi}\ . \tag{2.44}$$

Hence

$$E_z^{i,p}(\mathbf{r},s)=\lim_{r_0\to\infty}\left\{-\eta_0\frac{4}{\mu_0}\left[\frac{\pi s r_0/c}{2}\right]^{1/2}e^{\frac{s}{c}(r_0-a)}E_z^i(\mathbf{r},s)\right\}\ . \tag{2.45}$$

Therefore the Laplace transform of the current density induced on the cylinder surface by the impulsive plane wave can be derived directly from

$$J_z^p(\phi,s)=\lim_{r_0\to\infty}\left\{-\eta_0\frac{4}{\mu_0}\left[\frac{\pi s r_0/c}{2}\right]^{1/2}e^{\frac{s}{c}(r_0-a)}J_z(\phi,s)\right\}. \tag{2.46}$$

For the shadow region, using the expression in (2.16) and taking into account only the terms corresponding to $n=h=1$, we obtain

$$J_z^p(\phi,s)=\frac{1}{Ai'(-\alpha_1)}\left(\frac{sa}{2c}\right)^{-1/3}\sum_{i=1}^{2}e^{-\frac{sa}{c}(\phi_i-\frac{\pi}{2}+1)-\beta_{i1}(\frac{sa}{2c})^{1/3}}. \tag{2.47}$$

Applying the formula [26],[14]

$$\frac{1}{2\pi j}\int_{s_0-j\infty}^{s_0+j\infty}s^{-1/3}e^{sT-\beta_i s^{1/3}}ds=\frac{3Ai'[\beta_i/(3T)^{1/3}]}{(3T)^{2/3}} \tag{2.48}$$

the early-time induced current density in the shadow region due to the impulsive plane wave under consideration is obtained as

$$J_z^p(\phi,t)=\frac{6^{1/3}c/a}{Ai'(-\alpha_1)}\sum_{i=1}^{2}Ai'\left[\frac{\alpha_1(\phi_i-\frac{\pi}{2})}{\left\{6[(\frac{ct}{a}-1)-(\phi_i-\frac{\pi}{2})]\right\}^{1/3}}\right]\frac{u\left[(\frac{ct}{a}-1)-(\phi_i-\frac{\pi}{2})\right]}{\left[(\frac{ct}{a}-1)-(\phi_i-\frac{\pi}{2})\right]^{2/3}}. \tag{2.49}$$

Using the relation (Appendix B)

$$\alpha_1=3^{-1/3}q_n\ ,\quad Ai'(-\alpha_1)=3^{2/3}\frac{1}{\pi}A'(q_1) \tag{2.50}$$

where $A(q)$ is another kind of Airy function which satisfies the equation

$$\frac{d^2A(q)}{dq^2}+\frac{q}{3}A(q)=0 \tag{2.51}$$

and $q_1=3.372134$ is the first zero of $A(q)$. (2.49) can now be written in a form

$$J_z^p(\phi,t)=\frac{6^{1/3}\pi c/a}{3^{2/3}}\frac{1}{1.059053}\sum_{i=1}^{2}Ai'\left[\frac{3.372134(\phi_i-\frac{\pi}{2})}{\left\{18[(\frac{ct}{a}-1)-(\phi_i-\frac{\pi}{2})]\right\}^{1/3}}\right]\frac{u\left[(\frac{ct}{a}-1)-(\phi_i-\frac{\pi}{2})\right]}{\left[(\frac{ct}{a}-1)-(\phi_i-\frac{\pi}{2})\right]^{2/3}} \tag{2.52}$$

which is exactly equation (20) in [7]. In deriving (2.52), $A(q_1)=1.059053$ [26] has been used. It should be noted that if we consider more terms in (2.16) when deriving $J_z^p(\phi,s)$ in (2.47), we can obtain more accurate results for this special case than those given in [7].

2.4 Numerical Results and Discussion

The normalized surface current density $-aJ_z$ in the shadow region at different angles, for $r_0/a=3$ and $r_0/a=6$, versus the normalized local time counted from the arrival of the first creeping wave, $\tau\equiv\tau_1$, is plotted in Figs. 2.3 and 2.4, respectively. For a given value of the local time, the magnitude of the current density decreases as ϕ increases from ϕ_b to π. This is due to the increased attenuation of the creeping waves traveling along a larger portion of the cylinder surface in the shadow region. For same ϕ and τ, the magnitude of the currents in the case of $r_0/a=3$ is smaller than that in the case of $r_0/a=6$, since for $r_0/a=3$, the resultant effect of the space attenuation of the incident cylindrical wave and the creeping wave attenuation is larger than that for $r_0/a=6$. In (2.20), the summation over n is found to be rapidly converging and hence only the values of $n=1$ to 5 are used in computation. Actually, even if we retain only the terms corresponding to $n=1$, we can still obtain a very good accuracy. As an example, for $r_0/a=3$, when $\phi=120^0$ and $\tau=0.2$, the difference between the results for $n=1$ and for n up to 5 is 4.33%. The results are compared with those obtained by using a double

Laplace transform approach (Section 2.2). It should be noted that the results in Figs. 2.3 and 2.4 obtained by applying a double Laplace transform correspond to the results in (2.20) when only the terms corresponding to $n=h=1$ are retained. The agreement is better for smaller values of the local time and for larger angles. Since the inverse Laplace transform formula [28] utilized in this paper is also an approximate one, we can only expect accurate results for τ up to such values, at each location, so that the contribution of the first term in (2.20) remains always larger than that of the other terms. For instance, for the case of $r_0/a=6$, when $\phi=180^0$ and $\tau=0.4$, the terms corresponding to h from 1 through 5 (with $i=1, 2; n=1, 2, 3, 4, 5$) are: 0.00373895, –0.00087922, 0.00034550, –0.00001475, –0.00001146.

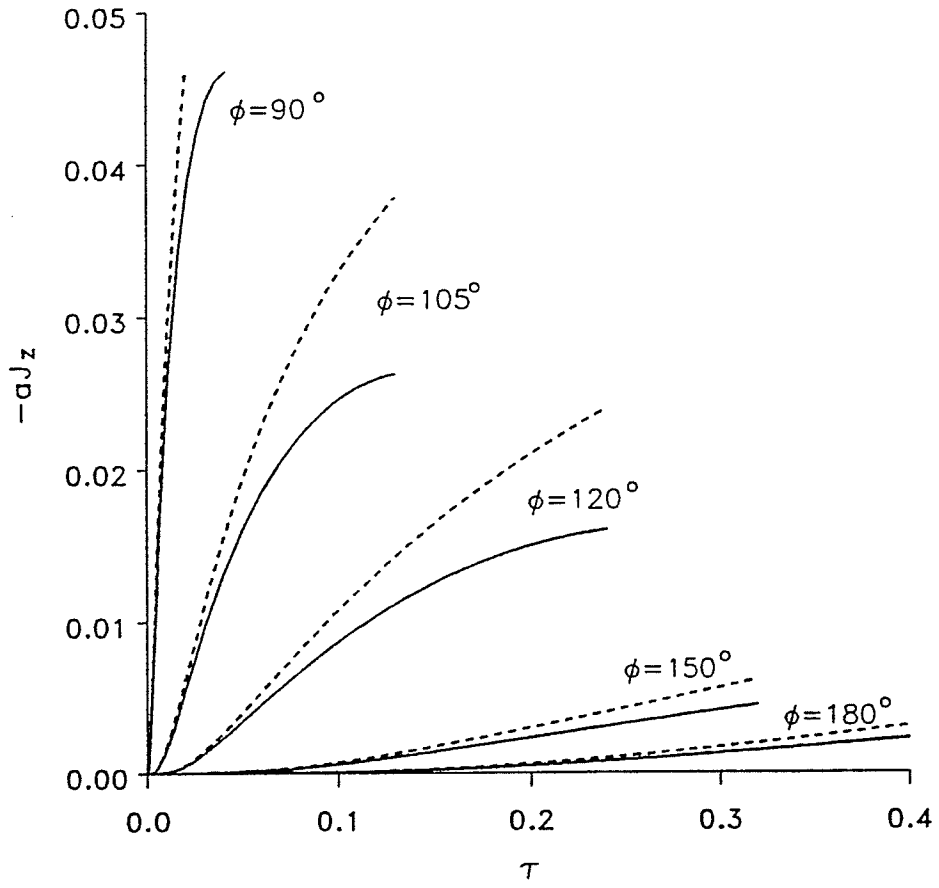

Fig. 2.3. Early-time current distribution in the shadow region for $r_0/a=3$;

—— Watson transformation, ------- double Laplace transform.

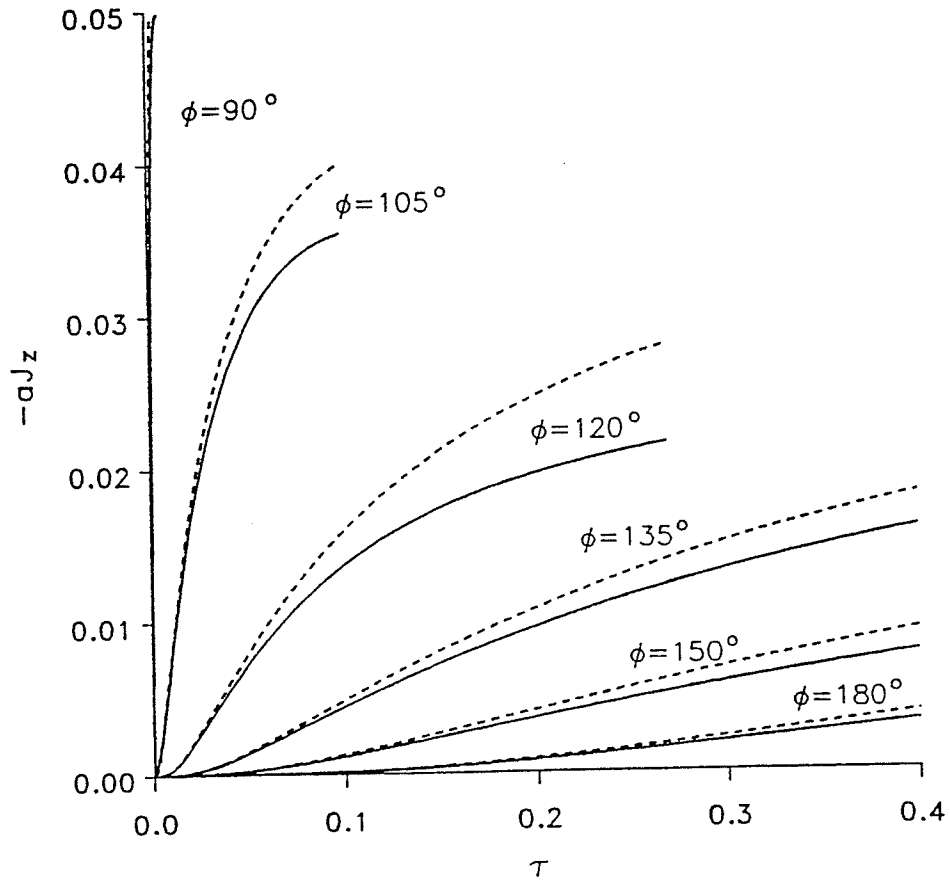

Fig. 2.4. Early-time current distribution in the shadow region for $r_0/a = 6$;

—— Watson transformation, ------- double Laplace transform.

CHAPTER 3

EARLY-TIME CURRENTS IN THE ILLUMINATED REGION

3.1 The Watson Transformation Solution

For the early-time solution in the illuminated region, the integral in (2.3), obtained via the Watson transformation, has to be evaluated in a different manner. Using the identity

$$\cos\nu(\phi-\pi)=e^{j\nu\pi}\cos\nu\phi-je^{j\nu\phi}\sin\nu\pi \tag{3.1}$$

(2.3) can be written as

$$J_z(\phi,s)=-\frac{1}{2\pi as}\int_{j\varepsilon-\infty}^{j\varepsilon+\infty}\frac{H_\nu^{(1)}(\frac{jsr_0}{c})}{H_\nu^{(1)}(\frac{jsa}{c})}e^{j\nu\phi}d\nu-\frac{j}{as}\sum_{i=1}^{2}\sum_{n=1}^{\infty}\sum_{q=0}^{\infty}\frac{H_{\nu_n}^{(1)}(\frac{jsr_0}{c})}{\dot{H}_{\nu_n}^{(1)}(\frac{jsa}{c})}e^{j\nu_n(2q\pi+\phi_i)} \tag{3.2}$$

where the triple sum is derived in a similar way as that in (2.7), with

$$\phi_i=\begin{cases}2\pi-\phi & \text{for } i=1\\ 2\pi+\phi & \text{for } i=2\end{cases}. \tag{3.3}$$

The integral term in (3.2) corresponds to the directly reflected wave and the triple sum to the creeping waves propagating along the cylinder circumference. Only the integral term in (3.2) needs to be retained, since even the smallest time delay in the creeping wave contribution, i.e. $\frac{a}{c}(2\pi-\phi)$, for $i=1$ and $q=0$, will be beyond the time range of the early-

time solution (Fig. 3.1).

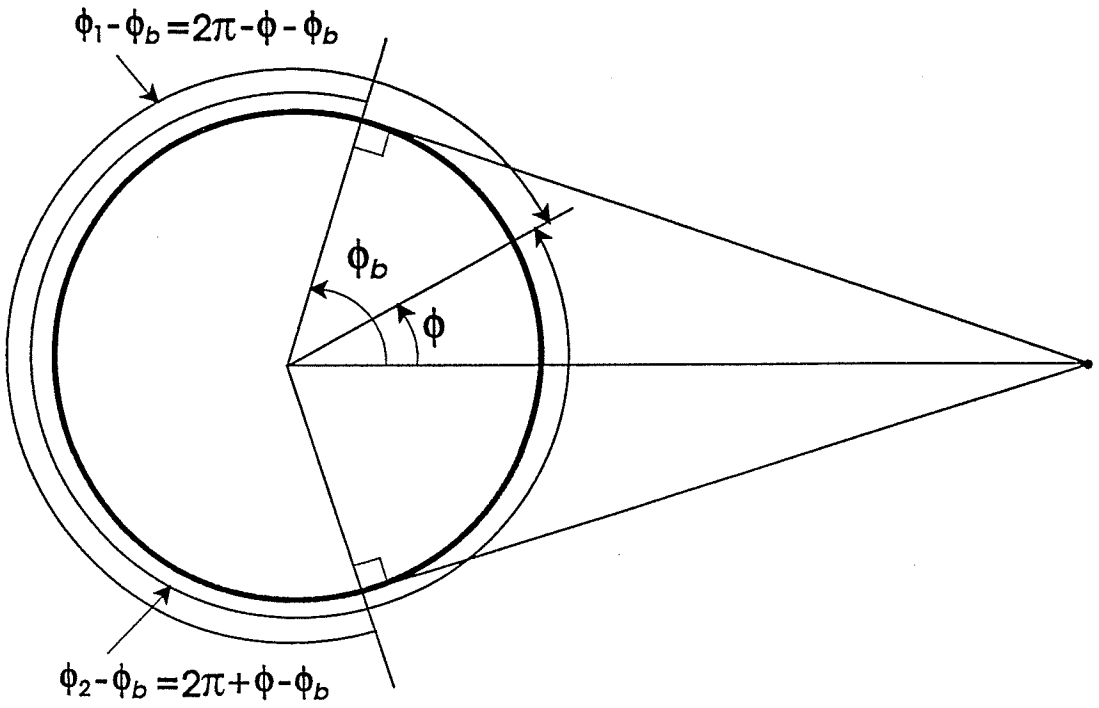

Fig. 3.1. Time delay of the creeping waves in the illuminated region.

The integral in (3.2) can be evaluated by applying the saddle point method. For the early-time solution we consider the behavior of the integrand in (3.2) as the real-valued $s\rightarrow\infty$ [9]. Taking into account the asymptotic expansion of $H_\nu(jsr_0/c)/H_\nu(jsa/c)$ when $|\nu/s|$ is small, the value of the integral is determined practically from large values of $|\nu|$ only. Using the asymptotic expansion in (2.13) and performing the change of variable $u=\nu/(jsa/c)$ yields

$$J_z(\phi,s)=-\frac{1}{2\pi j}\frac{1}{c}\int_{\sigma-j\infty}^{\sigma+j\infty}F(u)e^{\frac{sa}{c}G(u)}du \tag{3.4}$$

where σ is a small positive number and

$$F(u)=\left[\frac{1-u^2}{r_0'^2-u^2}\right]^{1/4}\frac{\sum_{m=0}^{\infty}\frac{A_m'}{(-\frac{1}{2}\frac{sa}{c}\sqrt{r_0'^2-u^2})^m}\frac{\Gamma(m+\frac{1}{2})}{\Gamma(\frac{1}{2})}}{\sum_{m=0}^{\infty}\frac{A_m}{(-\frac{1}{2}\frac{sa}{c}\sqrt{1-u^2})^m}\frac{\Gamma(m+\frac{1}{2})}{\Gamma(\frac{1}{2})}} \tag{3.5}$$

$$G(u)=-(r_0'^2-u^2)^{1/2}+(1-u^2)^{1/2}+u[\cos^{-1}(u/r_0')-\cos^{-1}u-\phi] \tag{3.6}$$

in which $r_0'\equiv r_0/a$. A_m are given by (2.14), and A_m' have the same expressions as A_m with γ replaced by γ',

$$\gamma=j\cos^{-1}u\,,\quad \gamma'=j\cos^{-1}(u/r_0')\,. \tag{3.7}$$

The saddle point u_0 satisfies the equation $G'(u)=0$, which reduces to

$$\cos^{-1}(u_0/r_0')-\cos^{-1}u_0-\phi=0\,. \tag{3.8}$$

u_0 can be obtained in the form

$$u_0=\frac{r_0\sin\phi}{R_0}=\sin\alpha=r_0'\sin\beta \tag{3.9}$$

where

$$R_0=(r_0^2+a^2-2r_0\,a\cos\phi)^{1/2} \tag{3.10}$$

and α, β are the angles shown in Fig. 1.1. The integral in (3.4) is calculated as [31]

$$J_z(\phi,s)=-\frac{1}{2\pi c}F(u_0)\,e^{\frac{sa}{c}G(u_0)}\left[\frac{2\pi}{\frac{sa}{c}G''(u_0)}\right]^{1/2} \tag{3.11}$$

which can finally be presented in the form

$$J_z(\phi, s) = -\frac{\cos\alpha}{\sqrt{2\pi R_0 cs}} \left[1 + \frac{1}{2}\frac{C_1}{sa/c} + \frac{3}{4}\frac{C_2}{(sa/c)^2} + \cdots\right] e^{-sR_0/c} \tag{3.12}$$

where

$$C_1 = \frac{1}{4r_0' \cos\alpha \cos\beta}\left[R_0' + \frac{5}{3}(r_0' \cos\beta \tan^2\alpha - \cos\alpha \tan^2\beta)\right] \tag{3.13}$$

$$\begin{aligned} C_2 = \frac{1}{r_0'^2 \cos^2\alpha \cos^2\beta}\Bigg\{ & \frac{5}{144} r_0' \cos\beta \left[R_0' \tan^2\alpha + (1 + \frac{5}{3}\tan^2\alpha)(r_0' \cos\beta \tan^2\alpha - \cos\alpha \tan^2\beta)\right] \\ & + \frac{77}{144}\left[(1 + \frac{5}{6}\tan^2\beta)\cos^2\alpha \tan^2\beta - (1 + \frac{5}{6}\tan^2\alpha) r_0'^2 \cos^2\beta \tan^2\alpha\right] \\ & - \frac{1}{96} R_0'(7R_0' + 16\cos\alpha)\Bigg\} \end{aligned} \tag{3.14}$$

with $R_0' \equiv R_0/a$.

The inverse Laplace transform of (3.12), evaluated by considering only three terms in the series expansion, gives the time dependent solution as

$$J_z(\phi, t) = -\frac{1}{\pi a}\frac{\cos\alpha}{\sqrt{2R_0/a}}\left(\frac{1}{\tau^{1/2}} + C_1\tau^{1/2} + C_2\tau^{3/2}\right) u(\tau) \tag{3.15}$$

where

$$\tau = \frac{c}{a}(t - R_0/c) \ . \tag{3.16}$$

3.2 The Luneberg-Kline Expansion

The current response in the illuminated region can also be determined by means of a

Luneberg-Kline expansion. The Laplace transform of the electric field in the absence of the cylinder can be written as [30]

$$E_z^i(r,\theta,s) = -j\frac{\mu_0}{4} H_0^{(1)}(jkR) \tag{3.17}$$

where r,θ are the cylindrical coordinates of the field point and R the distance from the line current to the field point (Fig. 3.2).

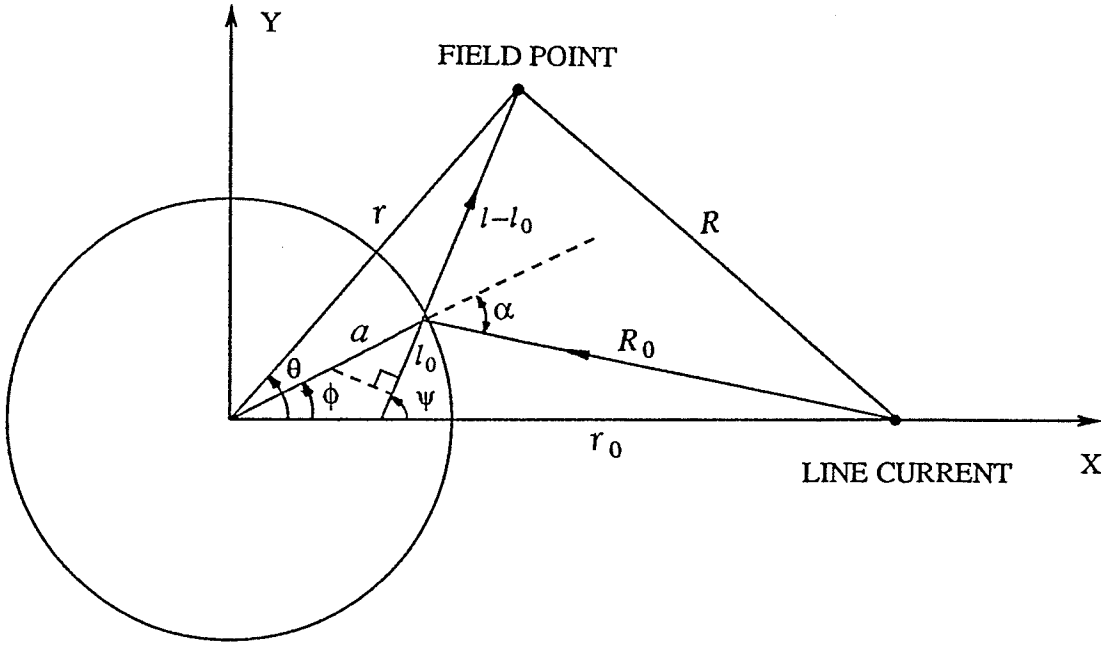

Fig. 3.2. Caustic coordinate system.

When $s \to \infty$, E_z^i can be written in the asymptotic form [29]

$$E_z^i(r,\theta,s) = -\frac{\mu_0}{2}\frac{1}{\sqrt{2\pi kR}} e^{-kR}\left[1 - \frac{1}{8}\frac{1}{kR} + \frac{9}{128}\frac{1}{(kR)^2} - \cdots\right] . \tag{3.18}$$

The Laplace transform of the scattered electric field satisfies the wave equation

$$\nabla^2 E_z^s(r,\theta,s)-k^2 E_z^s(r,\theta,s)=0\ . \tag{3.19}$$

Now we assume that E_z^s has the asymptotic expansion (for $k\to\infty$) of the form

$$E_z^s(r,\theta,s)=-\frac{\mu_0}{2}\frac{1}{\sqrt{2\pi k}}e^{-k\Psi(r,\theta)}\sum_{n=0}^{\infty}\frac{w_n(r,\theta)}{k^n} \tag{3.20}$$

in which $\Psi(r,\theta)$ and $w_n(r,\theta)$ are the unknown functions to be determined. The boundary condition requires that the total tangential electric field be equal to zero at the surface of the cylinder, which can be written as

$$E_z^i(a,\theta,s)+E_z^s(a,\theta,s)=0\ . \tag{3.21}$$

Substituting (3.18) and (3.20) in (3.21) gives

$$\Psi(a,\theta)=R_0 \tag{3.22}$$

$$w_0(a,\theta)=-R_0^{-1/2},\quad w_1(a,\theta)=\frac{1}{8}R_0^{-3/2},\quad w_2(a,\theta)=-\frac{9}{128}R_0^{-5/2},\quad \cdots \tag{3.23}$$

where $R_0=(r_0^2+a^2-2r_0 a\cos\phi)^{1/2}$ with ϕ as shown in Fig. 3.2. Then we substitute (3.20) into (3.19) to obtain

$$\begin{cases}(\nabla\Psi)^2=1\\ 2\nabla\Psi\cdot\nabla w_n+w_n\nabla^2\Psi=\nabla^2 w_{n-1}\quad n=0,1,2,\cdots;\ w_{-1}=0\ .\end{cases} \tag{3.24}$$

This equation can be solved in the caustic coordinate system to give [32]

$$w_n(l,\psi)=w_n(l_0,\psi)\left(\frac{l_0}{l}\right)^{1/2}+\frac{1}{2l^{1/2}}\int_{l_0}^{l} l'^{1/2}\,\nabla^2 w_{n-1}(l',\psi)dl' \tag{3.25}$$

where l and ψ are the caustic coordinates shown in Fig. 3.2 and $l_0=\frac{a}{2}\cos\alpha$ is the distance along the reflected ray from the caustic to the cylinder surface with α as shown in

Fig. 3.2. It can be shown that the Laplacian operator in caustic coordinates is (Appendix D)

$$\nabla^2=(1+\frac{A}{l^2})\frac{\partial^2}{\partial l^2}+(\frac{1}{l}-\frac{C}{l^2}-\frac{A}{l^3})\frac{\partial}{\partial l}-\frac{2B}{l^2}\frac{\partial^2}{\partial l\partial\psi}+\frac{1}{l^2}\frac{\partial^2}{\partial\psi^2}+\frac{B}{l^3}\frac{\partial}{\partial\psi} \quad (3.26)$$

where

$$A=\frac{a^2}{4}\sin^2\alpha(1+\frac{d\phi}{d\psi})^2,\quad B=\frac{a}{2}\sin\alpha(1+\frac{d\phi}{d\psi})$$

$$C=a\left[-\frac{1}{2}\cos\alpha(\frac{d\phi}{d\psi})^2+\cos\alpha(1-\frac{d\phi}{d\psi})+\frac{1}{2}\sin\alpha\frac{d^2\phi}{d\psi^2}\right]. \quad (3.27)$$

The phase function $\Psi(r,\theta)$ can be written as

$$\Psi(r,\theta)=R_0+l-\frac{a}{2}\cos\alpha\ . \quad (3.28)$$

From (3.20)–(3.27), expressions for w_0, w_1 and w_2 are obtained. The sum of the incident and scattered electric fields gives the total electric field

$$E_z(r,\theta)=-\frac{\mu_0}{2}\frac{1}{\sqrt{2\pi k}}\left\{[\frac{1}{R^{1/2}}e^{-kR}-\frac{1}{R_0^{1/2}}(\frac{l_0}{l})^{1/2}e^{-k(R_0+l-\frac{a}{2}\cos\alpha)}]\right.$$

$$+\frac{1}{k}[-\frac{1}{8}\frac{1}{R^{3/2}}e^{-kR}+\frac{1}{8}\frac{1}{R_0^{3/2}}(\frac{l_0}{l})^{1/2}e^{-k(R_0+l-\frac{a}{2}\cos\alpha)}]+\frac{1}{k}\frac{1}{2l^{1/2}}e^{-k(R_0+l-\frac{a}{2}\cos\alpha)}$$

$$\cdot\left[[\frac{1}{4}(\frac{l_0}{R_0})^{1/2}\frac{\partial^2}{\partial\psi^2}(\frac{l_0}{R_0})^{1/2}]\frac{1}{l}+[\frac{1}{4}(\frac{l_0}{R_0})^{1/2}C+B\frac{\partial}{\partial\psi}(\frac{l_0}{R_0})^{1/2}]\frac{1}{l^2}+\frac{5}{12}A(\frac{l_0}{R_0})^{1/2}\frac{1}{l^3}\right]_{l_0}^{l}$$

$$\left.+\frac{1}{k^2}[\frac{9}{128}\frac{1}{R^{5/2}}e^{-kR}-\frac{9}{128}\frac{1}{R_0^{5/2}}(\frac{l_0}{l})^{1/2}e^{-k(R_0+l-\frac{a}{2}\cos\alpha)}]+\cdots\right\}. \quad (3.29)$$

The surface current density is equal to the tangential component of the magnetic field

intensity on the surface of the cylinder, $J_z(\phi, s)=\frac{1}{\mu_0 s}\frac{\partial E_z}{\partial r}|_{r=a}$. After a lengthy but straightforward derivation, we finally obtain the Laplace transform of the current density up to the power of $s^{-5/2}$ as (Appendix E)

$$J_z(\phi, s)=-\frac{1}{2c\sqrt{2\pi}}e^{-sR_0/c}\left\{\frac{2\cos\alpha}{R_0^{1/2}}(c/s)^{1/2}+\frac{1}{4\cos\alpha}\frac{1}{R_0^{3/2}}(3\cos^2\alpha-2+2R_0/l_0)(c/s)^{3/2}\right.$$

$$\left.+\frac{D}{512\cos\alpha}\frac{R_0^{1/2}}{(l_0+R_0)^3}(c/s)^{5/2}\right\} \tag{3.30}$$

where

$$D=-3(5\cos^2\alpha-4)\cos^3\alpha(R_0/a)^{-3}-2(45\cos^2\alpha-32)\cos^2\alpha(R_0/a)^{-2}$$

$$-4(45\cos^2\alpha+8-\frac{24}{\cos^2\alpha})\cos\alpha(R_0/a)^{-1}-8(15\cos^2\alpha+8+\frac{40}{\cos^2\alpha})$$

$$+320(1-\frac{40}{\cos^2\alpha})\frac{1}{\cos\alpha}(R_0/a)+512(3-\frac{4}{\cos^2\alpha})\frac{1}{\cos^2\alpha}(R_0/a)^2\ . \tag{3.31}$$

The inverse Laplace transform of (3.30) gives the time dependent solution as

$$J_z(\phi, t)=-\frac{1}{\sqrt{2}\pi a}\left\{\frac{\cos\alpha}{(R_0/a)^{1/2}}\frac{1}{\tau^{1/2}}+\frac{1}{4\cos\alpha}\frac{1}{(R_0/a)^{3/2}}[3\cos^2\alpha-2+\frac{4}{\cos\alpha}(R_0/a)]\tau^{1/2}\right.$$

$$\left.+\frac{D}{96}\frac{1}{\cos\alpha}\frac{(R_0/a)^{1/2}}{(\cos\alpha+2R_0/a)^3}\tau^{3/2}\right\}u(\tau) \tag{3.32}$$

where $\tau=\frac{c}{a}(t-R_0/c)$.

3.3 Special Case: Current Response to an Impulsive Plane Wave

As in Section 2.3, the induced current density on the cylinder surface in the

illuminated region due to a TM polarized impulsive plane electromagnetic wave can also be determined as a special case of the above results. The incident electric field is given in (2.41). Using (3.12) in (2.46) and noting that when $r_0 \to \infty$,

$$\alpha \to \phi\,, \quad \beta \to 0\,, \quad r_0'/R_0' \to 1 \tag{3.33}$$

we obtain

$$J_z^p(\phi, s) = e^{-\frac{sa}{c}(1-\cos\phi)} \left[2\cos\phi + \frac{1}{4}(1+\frac{5}{3}\tan^2\phi)\frac{1}{sa/c} \right.$$

$$\left. - \frac{1}{32\cos\phi}(\frac{7}{2}+\frac{67}{3}\tan^2\phi+\frac{335}{18}\tan^4\phi)\frac{1}{(sa/c)^2} \right] . \tag{3.34}$$

The inverse Laplace transform of (3.33) gives the time domain solution as

$$J_z^p(\phi, t) = 2\,\delta(t')\cos\phi + \frac{1}{4}(1+\frac{5}{3}\tan^2\phi)(c/a)\,u(t')$$

$$- \frac{1}{32\cos\phi}(\frac{7}{2}+\frac{67}{3}\tan^2\phi+\frac{335}{18}\tan^4\phi)(c/a)^2 t' u(t') \tag{3.35}$$

where $t' = t - \frac{a}{c}(1-\cos\phi)$.

If we use the Luneberg-Kline expansion solution (3.30) instead of (3.12), we have

$$J_z^p(\phi, s) = e^{-\frac{sa}{c}(1-\cos\phi)} \left[2\cos\phi + \frac{1}{2\cos^2\phi}\frac{1}{sa/c} + \frac{1}{\cos^3\phi}(3-\frac{4}{\cos^2\phi})\frac{1}{(sa/c)^2} \right] \tag{3.36}$$

and

$$J_z^p(\phi, t) = 2\delta(t')\cos\phi + \frac{(c/a)}{\cos^2\phi}u(t') - \frac{(c/a)^2(1+3\sin^2\phi)}{\cos^5\phi}t'u(t') \tag{3.37}$$

which is exactly equation (13) in [7]. It should be noted that the first term in (3.34) is the same as that in (3.36), which represents the physical optics solution.

3.4 Numerical Results and Discussion

Numerical results of the normalized surface current density for the illuminated region when $r_0 = 3a$ and $r_0 = 6a$, are presented in Figs. 3.3 and 3.4, respectively, where τ is the normalized local time, counted from the arrival of the wave front. Due to the nature of the series in (3.15), we expect accurate results for points which are not close to the shadow boundary and for times such that the subsequent terms in (3.15) bring a contribution which remains small as compared to that of the previous ones. Theoretically, there is an infinite current density at the arrival of the wave front, which does not exist in the shadow region. For a given value of τ, the magnitude of the current density decreases as ϕ increases from 0 to ϕ_b. Due to the space attenuation for a cylindrical wave, the magnitude of the current density for $r_0/a = 6$ is smaller than that for $r_0/a = 3$, when ϕ is not close to ϕ_b. It should be remarked that the first term in the Luneberg-Kline expansion solution (3.32) and that in the Watson transformation solution in (3.15) are the same, being approximately given by the physical optics solution [33,34]. Comparison of the results from the physical optics approximation, the Watson transformation, and from the Luneberg-Kline expansion, shows that for the early-time response in the illuminated region the Watson transformation solution has at each location a range of validity up to greater times than the Luneberg-Kline expansion solution. On the other hand, the simple physical optics solution provides reasonably good results at all locations for an increased time range.

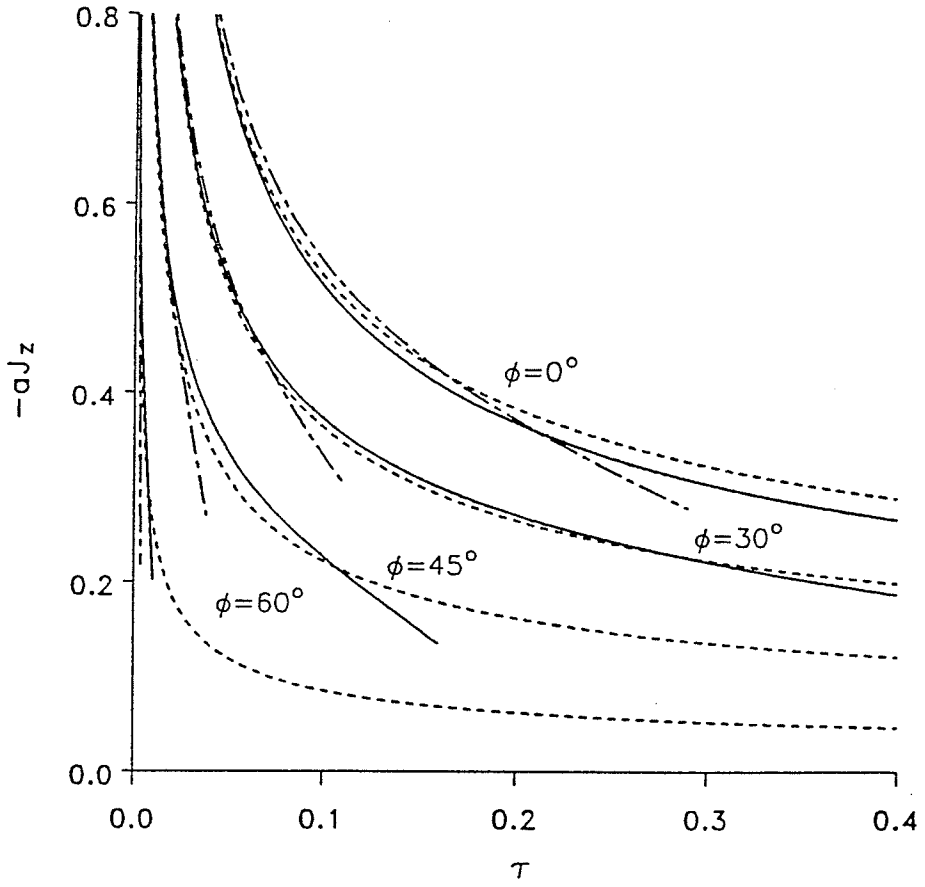

Fig. 3.3. Early-time current distribution in the illuminated region for $r_0/a=3$; —— Watson transformation, - —- Luneberg–Kline expansion, ------- physical optics.

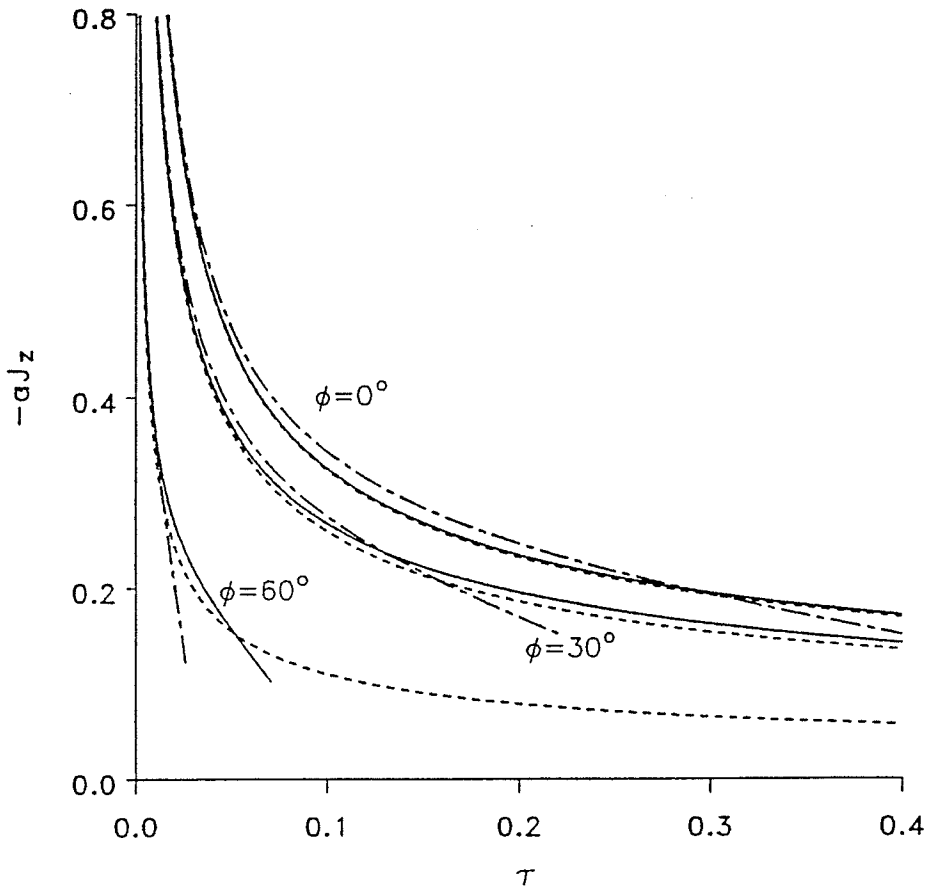

Fig. 3.4. Early-time current distribution in the illuminated region for $r_0/a=6$; —— Watson transformation, -—- Luneberg–Kline expansion, ------- physical optics.

CHAPTER 4

LATE-TIME CURRENT RESPONSE

The initial objective in this chapter is to derive analytical expressions for the late-time current density induced on the perfectly conducting circular cylinder by a cylindrical wave. However, we will show that, in fact, the single expression obtained is mathematically valid for all the time ranges and numerically useful for times after the initial wavefront passes the cylinder axis, which corresponds to all the time ranges in the shadow region and for larger angles in the illuminated region. This is different from the conventional definition of "late-time", i.e. the time range after the initial wavefront has completely passed the cylinder. The series expression of the induced current density does not converge rapidly for small values of time. Hence in these cases we can use the early-time results obtained in Chapters 2 and 3. For larger values of time, the series expression converges very rapidly and only the first few terms are needed to give accurate results. Unlike the early-time solution, the late-time solution for both the shadow and the illuminated region can be represented by a single expression.

In our derivation, we use two different procedures: one starts from the frequency domain eigenfunction solution of the total induced current density and the other from that of the magnetic fields at the cylinder surface and deals with the scattered and incident magnetic fields separately. It is found that the results obtained by the first approach has a wide range of validity.

4.1 The Inverse Laplace Transform of the Total Current Density

The Laplace transform of the total induced current density can be expressed in terms of the modified Bessel functions as

$$J_z(\phi, s) = -\frac{1}{2\pi as} \sum_{n=0}^{\infty} \varepsilon_n \frac{K_n(sr_0/c)}{K_n(sa/c)} \cos n\phi \tag{4.1}$$

where $\varepsilon_n = 1$ for $n = 0$ and $\varepsilon_n = 2$ for $n \neq 0$, K_n is the modified Bessel function of the second kind and order n. Taking the inverse Laplace transform of (4.1), we have

$$J_z(\phi, t) = \frac{1}{2\pi j} \int_{s_0 - j\infty}^{s_0 + j\infty} e^{st} J_z(\phi, s)\, ds \ . \tag{4.2}$$

Using (4.1) in (4.2) we obtain

$$J_z(\phi, t) = -\frac{1}{2\pi j} \frac{1}{2\pi a} \sum_{n=0}^{\infty} \varepsilon_n h_n(\tau) \cos n\phi \tag{4.3}$$

where

$$h_n(\tau) = \int_{\zeta_0 - j\infty}^{\zeta_0 + j\infty} H_n(\zeta, \tau)\, d\zeta \tag{4.4}$$

in which

$$H_n(\zeta, \tau) = \frac{K_n(\zeta r_0')}{K_n(\zeta)} \frac{e^{\zeta\tau}}{\zeta} \tag{4.5}$$

with ζ, τ and r_0 being normalized quantities defined as

$$\zeta = sa/c \ , \ \tau = ct/a \ , \ r_0' = r_0/a \ . \tag{4.6}$$

The integration contours are chosen as shown in Fig. 4.1.

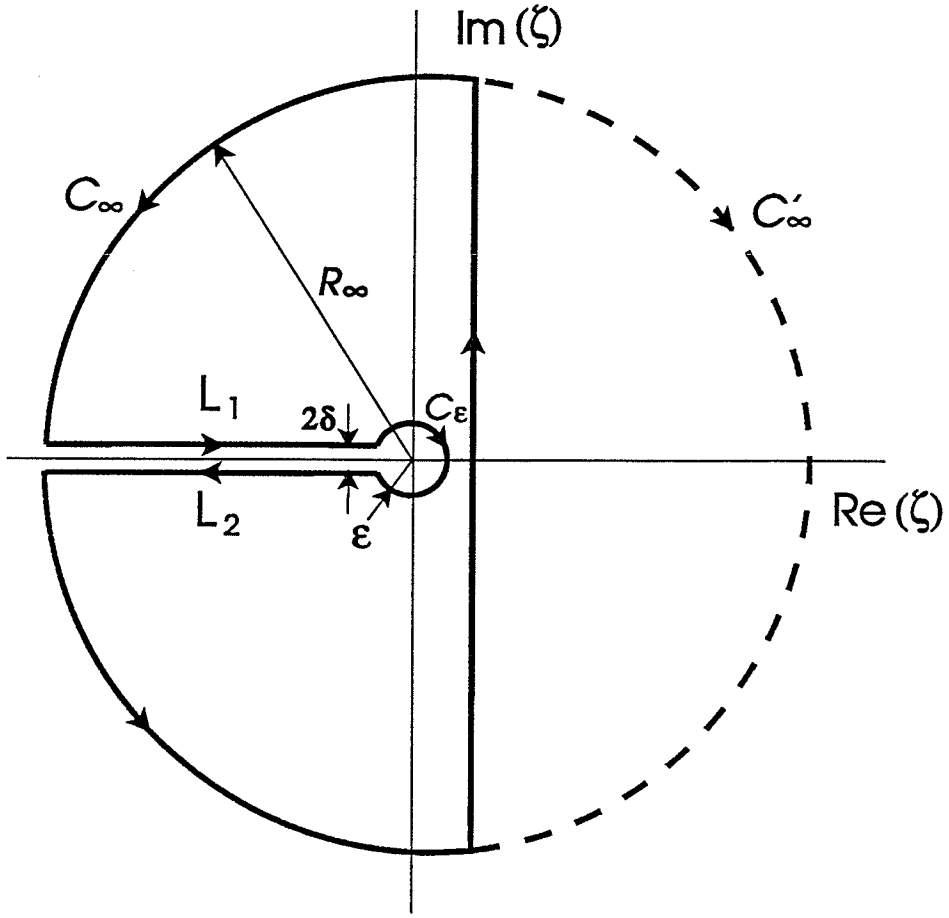

Fig. 4.1. Integration contours in the complex ζ-plane.

When the contour is closed in the right half plane along C'_∞ , we have

$$h_n(\tau)=0 \quad \text{for} \quad \tau < r'_0 - 1 \tag{4.7}$$

since $K_n(\zeta)$ has no zeros in the right half plane and the integral along C'_∞ vanishes. The physical interpretation of this result is obvious. When the contour is closed along $C_\infty + L_1 + C_\varepsilon + L_2$ in the left half plane, $h_n(\tau)$ can be written as

$$h_n(\tau)=2\pi j \sum_l R_{nl} - \left[\int_{C_\infty} + \int_{C_\varepsilon} + \int_{L_1} + \int_{L_2}\right] H_n(\zeta,\tau)\, d\zeta \tag{4.8}$$

where R_{nl} are the residues of $H_n(\zeta,\tau)$ at the simple poles ζ_{nl} given by $K_n(\zeta_{nl})=0$. It can be shown that (Appendix F)

$$\lim_{\varepsilon\to 0} \int_{C_\varepsilon} H_n(\zeta,\tau) d\zeta = -2\pi j \frac{1}{r'^{\,n}_0} \tag{4.9}$$

and

$$\lim_{R_\infty\to\infty} \int_{C_\infty} H_n(\zeta,\tau) d\zeta = 0 \quad \text{for} \quad \tau > r'_0 - 1 \ . \tag{4.10}$$

Exploiting appropriately the analytic continuation of Bessel functions, the contributions from the line integrals along the branch cut can be evaluated as (Appendix G)

$$\int_{L_1} H_n(\zeta,\tau)\, d\zeta + \int_{L_2} H_n(\zeta,\tau)\, d\zeta = (-1)^n 2\pi j\, B_n(\tau) \tag{4.11}$$

where

$$B_n(\tau) = \int_0^\infty \frac{I_n(zr'_0)\, K_n(z) - I_n(z)\, K_{n+1}(zr'_0)}{K_n^2(z) + \pi^2 I_n^2(z)} \frac{e^{-z\tau}}{z}\, dz \tag{4.12}$$

in which I_n is the modified Bessel function of the first kind and order n. The residues R_{nl} can be expressed as

$$R_{nl} = -\frac{K_n(\zeta_{nl} r_0')}{K_{n-1}(\zeta_{nl})} \frac{e^{\zeta_{nl}\tau}}{\zeta_{nl}} \tag{4.13}$$

and the summation in (4.8) as

$$\sum_l R_{nl} = -\sum_{l=1}^{V(n)} \frac{K_n(\zeta_{nl} r_0')}{K_{n-1}(\zeta_{nl})} \frac{e^{\zeta_{nl}\tau}}{\zeta_{nl}} \tag{4.14}$$

where $V(n)$ is the number of zeros of $K_n(\zeta)$ and depends on n. Since the zeros of $K_n(\zeta)$ appear in conjugate pairs [29] and $V(n)$ is twice the integer part of $n/2$, (4.14) can be written in the form

$$\sum_l R_{nl} = -2\sum_{l=1}^{[n/2]} \mathrm{Re}\left[\frac{K_n(\zeta_{nl} r_0')}{K_{n-1}(\zeta_{nl})} \frac{e^{\zeta_{nl}\tau}}{\zeta_{nl}}\right] \tag{4.15}$$

where $[n/2]$ represents the integer part of $n/2$ and the zeros of $K_n(\zeta)$ are now either those in the second quadrant or in the third quadrant. The zeros of $K_n(\zeta)$ for n up to 30 in the second quadrant are plotted in Fig. 4.2 and those for n up to 20 are listed in Appendix H.

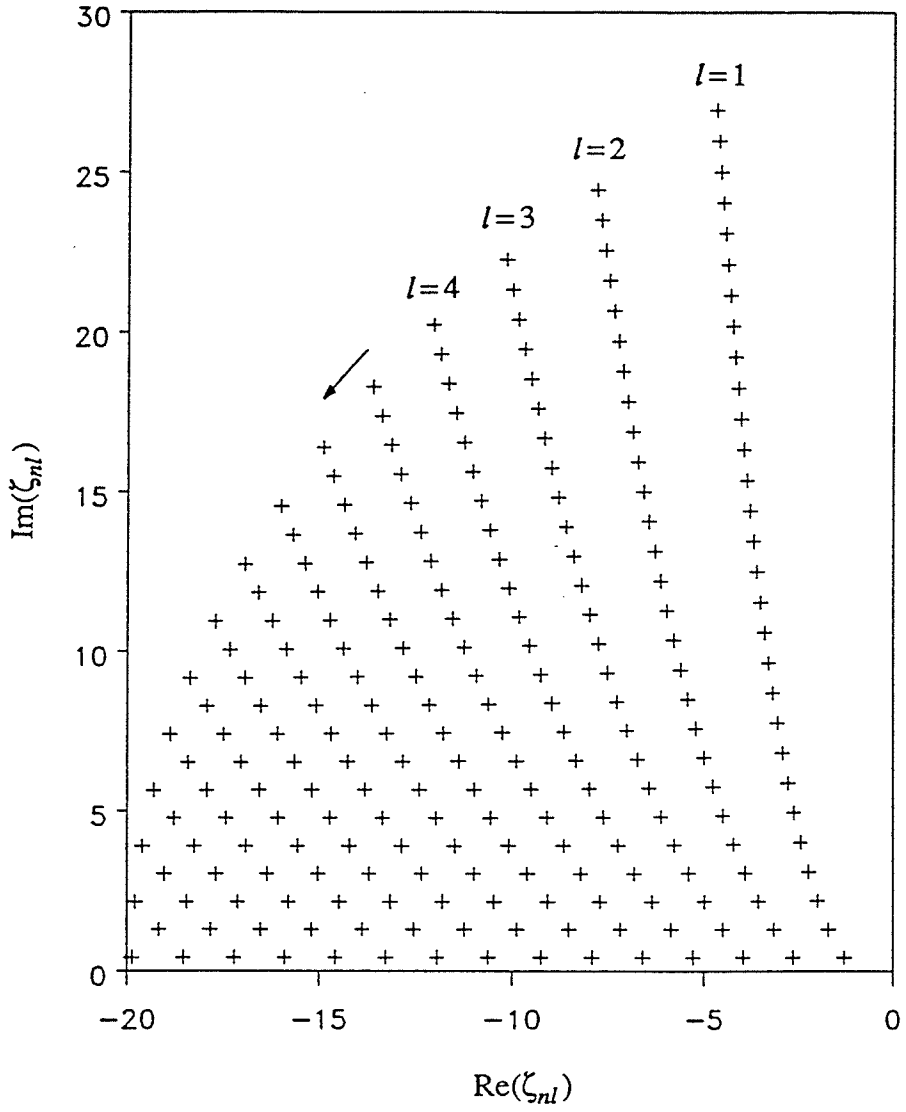

Fig. 4.2. Distribution of the zeros of $K_n(\zeta)$.

With (4.9)-(4.15) in (4.8), we obtain

$$h_n(\tau)=2\pi j\left\{\frac{1}{r_0'^{\,n}}-2\sum_{l=1}^{[n/2]}\mathrm{Re}\left[\frac{K_n(\zeta_{nl}r_0')}{K_{n-1}(\zeta_{nl})}\frac{e^{\zeta_{nl}\tau}}{\zeta_{nl}}\right]\right.$$

$$\left.-(-1)^n\int_0^\infty\frac{I_n(zr_0')K_n(z)-I_n(z)K_{n+1}(zr_0')}{K_n^2(z)+\pi^2 I_n^2(z)}\frac{e^{-z\tau}}{z}dz\right\}\quad . \tag{4.16}$$

Substituting in (4.3) and using the identity

$$\sum_{n=0}^{\infty}\varepsilon_n\frac{\cos n\phi}{r_0'^{\,n}}=\frac{r_0'^{\,2}-1}{r_0'^{\,2}-2r_0'\cos\phi+1} \tag{4.17}$$

yields finally

$$J_z(\phi,t)=-\frac{1}{2\pi a}\frac{r_0'^{\,2}-1}{r_0'^{\,2}-2r_0'\cos\phi+1}$$

$$+\frac{1}{2\pi a}\sum_{n=0}^{\infty}(-1)^n\varepsilon_n\cos n\phi\int_0^\infty\frac{I_n(zr_0')K_n(z)-I_n(z)K_n(zr_0')}{K_n^2(z)+\pi^2 I_n^2(z)}\frac{e^{-z\tau}}{z}dz$$

$$+\frac{2}{\pi a}\sum_{n=2}^{\infty}\cos n\phi\sum_{l=1}^{[n/2]}\mathrm{Re}\left[\frac{K_n(\zeta_{nl}r_0')}{K_{n-1}(\zeta_{nl})}\frac{e^{\zeta_{nl}\tau}}{\zeta_{nl}}\right] \tag{4.18}$$

which is valid for $\tau>(r_0'-1)$, that is for all time ranges after the initial incident wave-front reaches the cylinder, and for both the illuminated and shadow regions.

4.2 The Inverse Laplace Transforms of the Magnetic Fields

In this section, we start from the expressions of the magnetic fields and use the relations

$$J_z(\phi,s)=H_\phi^i(a,\phi,s)+H_\phi^s(a,\phi,s) \tag{4.19}$$

$$J_z(\phi, t) = H_\phi^i(a, \phi, t) + H_\phi^s(a, \phi, t) \tag{4.20}$$

to obtain $J_z(\phi, t)$, where H_ϕ^i and H_ϕ^s represent the incident and scattered magnetic fields on the cylinder surface, respectively. The Laplace transforms of incident and scattered magnetic fields expressed in terms of the modified Bessel functions can be derived, respectively, as

$$H_\phi^i(a, \phi, s) = -\frac{1}{2\pi c} \frac{r_0' \cos\phi - 1}{R_0'} K_1(\zeta R_0') \tag{4.21}$$

$$H_\phi^s(a, \phi, s) = \frac{1}{2\pi c} \sum_{n=0}^{\infty} \varepsilon_n \frac{I_n(\zeta)}{K_n(\zeta)} K_n'(\zeta) K_n(\zeta r_0') \cos n\phi \tag{4.22}$$

where $R_0' = (r_0'^{\,2} - 2r_0' \cos\phi + 1)^{1/2}$ and K_n' is the derivative of K_n with respect to the argument. The inverse Laplace transform of (4.21) gives [36]

$$H_\phi^i(a, \phi, t) = -\frac{1}{2\pi a} \frac{r_0' \cos\phi - 1}{R_0'^{\,2}} \frac{\tau}{(\tau^2 - R_0'^{\,2})^{1/2}} \quad \text{for } \tau > R_0' \ . \tag{4.23}$$

By following the same procedure as in Section 4.1, we obtain the time domain scattered magnetic field at the cylinder surface as

$$H_\phi^s(a, \phi, t) = -\frac{1}{2\pi a} \sum_{n=0}^{\infty} \frac{\cos n\phi}{r_0'^{\,n}} - \frac{1}{2\pi a} \sum_{n=0}^{\infty} (-1)^n \varepsilon_n \cos n\phi \, B_n^s(\tau)$$

$$+ \frac{1}{2\pi a} \sum_{n=0}^{\infty} 4\cos n\phi \sum_{l=1}^{[n/2]} \mathrm{Re}[e^{\zeta_{nl}\tau} I_n(\zeta_{nl}) K_n(\zeta_{nl} r_0')] \quad \text{for } \tau > r_0' + 1 \tag{4.24}$$

where

$$B_n^s(\tau) = \int_0^{\infty} e^{-z\tau} I_n(z) \frac{K_n(zr_0')/z + I_n(zr_0')[K_n(z)K_n'(z) + \pi^2 I_n(z) I'_n(z)]}{K_n^2(z) + \pi^2 I_n^2(z)} dz \ . \tag{4.25}$$

Using (4.20), (4.23) and (4.24), we finally obtain $J_z(\phi, t)$ as

$$J_z(\phi,t)=-\frac{1}{2\pi a}\frac{r_0'\cos\phi-1}{R_0'^{\,2}}\frac{\tau}{(\tau^2-R_0'^{\,2})^{1/2}}$$

$$-\frac{1}{2\pi a}\sum_{n=0}^{\infty}\frac{\cos n\phi}{r_0'^{\,n}}-\frac{1}{2\pi a}\sum_{n=0}^{\infty}(-1)^n\varepsilon_n\cos n\phi\, B_n^s(\tau)$$

$$-\frac{1}{2\pi a}\sum_{n=2}^{\infty}4\cos n\phi\sum_{l=1}^{[n/2]}\mathrm{Re}[e^{\zeta_{nl}\tau}I_n(\zeta_{nl})K_n(\zeta_{nl}r_0')] \qquad (4.26)$$

which is valid for $\tau > r_0' + 1$, that is for the time range after the initial incident wavefront has completely passed the cylinder.

4.3 Discussion of the Two Approaches

We have obtained two different expressions of the current density by following two procedures in Section 4.1 and 4.2, respectively. The first expression is valid for $\tau > r_0' - 1$ and the second for $\tau > r_0' + 1$. It should be noted that $\tau > r_0' - 1$ corresponds to the time range after the initial incident wavefront has reached the cylinder and $\tau > r_0' + 1$ to the time range after the initial incident wavefront has completely passed the cylinder. The questions now are: (1) Are the two different expressions identical for $\tau > r_0' + 1$? (2) Why do they have different ranges of validity? In order to answer the first question, we expand the Laplace transform of the incident magnetic field as

$$H_\phi^i(a,\phi,s)=-\frac{1}{2\pi c}\sum_{n=0}^{\infty}\varepsilon_n I_n'(\zeta)K_n(\zeta r_0')\cos n\phi \qquad (4.27)$$

where I_n' is the derivative of I_n with respect to the argument. By choosing the same contours as in Fig. 4.1 and noting that except the branch point at the origin, $H_\phi^i(a,\phi,s)$ has no poles in the ζ-plane, we obtain the inverse Laplace transform of (4.27) as

$$H_\phi^i(a,\phi,t)=-\frac{1}{2\pi a}\sum_{n=1}^{\infty}\frac{\cos n\phi}{r_0'^{\,n}}+\frac{1}{2\pi a}\sum_{n=0}^{\infty}(-1)^n\varepsilon_n\cos n\phi\, B_n^i(\tau)\quad\text{for }\tau>r_0'+1 \tag{4.28}$$

where

$$B_n^i(\tau)=\int_0^{\infty}e^{-z\tau}\,I_n'(z)I_n(zr_0')\,dz\ . \tag{4.29}$$

Comparing (4.23) with (4.28), we obtain a mathematical identity

$$\frac{r_0'\cos\phi-1}{R_0'^{\,2}}\,\frac{\tau}{(\tau^2-R_0'^{\,2})^{1/2}}=-\frac{1}{2\pi a}\sum_{n=1}^{\infty}\frac{\cos n\phi}{r_0'^{\,n}}+\frac{1}{2\pi a}\sum_{n=0}^{\infty}(-1)^n\varepsilon_n\cos n\phi\, B_n^i(\tau) \tag{4.30}$$

which is valid for $\tau>r_0'+1$. Computed results from both sides of (4.30) for $r_0'=3$, $\phi=0^0$, 90^0 and 180^0 are given in Table II, showing the convergence of the series involved (for $n=15$). Using (4.24) and (4.28) in (4.20) we obtain another form for the current density expression

$$J_z(\phi,t)=-\frac{1}{2\pi a}\frac{r_0'^{\,2}-1}{r_0'^{\,2}-2r_0'\cos\phi+1}+\frac{1}{2\pi a}\sum_{n=0}^{\infty}(-1)^n\varepsilon_n\cos n\phi\,[B_n(\tau)-B_n^s(\tau)]$$

$$+\frac{1}{2\pi a}\sum_{n=2}^{\infty}4\cos n\phi\sum_{l=1}^{[n/2]}\mathrm{Re}[e^{\zeta_{nl}\tau}I_n(\zeta_{nl})K_n(\zeta_{nl}r_0')]\ . \tag{4.31}$$

By using the Wronskians for I_n and K_n, it can be shown that

$$B_n(\tau)=B_n^i(\tau)+B_n^s(\tau) \tag{4.32}$$

and

$$I_n(\zeta_{nl})K_n(\zeta_{nl}r_0')=\frac{1}{\zeta_{nl}}\,\frac{K_n(\zeta_{nl}r_0')}{K_{n-1}(\zeta_{nl})}\ . \tag{4.33}$$

As a result, (4.18) and (4.26) are identical for $\tau>r_0'+1$.

Table II

Computed results from the identity (4.30)

ϕ	$\tau-(r_0'+1)$	L.H.S. of (4.30)	R.H.S. of (4.30)
0^0	0.10	-0.5727687	-0.5727540
	0.50	-0.5581563	-0.5581558
	1.00	-0.5455447	-0.5455442
	2.00	-0.5303301	-0.5303296
	3.00	-0.5217492	-0.5217487
	4.00	-0.5163978	-0.5163973
	5.00	-0.5128226	-0.5128221
	6.00	-0.5103104	-0.5103099
	7.00	-0.5084752	-0.5084747
	8.00	-0.5070925	-0.5070921
	9.00	-0.5060243	-0.5060238
	10.00	-0.5051815	-0.5051810
90^0	0.10	0.1571124	0.1571044
	0.50	0.1405564	0.1405562
	1.00	0.1290995	0.1290992
	2.00	0.1176697	0.1176694
	3.00	0.1120897	0.1120895
	4.00	0.1088662	0.1088660
	5.00	0.1068104	0.1068101
	6.00	0.1054093	0.1054090
	7.00	0.1044074	0.1044071
	8.00	0.1036642	0.1036640
	9.00	0.1030967	0.1030965
	10.00	0.1026530	0.1026528
180^0	0.10	1.1388890	1.1228971
	0.50	0.5457052	0.5457041
	1.00	0.4166667	0.4166657
	2.00	0.3354102	0.3354092
	3.00	0.3046359	0.3046349
	4.00	0.2886751	0.2886741
	5.00	0.2790782	0.2790772
	6.00	0.2727723	0.2727714
	7.00	0.2683725	0.2683715
	8.00	0.2651651	0.2651640
	9.00	0.2627469	0.2627459
	10.00	0.2608746	0.2608736

The second question relates to the range of validity of the current density expressions. From the derivation, we have noticed that it is the integral along C_∞ that determines the condition for the expression to be valid. In both cases, we require that $\lim_{R_\infty \to \infty} \int_{C_\infty} = 0$. Since the first expression is valid for $\tau > r_0' - 1$ and the second for $\tau > r_0' + 1$, it can be concluded that for $r_0' - 1 < \tau < r_0' + 1$, the integral along C_∞ for $H_\phi^i(a, \phi, s)$ and that for $H_\phi^s(a, \phi, s)$ cancel each other.

4.4 A Limiting Case

Let us consider the limiting case of (4.18) as $t \to \infty$ ($\tau \to \infty$). From (4.18), since $\lim_{\tau \to \infty} B_n(\tau) = 0$ and the residue contribution also vanishes when $\tau \to \infty$, we have

$$\lim_{t \to \infty} J_z(\phi, t) = -\frac{1}{2\pi a} \frac{r_0'^2 - 1}{r_0'^2 - 2r_0' \cos\phi + 1} \quad . \tag{4.34}$$

On the other hand, we consider the problem as the line current being a steady state current. By solving this steady state problem we obtain the same expression of the induced current as (4.34), which is expected.

Another check can be done by using one of the properties of the Laplace transform [9]

$$\lim_{t \to \infty} f(t) = \lim_{s \to 0} sF(s) \tag{4.35}$$

where $f(t)$ and $F(s)$ are a Laplace transform pair. Applying (4.35) to (4.1), we obtain

$$\lim_{t \to \infty} J_z(\phi, t) = -\frac{1}{2\pi a} \sum_{n=0}^{\infty} \varepsilon_n \frac{\cos n\phi}{r_0'^n} = -\frac{1}{2\pi a} \frac{r_0'^2 - 1}{r_0'^2 - 2r_0' \cos\phi + 1} \tag{4.36}$$

which is also expected.

4.5 Numerical Results and Discussion

Expression (4.18) is analytically valid for all the time ranges, and the branch cut and the residue series converge rapidly everywhere except for $\tau < r_0'$. This time range corresponds to the early time in the illuminated region, for which the results were obtained in Chapter 3, and to the initial part of the intermediate time in the same region. For the remaining part of the intermediate time and for the late time in the illuminated region, as well as for all the time ranges in the shadow region, only the first few terms in the series in (4.18) are needed to obtain accurate numerical results.

Computed results for the normalized surface current density at different angles, for r_0=3a and r_0=6a, are plotted in Figs. 4.3 and 4.4, respectively, versus the normalized time $\tau_c = \tau - (r_0' - 1)$, which is counted from the arrival of the initial incident wavefront at the cylinder surface, at $\phi = 0$. For the numerical calculation of the integral term $B_n(\tau)$, we separate the integral as

$$B_n(\tau) = \int_0^{\delta'} + \int_{\delta'}^{Z} + \int_{Z}^{\infty} . \tag{4.37}$$

where δ' is a small positive number. By using large argument approximations of I_n and K_n, we can estimate the truncation error $\int_Z^\infty$ and hence we are able to choose an appropriate upper limit Z. It is found that the significant contributions of the integrands occur for $z < 10$. For example, when $Z = 10$ the truncation error is of the order of 10^{-11}. The numerical results shown in Figs. 4.3 and 4.4 are calculated by using $Z = 10$. Comparison

with results by using $Z=5$ and 30 shows that the maximum difference from the results is 0.1% when using $Z=5$ and 0.001% when using $Z=30$. The integral $\int_0^{\delta'}$ can be evaluated by using small argument approximations of I_n and K_n. Since for $n\neq 0$ the value of integrand is 0 at $z=0$, the contribution from $\int_0^{\delta'}$ can be neglected when δ' is sufficiently small. However, for $n=0$ the contribution from $\int_0^{\delta'}$ is significant even for extremely small δ' since in this case the integrand is infinite at $z=0$. Denoting

$$\Delta \equiv \int_0^{\delta'} \frac{I_0(zr_0')K_0(z)-I_0(z)K_0(zr_0')}{K_0^2(z)+\pi^2 I_0^2(z)} \frac{e^{-z\tau}}{z} dz \tag{4.38}$$

we have, for z small,

$$\Delta \approx \int_0^{\delta'} \frac{\ln r_0'}{\ln^2 z+\pi^2} \frac{e^{-z\tau}}{z} dz \ . \tag{4.39}$$

Making the change of variable $y=-\ln z$, we obtain

$$\Delta \approx \ln r_0' \int_{-\ln\delta'}^{\infty} \frac{e^{-\tau e^{-y}}}{y^2+\pi^2} dy \ . \tag{4.40}$$

For δ' very small, $-\ln\delta'$ is a large positive number and the exponential part in (4.39) is very close to 1. Therefore, (4.39) can be approximately integrated as

$$\Delta \approx \frac{\ln r_0'}{\pi}\left[\frac{\pi}{2}-\tan^{-1}(-\ln\delta')\right] \ . \tag{4.41}$$

The series of the integral terms is found to converge rapidly and 6 terms are sufficient in the calculations. Comparison with results by using 11 and 16 terms shows that they are

the same in the first three decimal places.

For the calculation of the residue contributions in (4.18), n is taken from 2 up to 10. Comparison with the results for n from 2 to 20 and 30 shows that they are the same in their first three decimal places. The zeros of $K_n(\zeta)$ have been evaluated by using very efficient and accurate techniques [37]. From Fig. 4.2 we can see that the zeros in the first layer (l=1) have smaller magnitude of the real part. Due to the exponential factor in (4.15), the zeros in this first layer will give the biggest contribution for large τ.

It can be seen from Figs. 4.3 and 4.4 that the currents in the illuminated region first decrease and then slowly increase, while in the shadow region the currents start from 0 by increasing rapidly in the beginning, with a slower and slower increase at later times. The starting times of the currents in the shadow region are different for different angles, which corresponds to the time needed for the incident wave to travel from the line current to the point under consideration on the cylinder surface. For example, when $\phi = 180^0$ in the case of $r_0 = 3a$, the starting time is $\tau_c = 2.74$. It is interesting to note from Figs. 4.3 and 4.4 that in the illuminated region the magnitude of the current density for $r_0 = 6a$ is smaller than that for $r_0 = 3a$ at the same location. This is due to the space attenuation of the cylindrical wave which is larger for $r_0 = 6a$ than for $r_0 = 3a$. On the contrary, in the shadow region, not very close to the shadow boundary, the magnitude of the current density for $r_0 = 3a$ is smaller than that for $r_0 = 6a$, which is due to the resultant effect of the space attenuation of the incident cylindrical wave and the creeping wave attenuation, the latter being larger for $r_0 = 3a$ than for $r_0 = 6a$.

Since the current response expression obtained in this chapter is valid for all the time ranges in the shadow region, we present in Fig. 4.5 a comparison of the results with

the early-time results obtained in Chapter 2 by using the Watson transformation. It can be seen that the results are in good agreement. The time parameter in Fig. 4.5 is the normalized local time τ_l, which is τ_1 defined in Chapter 2 and is counted from the moment the initial wave excitation reaches the point considered on the cylinder surface.

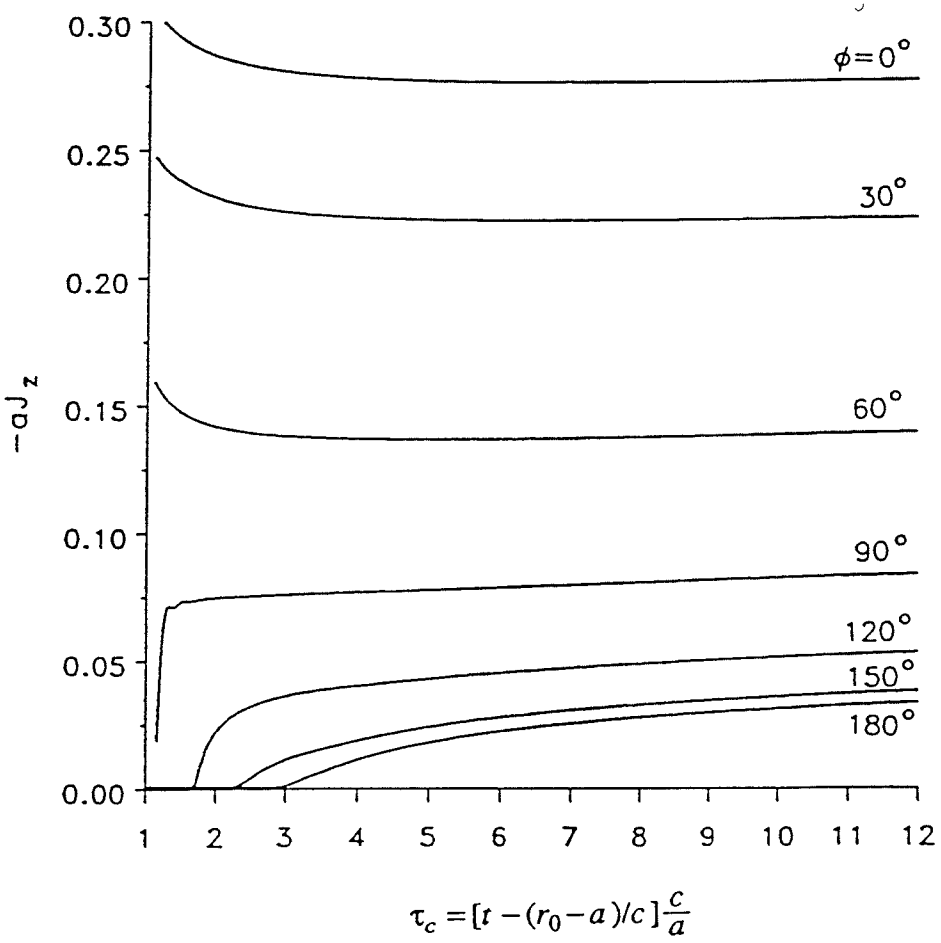

Fig. 4.3. Current distribution for $r_0/a=3$.

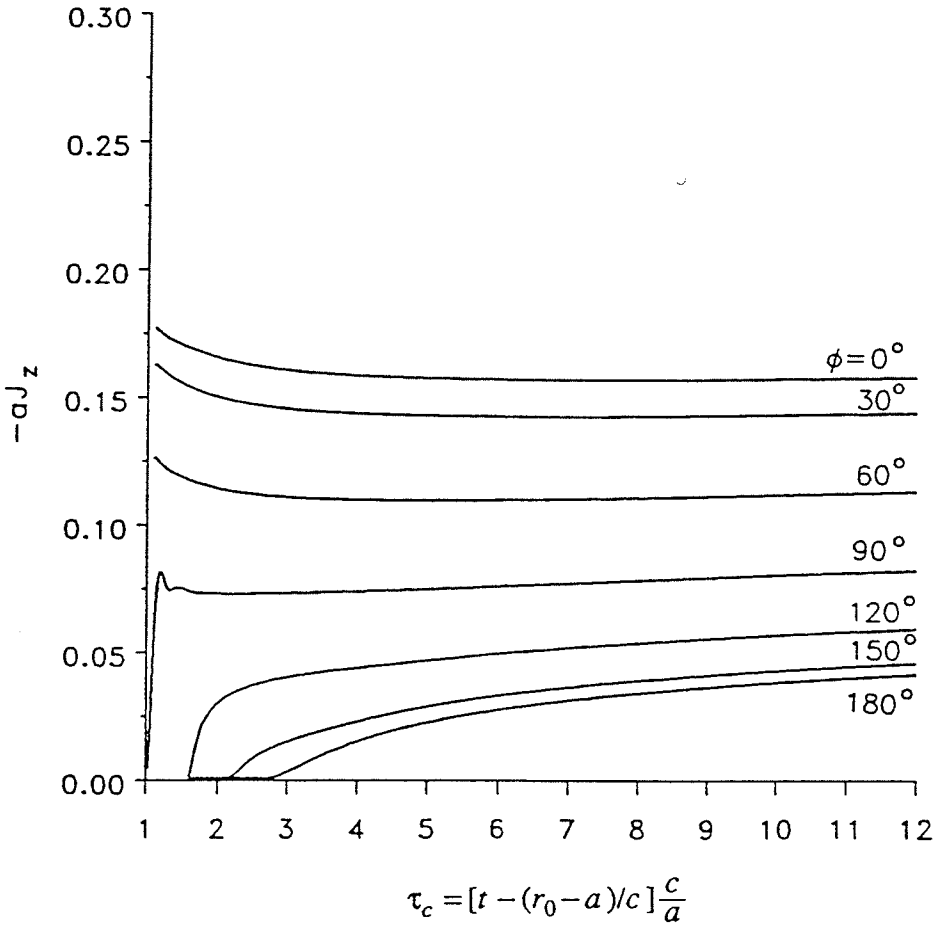

Fig. 4.4. Current distribution for $r_0/a=6$.

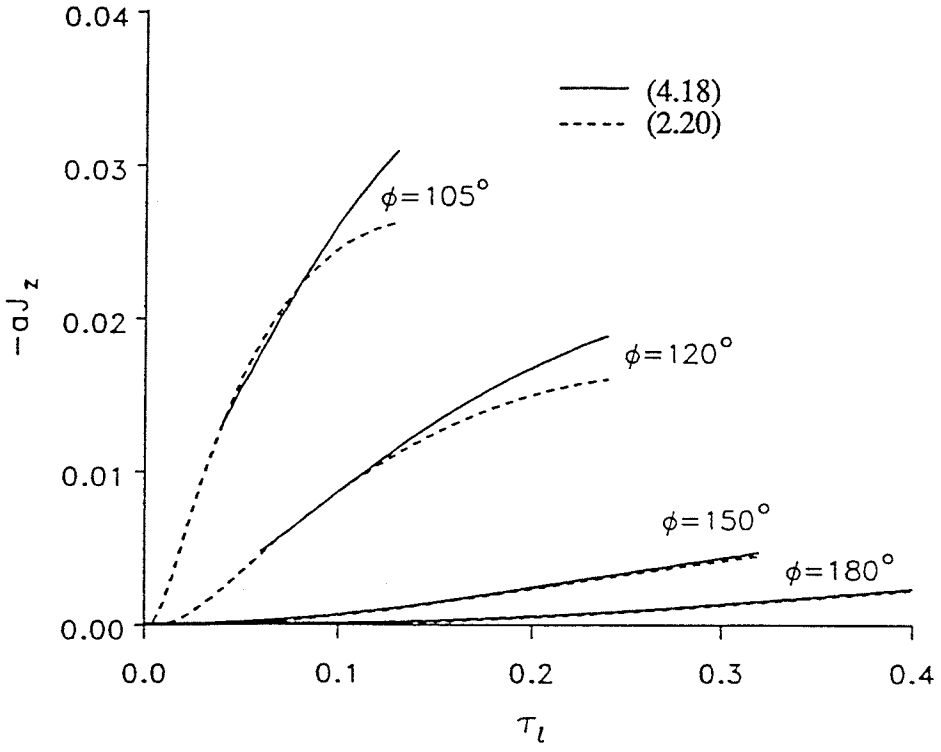

Fig. 4.5. Comparison of early-time results for $r_0/a=3$.

4.6 Special Case: Current Response to an Impulsive Plane Wave

We will apply now the procedure presented in this chapter to derive an analytical expression for the transient current induced on a perfectly conducting circular cylinder illuminated by an impulsive plane wave. This new expression has a larger range of validity than previous results [7,14]. The geometry of the problem is shown in Fig. 2.2. The incident electric field is given by (2.41). The Laplace transform of the induced current density on the cylinder surface can be derived as [30]

$$J_z(\phi, s) = e^{-\zeta} \sum_{n=0}^{\infty} \varepsilon_n \cos n\phi \, \frac{1}{\zeta K_n(\zeta)} \tag{4.42}$$

where again $\zeta = sa/c$. Taking the inverse Laplace transform of (4.42), we have

$$J_z(\phi, t) = \frac{c}{a} \sum_{n=0}^{\infty} \varepsilon_n \cos n\phi \, h_n(\tau) \tag{4.43}$$

where $\tau = ct/a$ and

$$h_n(\tau) = \frac{1}{2\pi j} \int_{\zeta_0 - j\infty}^{\zeta_0 + j\infty} H_n(\zeta, \tau) \, d\zeta \tag{4.44}$$

in which

$$H_n(\zeta, \tau) = \frac{e^{\zeta(\tau - 1)}}{\zeta K_n(\zeta)} \ . \tag{4.45}$$

In order to evaluate (4.45), the contour shown in Fig. 4.1 is again used. Hence

$$h_n(\tau) = -\frac{1}{2\pi j} \left[\int_{C_\infty} + \int_{C_\varepsilon} + \int_{L_1} + \int_{L_2} \right] H_n(\zeta, \tau) d\zeta + \sum_l R_{nl} \tag{4.46}$$

where R_{nl} is the residue of $H_n(\zeta, \tau)$ at the pole ζ_{nl} at which $K_n(\zeta) = 0$. It can be shown that (Appendix I)

$$\lim_{\varepsilon \to 0} \int_{C_\varepsilon} H_n(\zeta, \tau) \, d\zeta = 0 \tag{4.47}$$

and when $\tau > 0$

$$\lim_{R_\infty \to \infty} \int_{C_\infty} H_n(\zeta,\tau)\, d\zeta = 0 \ . \tag{4.48}$$

Using appropriate analytic continuation of the modified Bessel functions, the contributions from the line integrals along the branch cut can be evaluated as (Appendix I)

$$\int_{L_1} H_n(\zeta,\tau)\, d\zeta + \int_{L_2} H_n(\zeta,\tau)\, d\zeta = -2\pi j\, B_n(\tau) \tag{4.49}$$

where

$$B_n(\tau) = \int_0^\infty \frac{I_n(y)\, e^{-y(\tau-1)}}{y[K_n^2(y) + \pi^2 I_n^2(y)]}\, dy \tag{4.50}$$

For the residue terms, since the zeros of $K_n(\zeta)$ appear in conjugate pairs, $\sum_l R_{nl}$ can be obtained as

$$\sum_l R_{nl} = -2 \sum_{l=1}^{[n/2]} \mathrm{Re}\left[\frac{e^{\zeta_{nl}(\tau-1)}}{\zeta_{nl} K_{n+1}(\zeta_{nl})}\right] \tag{4.51}$$

where $[n/2]$ represents the integer part of $n/2$. From (4.43) – (4.51), we finally obtain

$$J_z(\phi, t) = \frac{c}{a} \sum_{n=0}^{\infty} \varepsilon_n \cos n\phi\, [B_n(\tau) + \sum_l R_{nl}] \quad \text{for } \tau > 0 \tag{4.52}$$

with $B_n(\tau)$ and $\sum_l R_{nl}$ given by (4.50) and (4.51), respectively.

Numerical results of the induced current density are presented in Figs. 4.6-4.9 where $ct'/d = (\tau - 1)/2$ in which $d = 2a$. The results are compared with those in [14] and $c/a = 20\pi$ was chosen in using (4.52) in order to make the comparison. It should be noted that the results in [14] are calculated by using three different formulas corresponding to: the early-time approximation, the late-time approximation and the approximation for

intermediate times by using interpolation between early- and late-time solutions. It can be seen from the Figs. that the results from the single expression (4.52) cover all the time ranges in the shadow region. They also cover the late time range in the illuminated region and part of the early and intermediate time ranges for large angles in this region. This shows that expression (4.52) has a larger range of validity than the late-time approximation given in [7,14].

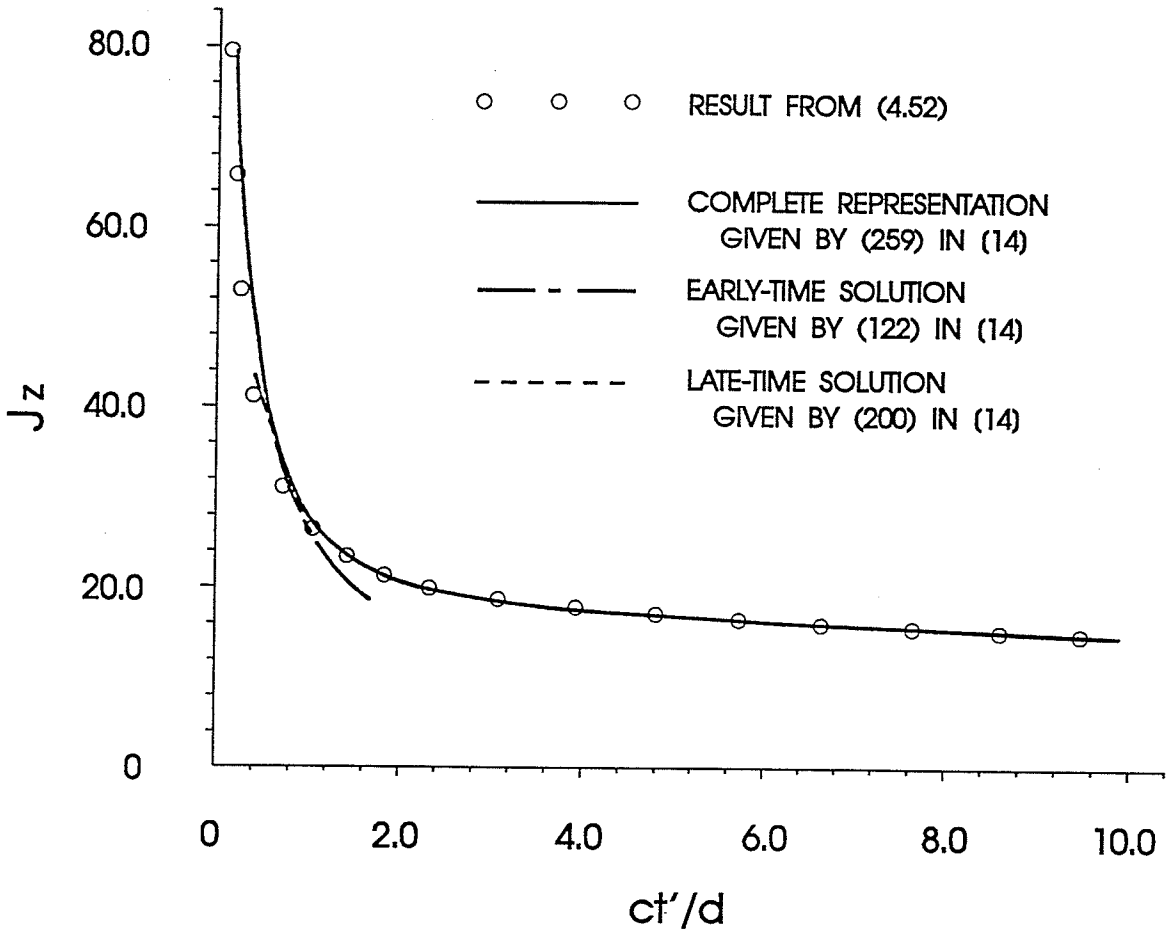

Fig. 4.6. Current distribution for plane wave incidence: $\phi = 90^0$.

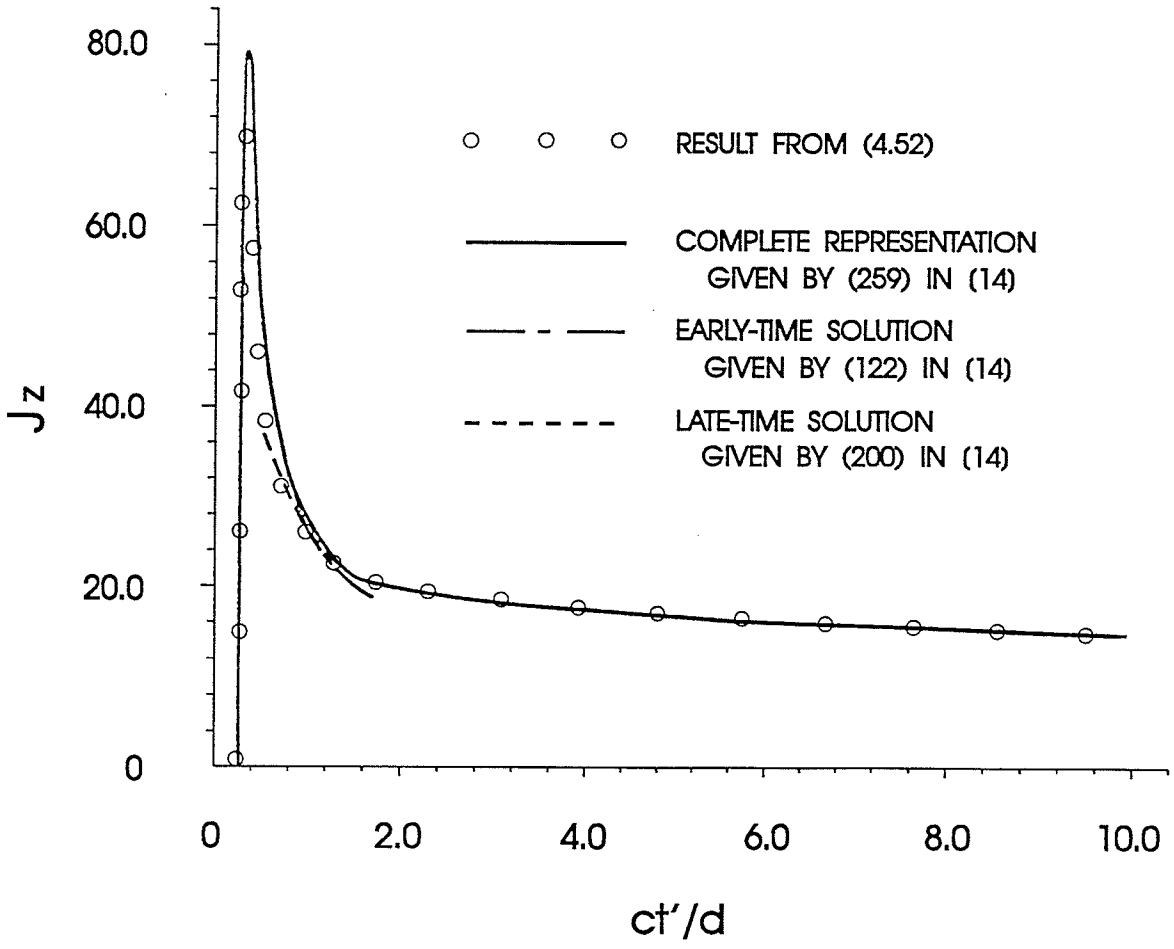

Fig. 4.7. Current distribution for plane wave incidence: $\phi = 120^0$.

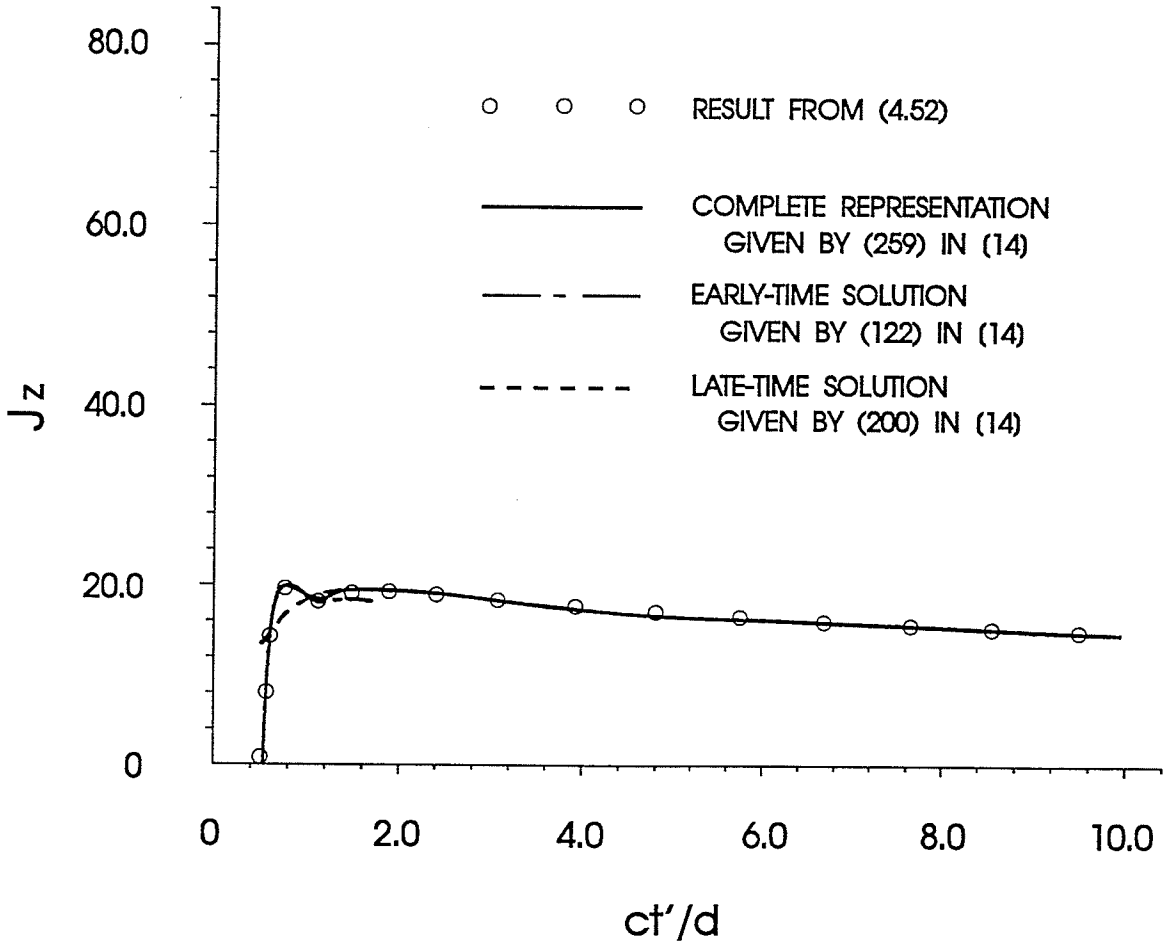

Fig. 4.8. Current distribution for plane wave incidence: $\phi = 150^0$.

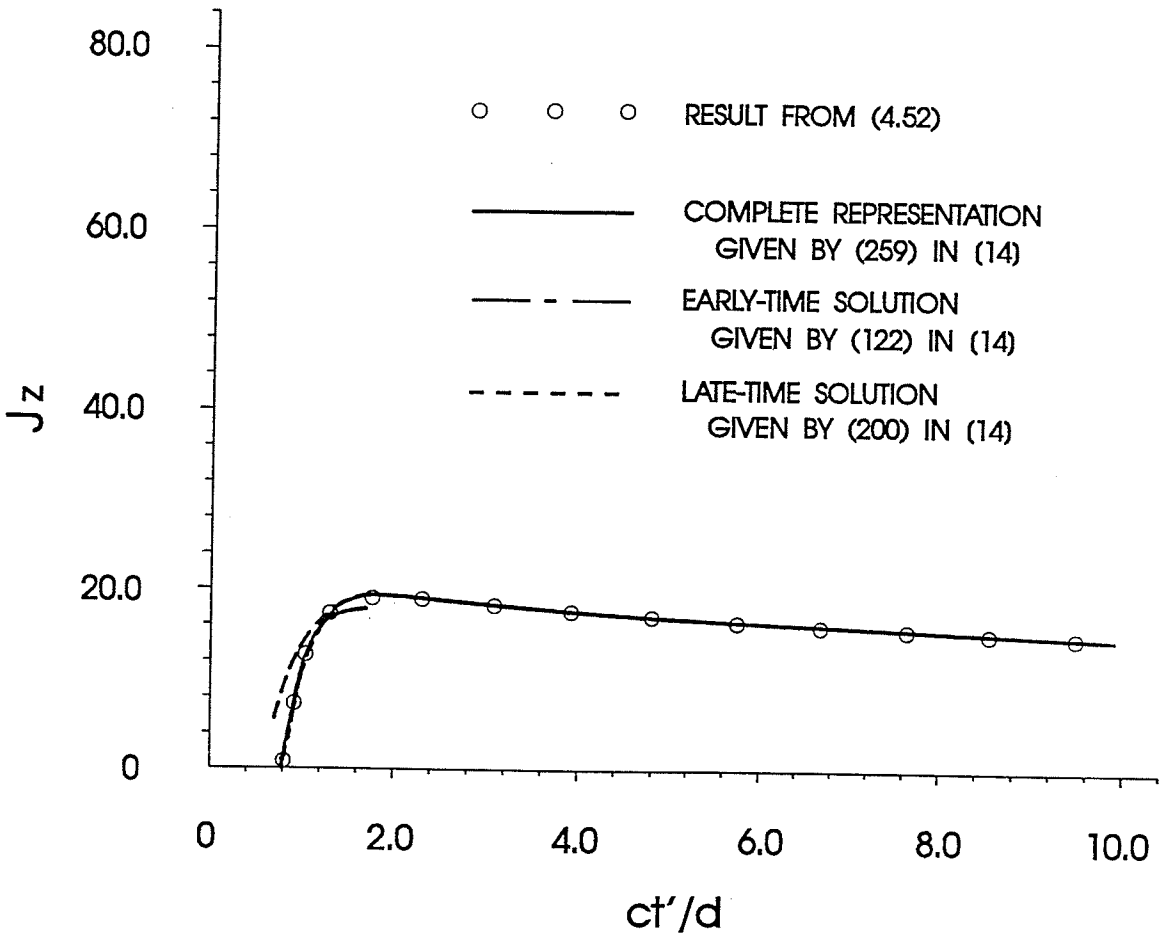

Fig. 4.9. Current distribution for plane wave incidence: $\phi = 180^0$.

CHAPTER 5

TRANSIENT RESPONSE TO A PLANE ELECTROMAGNETIC PULSE

The analytical procedure presented in Chapter 4 is applied in this chapter to treat the problem of the transient current response of a perfectly conducting circular cylinder to a plane electromagnetic pulse of a double exponential type.

5.1 Formulation and Analysis

Consider an infinitely long, perfectly conducting circular cylinder illuminated by a TM polarized plane electromagnetic pulse (see Fig. 5.1). The incident electric field is of a double exponential type given by

$$E_z^i(r,\phi,t)=\eta_0\,[e^{-\gamma_1(t+\frac{x}{c}-\frac{a}{c})}-e^{-\gamma_2(t+\frac{x}{c}-\frac{a}{c})}]\,u(t+\frac{x}{c}-\frac{a}{c}) \tag{5.1}$$

where γ_1 and γ_2 are the decay constants of the double exponential pulse with $\gamma_2>\gamma_1>0$. Note that at time $t=0$ the incident plane wavefront is tangent to the cylinder at $r=a$, $\phi=0$. The Laplace transform of the induced current density on the cylinder surface can be derived as

$$J_z(\phi,s)=\frac{a}{c}\sum_{n=0}^{\infty}\varepsilon_n\cos n\phi\,(\frac{1}{\zeta+\gamma_1'}-\frac{1}{\zeta+\gamma_2'})\,\frac{e^{-\zeta}}{\zeta K_n(\zeta)} \tag{5.2}$$

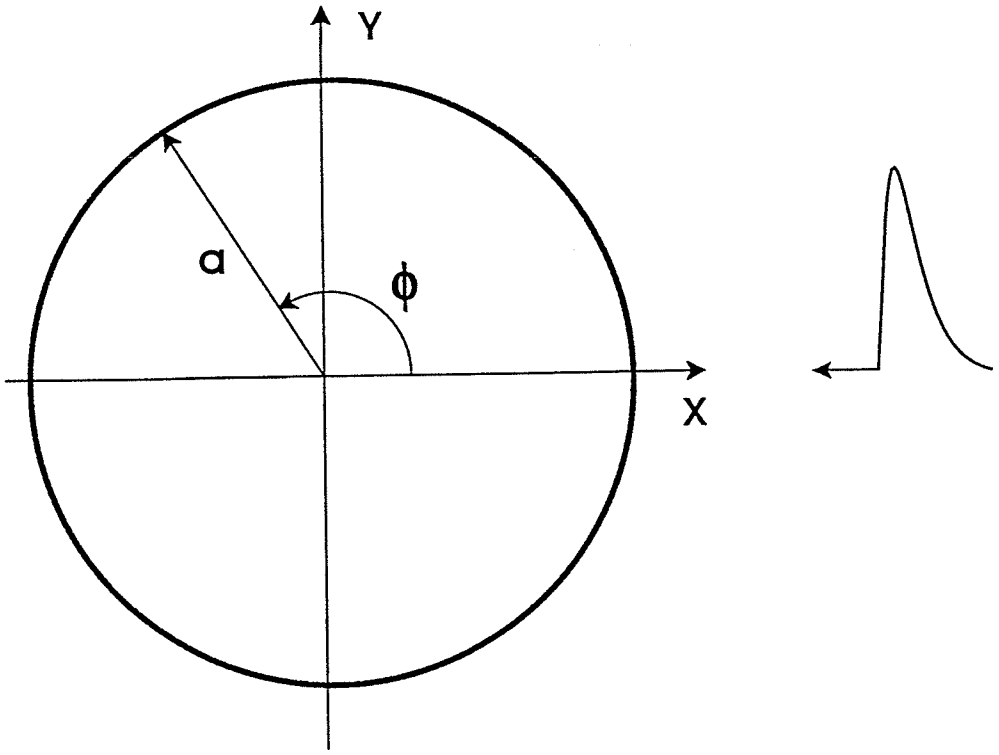

Fig. 5.1. Cross section of the circular cylinder illuminated by an electromagnetic pulse.

where ζ, γ_1' and γ_2' are normalized quantities defined by

$$\zeta = sa/c\ , \quad \gamma_1' = \gamma_1 a/c\ , \quad \gamma_2' = \gamma_2 a/c\ . \tag{5.3}$$

The inverse Laplace transform of (5.2) can be written in a form

$$J_z(\phi, t) = \sum_{n=0}^{\infty} \varepsilon_n h_n(\tau) \cos n\phi \tag{5.4}$$

where

$$h_n(\tau) = \frac{1}{2\pi j} \int_{\zeta_0 - j\infty}^{\zeta_0 + j\infty} H_n(\zeta, \tau)\, d\zeta \tag{5.5}$$

in which

$$H_n(\zeta, \tau) = \left(\frac{1}{\zeta + \gamma_1'} - \frac{1}{\zeta + \gamma_2'}\right) \frac{e^{\zeta(\tau - 1)}}{\zeta K_n(\zeta)} \tag{5.6}$$

and τ is the normalized time defined as $\tau = ct/a$. Note that the normalized time τ is dimensionless and its unit is the time needed for the wave to travel a distance of the radius a.

In order to evaluate the integrals in (5.5), we choose the integration contours as shown in Fig. 5.2.

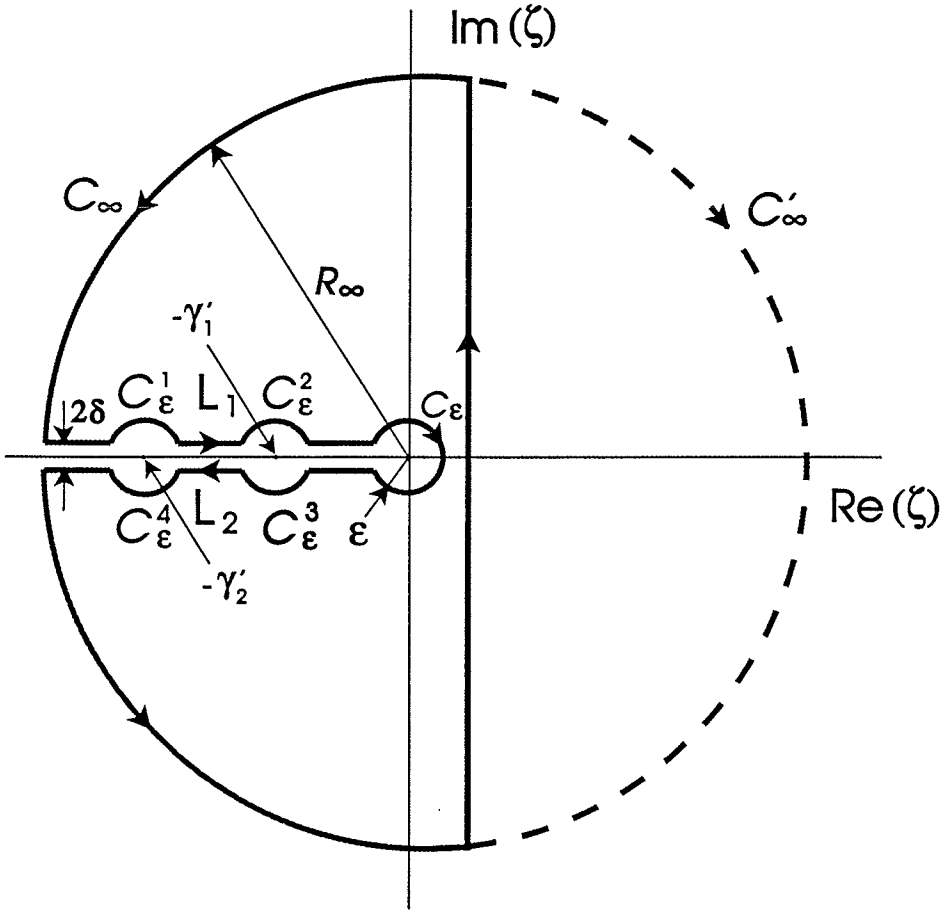

Fig. 5.2. Integration contours in the complex ζ-plane.

When the contour is closed in the right half plane along C'_∞, we have

$$h_n(\tau)=0 \quad \text{for} \quad \tau<0 \tag{5.7}$$

since $H_n(\zeta,\tau)$ has no poles in the right half plane and the integral along C'_∞ vanishes. This result is obvious taking into account the physical causality. When the contour is closed along $C_\infty+L_1+C_\varepsilon^1+C_\varepsilon^2+C_\varepsilon+C_\varepsilon^3+C_\varepsilon^4+L_2$ in the left half plane, $h_n(\tau)$ can be written as

$$h_n(\tau)=-\frac{1}{2\pi j}\left[\int_{C_\infty}+\int_{C_\varepsilon}+\int_{L_1}+\int_{L_2}+\int_{C_\varepsilon^1}+\int_{C_\varepsilon^2}+\int_{C_\varepsilon^3}+\int_{C_\varepsilon^4}\right]H_n(\zeta,\tau)d\zeta+\sum_l R_{nl} \tag{5.8}$$

where R_{nl} are the residues of $H_n(\zeta,\tau)$ at its simple poles ζ_{nl}, which are the zeros of K_n (see Fig. 4.2 and Appendix H). It can be shown that (Appendix J)

$$\lim_{\varepsilon\to 0}\int_{C_\varepsilon} H_n(\zeta,\tau)\,d\zeta=0 \tag{5.9}$$

and also that for $\tau>0$

$$\lim_{R_\infty\to\infty}\int_{C_\infty} H_n(\zeta,\tau)\,d\zeta=0\ . \tag{5.10}$$

Exploiting appropriately the analytic continuation of Bessel functions, the contributions from the integrals along the branch cut can be evaluated as (Appendix J)

$$\left[\int_{L_1}+\int_{L_2}\right]H_n(\zeta,\tau)\,d\zeta=-2\pi j\,B_n(\tau) \tag{5.11}$$

where

$$B_n(\tau)=\int_0^\infty\left(\frac{1}{\gamma'_1-z}-\frac{1}{\gamma'_2-z}\right)\frac{I_n(z)e^{-z(\tau-1)}}{z[K_n^2(z)+\pi^2 I_n^2(z)]}\,dz \tag{5.12}$$

and I_n is the modified Bessel function of the first kind and order n. The contributions

from the integrals along the infinitesimal semicircles C_ε^1, C_ε^2, C_ε^3 and C_ε^4 are (Appendix J)

$$\left[\int_{C_\varepsilon^1}+\int_{C_\varepsilon^4}\right] H_n(\zeta,\tau)\,d\zeta=-2\pi j\,F(\gamma_2',\tau)\,,\quad \left[\int_{C_\varepsilon^2}+\int_{C_\varepsilon^3}\right] H_n(\zeta,\tau)\,d\zeta=2\pi j\,F(\gamma_1',\tau) \tag{5.13}$$

in which

$$F(z,\tau)=(-1)^n\,\frac{K_n(z)e^{-z(\tau-1)}}{z[K_n^2(z)+\pi^2 I_n^2(z)]}\,. \tag{5.14}$$

The sum of the residues in (5.8) can be expressed as

$$\sum_l R_{nl}=-\sum_{l=1}^{V(n)}\left(\frac{1}{\zeta_{nl}+\gamma_1'}-\frac{1}{\zeta_{nl}+\gamma_2'}\right)\frac{e^{\zeta_{nl}(\tau-1)}}{\zeta_{nl}\,K_{n+1}(\zeta_{nl})} \tag{5.15}$$

where $V(n)$ is the number of zeros of $K_n(\zeta)$ and depends on n. Since the zeros ζ_{nl} of $K_n(\zeta)$ appear in conjugate pairs [29] and $V(n)$ is twice the integer part of $n/2$, (5.15) can be written in the form

$$\sum_l R_{nl}=-2\sum_{l=1}^{[n/2]}\mathrm{Re}\left[\left(\frac{1}{\zeta_{nl}+\gamma_1'}-\frac{1}{\zeta_{nl}+\gamma_2'}\right)\frac{e^{\zeta_{nl}(\tau-1)}}{\zeta_{nl}\,K_{n+1}(\zeta_{nl})}\right] \tag{5.16}$$

where $[n/2]$ represents the integer part of $n/2$ and the zeros ζ_{nl} are now either those in the second quadrant or in the third quadrant. With (5.9)-(5.16) in (5.8), we finally obtain the time domain induced surface current density as

$$\begin{aligned} J_z(\phi,t)=&-4\sum_{n=2}^{\infty}\cos n\phi\sum_{l=1}^{[n/2]}\mathrm{Re}\left[\left(\frac{1}{\zeta_{nl}+\gamma_1'}-\frac{1}{\zeta_{nl}+\gamma_2'}\right)\frac{e^{\zeta_{nl}(\tau-1)}}{\zeta_{nl}\,K_{n+1}(\zeta_{nl})}\right]\\ &+\sum_{n=0}^{\infty}\varepsilon_n\cos n\phi\left[\int_0^{\infty}\left(\frac{1}{\gamma_1'-z}-\frac{1}{\gamma_2'-z}\right)\frac{I_n(z)e^{-z(\tau-1)}}{z[K_n^2(z)+\pi^2 I_n^2(z)]}\,dz\right] \end{aligned} \tag{5.17}$$

$$-\sum_{n=0}^{\infty}(-1)^n\varepsilon_n\cos n\phi\left[\frac{K_n(\gamma_1')e^{-\gamma_1'(\tau-1)}}{\gamma_1'[K_n^2(\gamma_1')+\pi^2I_n^2(\gamma_1')]}-\frac{K_n(\gamma_2')e^{-\gamma_2'(\tau-1)}}{\gamma_2'[K_n^2(\gamma_2')+\pi^2I_n^2(\gamma_2')]}\right]$$

which is valid for $\tau>0$, that is for all time ranges after the initial incident wavefront reaches the cylinder, and for both the illuminated and shadow regions. The first summation in this expression represents the residue contribution, the second the branch cut contribution and the third the contributions due to the poles in s-plane introduced by the incident pulse.

5.2 Numerical Results and Discussion

Expression (5.17) is analytically valid for all the time ranges, with the series converging rapidly everywhere except for $\tau<1$. This time range corresponds to the early time in the illuminated region, for which the solution can be obtained by using methods described in Chapter 2 and 3 of this thesis. For larger τ, only the first few terms in the series in (5.17) are needed to obtain accurate numerical results.

Computed results for the surface current density at different angles, for $\gamma_1'=1$, $\gamma_2'=2$, and for $\gamma_1'=1$, $\gamma_2'=1.2$, are plotted in Figs. 5.3 and 5.4, respectively, versus the normalized time τ which is counted from the time when the initial incident wavefront reaches the cylinder surface, at $\phi=0$. It should be noted that the branch cut integral in (5.11) is not convergent in the general sense due to the appearance of the poles γ_1' and γ_2' in the integrand. However, it can be shown that this integral is convergent in the sense of the principal value. In fact this principal value of the integral is what is needed to obtain the inverse Laplace transform. For the numerical calculation of the principal value of the branch cut integral in (5.11), we separate the integral as

$$B_n(\tau)=\int_0^{\delta'}+\int_{\delta'}^{\gamma_1'-\varepsilon}+\int_{\gamma_1'+\varepsilon}^{\gamma_2'-\varepsilon}+\int_{\gamma_2'+\varepsilon}^{Z}+\int_{Z}^{\infty} \tag{5.18}$$

where δ' is a small positive number. By using large argument approximations of I_n and K_n, we can estimate the truncation error $\int_Z^\infty$ and hence we are able to choose an appropriate upper limit Z. It is found that the significant contributions of the integrands occur for $Z<10$. The numerical results shown in Figs. 5.3 and 5.4 are calculated by using $Z=25$. Comparison with results by using $Z=10$ and $Z=20$ shows that the maximum difference is 0.05%. The integral $\int_0^{\delta'}$ can be evaluated by using small argument approximations of I_n and K_n. Since for $n\neq 0$ the value of the integrand is 0 at $z=0$, the contribution from $\int_0^{\delta'}$ can be neglected when δ' is sufficiently small. However, for $n=0$ the contribution from $\int_0^{\delta'}$ is significant even for extremely small δ' since in this case the integrand is infinite at $z=0$. Letting Δ represent the integral $\int_0^{\delta'}$, we have, for z small,

$$\Delta\approx\int_0^{\delta'}\left(\frac{1}{\gamma_1'}-\frac{1}{\gamma_2'}\right)\frac{e^{-z(\tau-1)}}{z(\ln^2 z+\pi^2)}dz\ . \tag{5.19}$$

Making the change of variable $y=-\ln z$, we obtain

$$\Delta\approx\int_{-\ln\delta'}^{\infty}\left(\frac{1}{\gamma_1'}-\frac{1}{\gamma_2'}\right)\frac{e^{-(\tau-1)e^{-y}}}{y^2+\pi^2}dy\ . \tag{5.20}$$

This integral can be easily calculated numerically.

The value of ε in (5.18) is chosen to be 10^{-7} in the calculation. The value of the corresponding integral do not change practically when choosing a smaller value of ε.

For the evaluation of the integral series in (5.17), 21 terms have been used in the calculation. However, this is only necessary for τ close to 1. When τ is larger, say, $\tau > 1.5$, using 11 terms only gives a 0.5% difference. When $\tau > 2.5$, usage of 6 terms gives only a difference of 0.2%.

The series of the residue terms is found to converge rather rapidly and n from 2 up to 30 has been used in the calculation. This is again necessary only for accurate calculation when τ is close to 1. Comparison with results when using n from 2 up to 10 and up to 20 shows the maximum difference is less than 2%.

As shown in Figs. 5.3 and 5.4, the starting points of the currents in the shadow region are different for different angles, which correspond to the time needed for the incident wave to reach the point under consideration on the cylinder surface. For example, when $\phi = 180^0$, the starting time is $\tau = 2.57$. It should be noted that the difference between the magnitudes of the current density at different angles becomes smaller as τ increases. This means that after the incident wave has passed the cylinder and the creeping waves have traveled a few circumferences around the cylinder, the magnitude of the surface current density everywhere on the cylinder surface is almost the same. It slowly approaches zero as $\tau \to \infty$. It can also be seen from Figs. 5.3 and 5.4 that the magnitude of the current density for $\gamma_1' = 1, \gamma_2' = 2$ is larger than that for $\gamma_1' = 1, \gamma_2' = 1.2$ for a given ϕ and τ. This is due to the fact that the magnitude of the incident field is smaller in the latter case.

It should be noted that the surface current density given by (5.17), when considered as a function of the normalized quantities γ_1', γ_2', τ and the angular coordinate ϕ, is independent of the cylinder radius a. This implies that one can obtain J_z for any values of

a by simply converting γ_1, γ_2 and t to the normalized quantities γ_1', γ_2' and τ for a given value of a.

It should also be pointed out that the analytical expression given by (5.17) is theoretically valid for all time ranges and numerically useful for $\tau > 1$, instead of the conventional $\tau > 2$. Since for points at a finite distance in the plane of the complex variable s the series in (5.2) is uniformly convergent. As a consequence the series in expression (5.17) can be truncated appropriately to obtain numerical results. With such an expression the transient behavior can be determined for all the time ranges in the shadow region, for instance, without being necessary to derive separate expressions for the early times and for the late times, and to employ elaborate interpolation techniques to cover the intermediate times [7] The results obtained are also valid for the penumbral region [10].

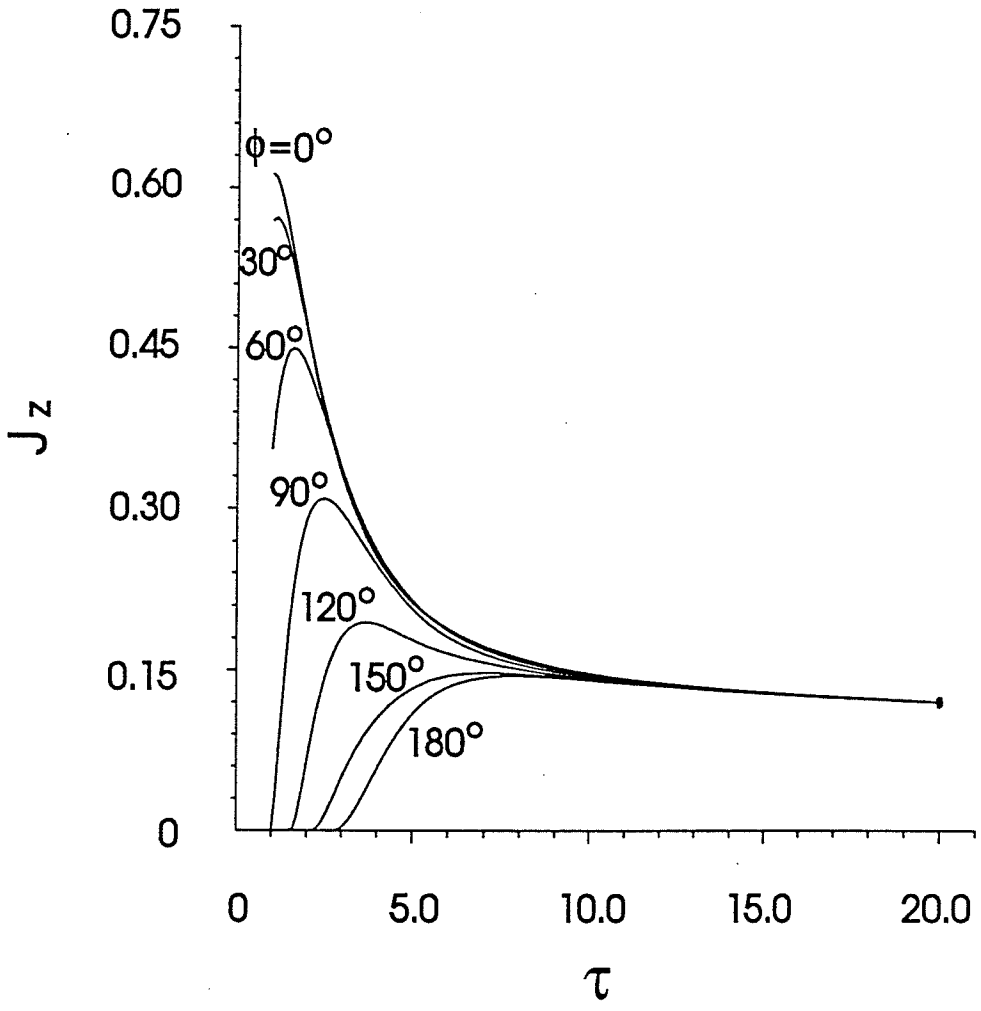

Fig. 5.3. Current density response for $\gamma_1' = 1, \gamma_2' = 2$.

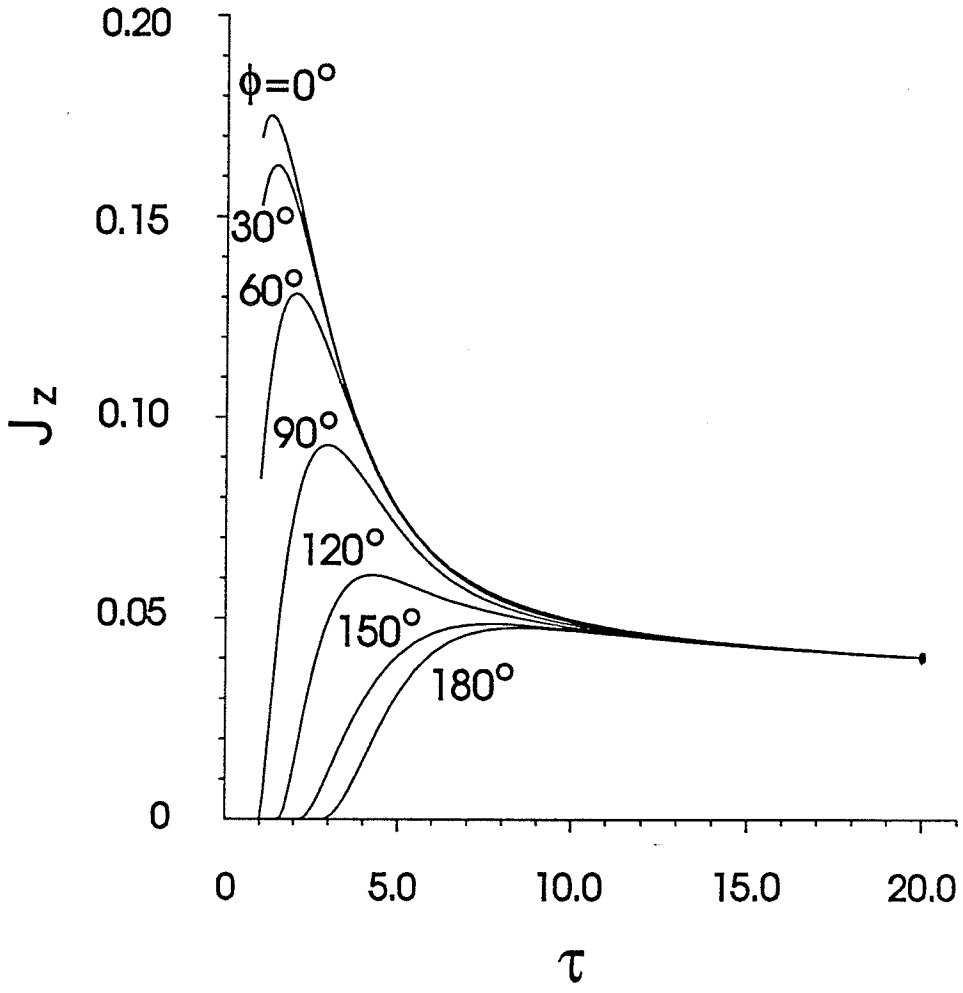

Fig. 5.4. Current density response for $\gamma_1' = 1, \gamma_2' = 1.2$.

CHAPTER 6

EARLY-TIME FIELD RESPONSE TO A CYLINDRICAL ELECTROMAGNETIC WAVE

In this Chapter, we derive the early-time field response of a conducting cylinder to a cylindrical electromagnetic wave by using the double Laplace transform approach as described in Chapter 2, Section 2.2.

6.1 The Frequency Domain Solution

We continue from Equation (2.26) of Section 2.2. The solution of this equation can be obtained as

$$A_{zm}(r, p, s)=\begin{cases} C_m K_{jp}(kr)+\dfrac{\mu_0}{kc}K_{jp}(kr_0)I_{jp}(kr) & r<r_0 \\ D_m K_{jp}(kr)+\dfrac{\mu_0}{kc}K_{jp}(kr)I_{jp}(kr_0) & r>r_0 \end{cases} \tag{6.1}$$

where I_{jp} is the modified Bessel function of the first kind and order jp, and C_m and D_m are constants to be determined by imposing the boundary condition $A_{zm}(a, p, s)=0$ and the continuity condition $\lim_{\varepsilon\to 0} A_{zm}(r_0-\varepsilon, p, s)=\lim_{\varepsilon\to 0} A_{zm}(r_0+\varepsilon, p, s)$. The transformed electric field can now be derived from (6.1) as

$$E_{zm}(r,p,s)=\begin{cases} \dfrac{\eta_0}{c}\dfrac{K_{jp}(kr_0)}{K_{jp}(ka)}[I_{jp}(ka)K_{jp}(kr)-I_{jp}(kr)K_{jp}(ka)] & r<r_0 \\ \dfrac{\eta_0}{c}\dfrac{K_{jp}(kr)}{K_{jp}(ka)}[I_{jp}(ka)K_{jp}(kr_0)-I_{jp}(kr_0)K_{jp}(ka)] & r>r_0 \end{cases} \tag{6.2}$$

6.2 The Time Domain Solution

The inverse of the two-sided Laplace transform in (6.2) is

$$\tilde{E}_{zm}(r,\phi_m,s)=\begin{cases}\dfrac{1}{2\pi j}\displaystyle\int_{\sigma-j\infty}^{\sigma+j\infty}\frac{\eta}{c}\frac{K_{jp}(kr_0)}{K_{jp}(ka)}[I_{jp}(ka)K_{jp}(kr)-I_{jp}(kr)K_{jp}(ka)]e^{p\phi_m}dp & r<r_0\\ \dfrac{1}{2\pi j}\displaystyle\int_{\sigma-j\infty}^{\sigma+j\infty}\frac{\eta}{c}\frac{K_{jp}(kr)}{K_{jp}(ka)}[I_{jp}(ka)K_{jp}(kr_0)-I_{jp}(kr_0)K_{jp}(ka)]e^{p\phi_m}dp & r>r_0\,.\end{cases} \tag{6.3}$$

As explained in section 2.2, we now use the following asymptotic expressions [26], [21]

$$K_{jp}(ka)\approx\frac{2^{1/2}\pi}{3(ka)^{1/3}}e^{-p\pi/2}f(x) \tag{6.4}$$

$$I_{jp}(ka)\approx-\frac{2^{1/2}}{3(ka)^{1/3}}e^{p\pi/2}[jf(x)+g(x)] \tag{6.5}$$

where $f(x)$ is given by (2.32) and

$$g(x)=3(2^{1/6})\,Bi(-2^{1/3}x)$$

$$x=[3ka(w\cosh w-\sinh w)]^{2/3}/2 \tag{6.6}$$

$$\cosh w=p/ka$$

in which Bi is the Airy function of the second kind corresponding to Equation (B.6) in Appendix B. The zeros of $K_{jp}(ka)$ corresponding to the zeros x_n of $f(x)$ are given in (2.32)

$$p_n\approx ka+x_n(ka)^{1/3} \tag{6.7}$$

Thus

$$\frac{\partial K_{jp}(ka)}{\partial p}\Big|_{p=p_n} \approx \frac{2^{1/2}\pi}{3(ka)^{2/3}} e^{-p_n\pi/2} f'(x_n) \ . \tag{6.8}$$

Since the zeros in (6.7) are in the right half-plane, the integrals in (6.3) are evaluated for $\phi_m < 0$, yielding for both $r < r_0$ and $r > r_0$

$$\tilde{E}_{zm}(r,\phi_m,s) = -\frac{\eta}{c}\sum_{n=1}^{\infty} e^{p_n\phi_m}[K_{jp}(kr_0)K_{jp}(kr)I_{jp}(ka)/\frac{\partial}{\partial p}K_{jp}(ka)]_{p=p_n} \ . \tag{6.9}$$

Using (6.5), (6.8) and the asymptotic approximation [29]

$$K_{jp}(z) \approx (\pi/2)^{1/2}(z^2-p^2)^{-1/4} e^{-(z^2-p^2)^{1/2}+p\cos^{-1}(p/z)-p\pi/2} \tag{6.10}$$

we obtain

$$\tilde{E}_{zm}(r,\phi_m,s) = \frac{\eta}{2c}\sum_{n=1}^{\infty}\frac{g(x_n)}{f'(x_n)}\frac{(ka)^{1/3}}{[(k^2r_0^2-p_n^{2)}(k^2r^2-p_n^2)]^{1/4}}$$

$$e^{-(k^2r_0^2-p_n^2)^{1/2}-(k^2r^2-p_n^2)^{1/2}+p_n[\cos^{-1}(p_n/kr_0)+\cos^{-1}(p_n/kr)+\phi_m]} \tag{6.11}$$

which can be written as

$$\tilde{E}_{zm}(r,\phi_m,s) = \sum_{n=1}^{\infty}\tilde{E}_{zm,n}(r,\ \phi_m,\ s) \ . \tag{6.12}$$

Since $\tilde{E}_{zm,n}$ decreases practically exponentially with p_n as n increases we may retain only the first term. Hence

$$\tilde{E}_{zm}(r,\phi_m,s) = -\frac{\eta}{2}\left(\frac{a}{c}\right)^{1/3}\frac{Bi(-\alpha_1)}{Ai'(-\alpha_1)}\frac{1}{[(k^2r_0^2-p_n^{2)}(k^2r^2-p_n^{2)}]^{+1/4}}s^{-2/3}e^{-t_{0m}s-\beta_m\left(\frac{sa}{2c}\right)^{1/3}} \tag{6.13}$$

where

$$\beta_m = \alpha_1 \theta_m$$

$$\theta_m = |\phi_m| - \cos^{-1}(p_n/kr_0) - \cos^{-1}(p_n/kr) \tag{6.14}$$

$$t_{0m} = [(r_0^2 - a^2)^{1/2} + (r^2 - a^2)^{1/2} + a\theta_m]/c \ .$$

To ensure that the summation in (6.11) is convergent for ϕ_m negative, we require that $|\phi_m| > \cos^{-1}(a/r_0) + \cos^{-1}(a/r_0)$, which shows that (6.13) is valid in the region of geometric shadow (Fig. 6.1).

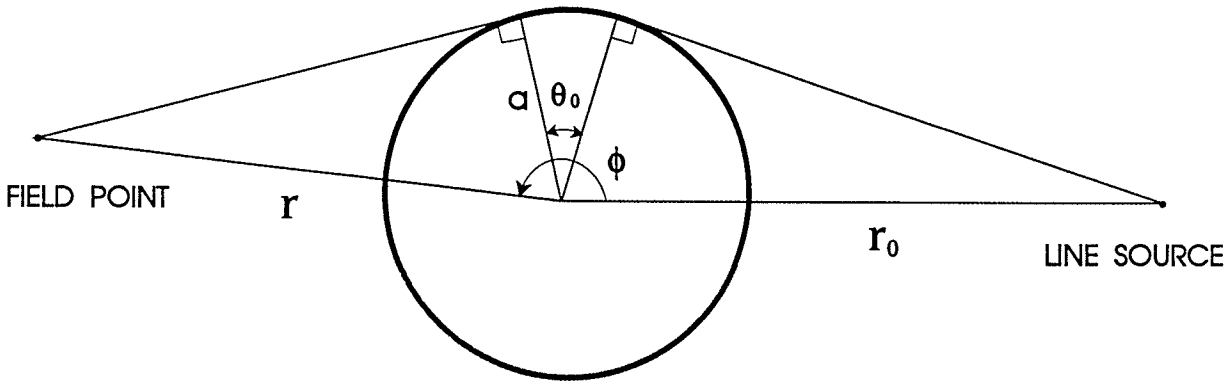

Fig. 6.1. Field point in the shadow region.

The total transformed electric field is given by

$$\tilde{E}_z(r, \phi, s) = \sum_{m=-\infty}^{\infty} \tilde{E}_{zm}(r, \phi_m, s) \tag{6.15}$$

For the early-time response we retain only two terms corresponding to the smallest

values of $|\phi_m|$ as

$$|\phi_m| = \begin{cases} |\phi| & \text{for } m=0 \\ 2\pi - |\phi| & \text{for } m=1 \end{cases} \tag{6.16}$$

Thus

$$\tilde{E}_{zm}(r,\phi_m,s) = -\frac{\eta}{2}\left(\frac{a}{c}\right)^{1/3} \frac{Bi(-\alpha_1)}{Ai'(-\alpha_1)} \frac{1}{[(k^2r_0^2-p_n^2)(k^2r^2-p_n^2)]^{+1/4}} s^{-2/3} \sum_{m=0}^{1} e^{-t_{0m}s-\beta_m\left(\frac{sa}{2c}\right)^{1/3}}. \tag{6.17}$$

From the integral [26]

$$\frac{1}{2\pi j}\int_{\sigma-j\infty}^{\sigma+j\infty} s^{-2/3} e^{sT-\gamma s^{1/3}}\, ds = 3^{2/3}T^{-1/3}Ai[(3T)^{-1/3}\gamma]u(T) \tag{6.18}$$

the inverse Laplace transform of (6.17) can be obtained in the form

$$E_z(r,\phi,t) = -\frac{\eta}{2}3^{2/3}\frac{Bi(-\alpha_1)}{Ai'(-\alpha_1)} \frac{1}{[(r_0^2-a^2)(r^2-a^2)]^{1/4}} \sum_{m=0}^{1} \tau_m^{-1/3} Ai[(6\tau_m)^{-1/3}\beta_m]\, u(\tau_m) \tag{6.19}$$

where $\tau_m = \frac{c}{a}(t-t_{0m})$.

For the illuminated region, the integrals in (6.3) can be evaluated using the saddle point method by employing the asymptotic expansions of both I and K. Since it yields only the same information as the physical optics solution we will not present the analysis. Interested reader may refer to [38].

6.3 Numerical Results and Discussion

Computed results for the early-time field response in the shadow region are shown in Figs. 6.2-6.5, where $E = aE_z$ and $\tau=\tau_0$ is the normalized local time, counted from the arrival of the wave front at the field point under consideration. Fig. 6.2 gives the (E, τ) curves for $r_0/a = 3$ and $r/a = 2$, when $\phi = 150^0$, 165^0 and 180^0. Fig. 6.3 gives the (E, τ) curves for $r_0/a = 3$ and $\phi = 180^0$, when $r/a = 2, 3$ and 4. Figs. 6.4 and 6.5 correspond to Figs. 6.2 and 6.3 for the case of $r_0/a = 6$. From these figures it is clear that the electric fields build up in an exponential manner. As the field point approaches the shadow boundary, the initial rise becomes very rapid. It can also be seen that the magnitude of the electric field in the case of $r_0/a = 3$, $r/a = 2$ and $\phi = 180^o$ is smaller than that in the case of $r_0/a = 6$, $r/a = 2$ and $\phi = 180^o$ for the same values of τ. This is due to the same reason as explained for case of current response.

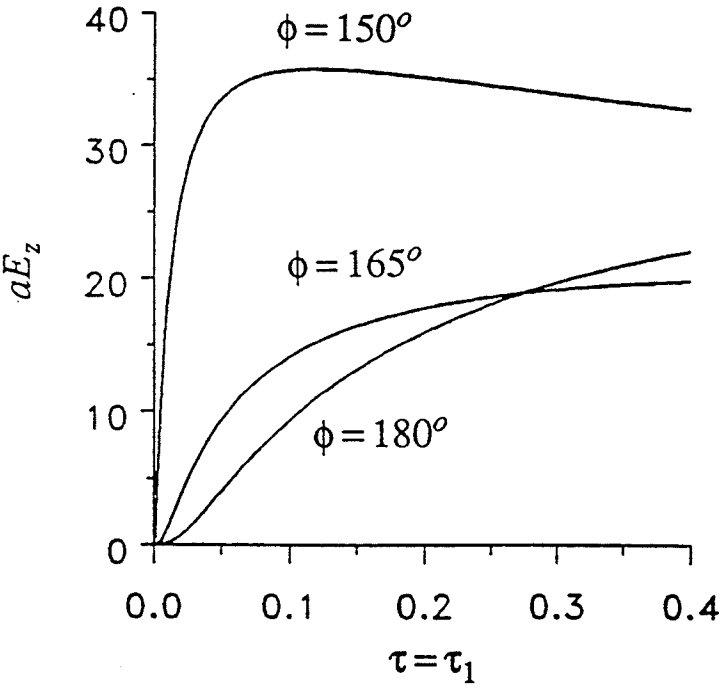

Fig. 6.2. Field response for $r_0 = 3a$ and $r = 2a$ at different ϕ.

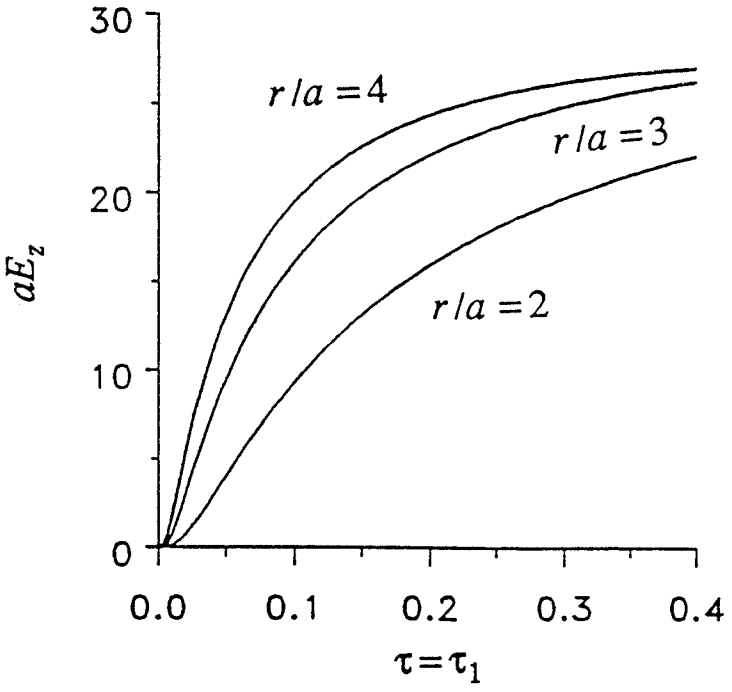

Fig. 6.3. Field response for $r_0=3a$ and $\phi=180^0$ at different r.

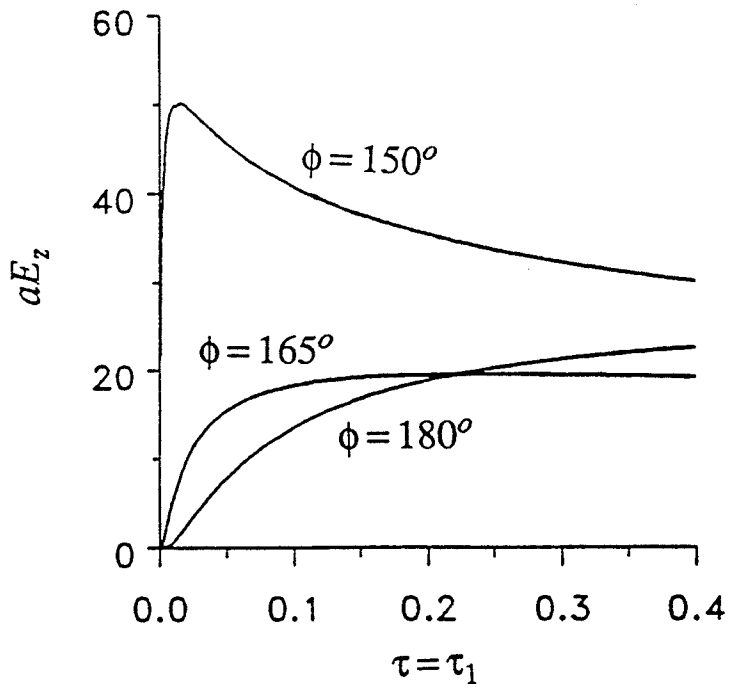

Fig. 6.4. Field response for $r_0 = 6a$ and $r = 2a$ at different ϕ.

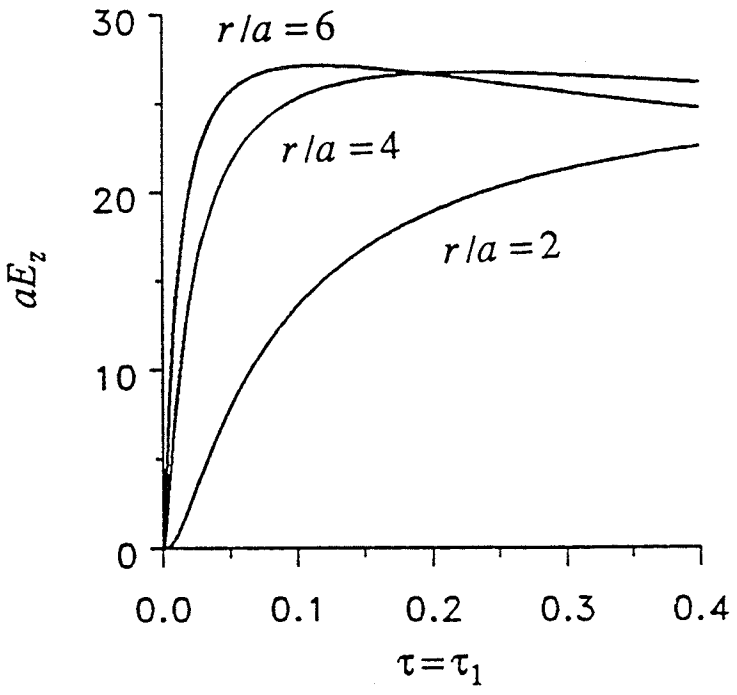

Fig. 6.5. Field response for $r_0=6a$ and $\phi=180^0$ at different r.

CHAPTER 7

FORMULATION OF THE TRANSIENT FIELD RESPONSE OF A DIELECTRIC CYLINDER

In this Chapter we derive analytical expressions of the transient field response of a dielectric circular cylinder to a cylindrical electromagnetic wave generated by a parallel filament carrying a unit-step current. The mathematical technique employed here is similar to that in Chapter 4.

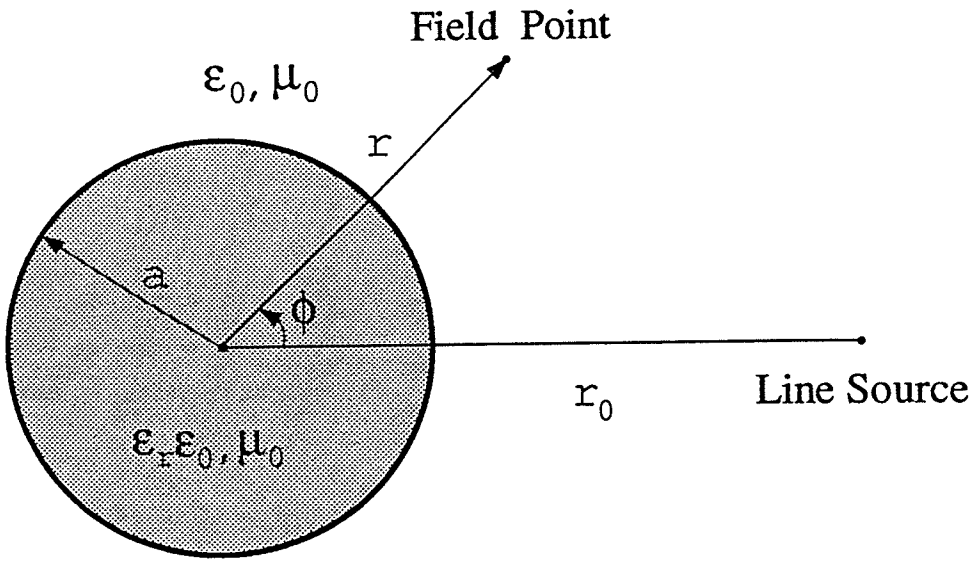

Fig. 7.1. Cross section of the dielectric cylinder to line source configuration.

7.1 The Frequency Domain Solution

The geometry is shown in Fig. 7.1 where a is the radius of the dielectric cylinder with permittivity $\varepsilon_r\varepsilon_0$, permeability $\mu=\mu_0$, and r_0 the distance from the line source to the cylinder axis. The surrounding medium is assumed to be free space with permittivity ε_0 and permeability μ_0. For a line source carrying a unit-step current, the Laplace transform of the electric field in the absence of the cylinder is

$$E_z^i(r,\phi,s)=-\frac{\mu_0}{2\pi}\begin{cases}\sum_{n=0}^{\infty}\varepsilon_n I_n(\frac{sr}{c})K_n(\frac{sr_0}{c})\cos n\phi & r<r_0\\ \sum_{n=0}^{\infty}\varepsilon_n I_n(\frac{sr_0}{c})K_n(\frac{sr}{c})\cos n\phi & r>r_0\end{cases}. \tag{7.1}$$

The Laplace transform of the scattered electric field outside the cylinder can be assumed as

$$E_z^s(r,\phi,s)=-\frac{\mu_0}{2\pi}\sum_{n=0}^{\infty}\varepsilon_n a_n K_n(\frac{sr}{c})K_n(\frac{sr_0}{c})\cos n\phi \tag{7.2}$$

and the Laplace transform of the electric field inside the cylinder as

$$E_z(r,\phi,s)=-\frac{\mu_0}{2\pi}\sum_{n=0}^{\infty}\varepsilon_n b_n I_n(\frac{sr}{c}\lambda)\cos n\phi \tag{7.3}$$

where $\lambda=\sqrt{\varepsilon_r}$. The magnetic fields corresponding to E_z^i, E_z^s and E_z are

$$H_z^i(r,\phi,s)=-\frac{1}{2\pi c}\begin{cases}\sum_{n=0}^{\infty}\varepsilon_n I_n'(\frac{sr}{c})K_n(\frac{sr_0}{c})\cos n\phi & r<r_0\\ \sum_{n=0}^{\infty}\varepsilon_n I_n(\frac{sr_0}{c})K_n'(\frac{sr}{c})\cos n\phi & r>r_0\end{cases} \tag{7.4}$$

$$H_z^s(r,\phi,s) = -\frac{1}{2\pi c}\sum_{n=0}^{\infty}\varepsilon_n a_n K_n'(\frac{sr}{c})K_n(\frac{sr_0}{c})\cos n\phi \tag{7.5}$$

$$H_z(r,\phi,s) = -\frac{\lambda}{2\pi c}\sum_{n=0}^{\infty}\varepsilon_n b_n I_n'(\frac{sr}{c}\lambda)\cos n\phi\ . \tag{7.6}$$

Using the boundary condition at $r=a$, the constants a_n and b_n can be obtained as

$$a_n = \frac{I_n(\frac{sa}{c}\lambda)I_{n+1}(\frac{sa}{c}) - \lambda I_n(\frac{sa}{c})I_{n+1}(\frac{sa}{c}\lambda)}{I_n(\frac{sa}{c}\lambda)K_{n+1}(\frac{sa}{c}) + \lambda K_n(\frac{sa}{c})I_{n+1}(\frac{sa}{c}\lambda)} \tag{7.7}$$

$$b_n = \frac{1}{sa/c}\,\frac{K_n(\frac{sr_0}{c})}{I_n(\frac{sa}{c}\lambda)K_{n+1}(\frac{sa}{c}) + \lambda K_n(\frac{sa}{c})I_{n+1}(\frac{sa}{c}\lambda)}\ . \tag{7.8}$$

From (7.2), (7.3), (7.7) and (7.8), we obtain the frequency domain solution of the scattered electric field outside the cylinder and the total electric field inside the cylinder, respectively, as

$$E_z^s(r,\phi,s) = -\frac{\eta_0}{2\pi c}\sum_{n=0}^{\infty}\varepsilon_n\cos n\phi\,\frac{I_n(\zeta\lambda)I_{n+1}(\zeta) - \lambda I_n(\zeta)I_{n+1}(\zeta\lambda)}{I_n(\zeta\lambda)K_{n+1}(\zeta) + \lambda K_n(\zeta)I_{n+1}(\zeta\lambda)}K_n(\zeta r')K_n(\zeta r_0') \tag{7.9}$$

and

$$E_z(r,\phi,s) = -\frac{\eta_0}{2\pi as}\sum_{n=0}^{\infty}\varepsilon_n\cos n\phi\,\frac{I_n(\zeta r'\lambda)K_n(\zeta r_0')}{I_n(\zeta\lambda)K_{n+1}(\zeta) + \lambda K_n(\zeta)I_{n+1}(\zeta\lambda)} \tag{7.10}$$

where $r' = r/a$ and ζ, r_0' and η_0 has the same definitions as before.

7.2 The Time Domain Solution

The inverse Laplace transform of (7.10) can be written as

$$E_z(r,\phi,t)=-\frac{\eta_0}{2\pi a}\sum_{n=0}^{\infty}\varepsilon_n\cos n\phi\, h_n(\tau) \tag{7.11}$$

where $\tau=ct/a$ and

$$h_n(\tau)=\frac{1}{2\pi j}\int_{\zeta_0-j\infty}^{\zeta_0+j\infty}H_n(\zeta)\,e^{\zeta\tau}d\zeta \tag{7.12}$$

in which

$$H_n(\zeta)=\frac{1}{\zeta}\,\frac{I_n(\zeta r'\lambda)\,K_n(\zeta r_0')}{I_n(\zeta\lambda)K_{n+1}(\zeta)+\lambda K_n(\zeta)I_{n+1}(\zeta\lambda)}\ . \tag{7.13}$$

The appropriate Bromwich contour and associated integration contours in the complex ζ plane are shown in Fig. 4.1. When the contour is closed in the right half plane, we have

$$h_n(\tau)=0 \qquad \text{for} \quad \tau<(r_0'-1)+\lambda(1-r') \tag{7.14}$$

since it can be shown that $f_n(\zeta)=I_n(\zeta\lambda)K_{n+1}(\zeta)+\lambda K_n(\zeta)I_{n+1}(\zeta\lambda)$ has no zeros in the right half plane and the contour integral along C_∞' vanishes. When the contour is closed along $C_\infty+L_1+C_\varepsilon+L_2$ in the left half plane, $h_n(\tau)$ can be written as

$$h_n(\tau)=-\frac{1}{2\pi j}\left[\int_{C_\infty}+\int_{C_\varepsilon}+\int_{L_1}+\int_{L_2}\right]H_n(\zeta)\,e^{\zeta\tau}\,d\zeta+\sum_l R_{nl} \tag{7.15}$$

where R_{nl} is the residue of $H_n(\zeta)\,e^{\zeta\tau}$ at the pole ζ_{nl} at which $f_n(\zeta)=0$. It can be shown that

$$\lim_{\varepsilon\to 0}\int_{C_\varepsilon} H_n(\zeta)\,e^{\zeta\tau}d\zeta=0 \tag{7.16}$$

and, when $\tau>(r_0'-1)+\lambda(1-r')$,

$$\lim_{R_\infty\to\infty}\int_{C_\infty} H_n(\zeta)\,e^{\zeta\tau}d\zeta=0\ . \tag{7.17}$$

Using appropriate analytic continuation of the modified Bessel functions, the contributions from the line integrals along the branch cut can be evaluated as

$$\int_{L_1} H_n(\zeta)\,e^{\zeta\tau}d\zeta+\int_{L_2} H_n(\zeta)\,e^{\zeta\tau}d\zeta=(-1)^{n+1}2\pi j\,B_n(\tau) \tag{7.18}$$

where

$$B_n(\tau)=\int_0^\infty \frac{e^{-z\tau}}{z}\,\frac{I_n(zr'\lambda)\,[K_n(zr_0')B+I_n(zr_0')A]}{A^2+\pi^2B^2}\,dz \tag{7.19}$$

in which

$$A=I_n(z\lambda)\,K_{n+1}(z)+\lambda\,I_{n+1}(z\lambda)\,K_n(z) \tag{7.20}$$

$$B=I_n(z\lambda)\,I_{n+1}(z)-\lambda\,I_{n+1}(z\lambda)\,I_n(z)\ . \tag{7.21}$$

For the residue terms, since the zeros of $f_n(\zeta)$ appear in conjugate pairs, R_{nl} can be obtained as

$$R_{nl}=2\mathrm{Re}\left[\frac{e^{\zeta_{nl}\tau}}{\zeta_{nl}}\,\frac{I_n(\lambda r'\zeta_{nl})K_n(r_0'\zeta_{nl})}{\lambda^2 I_{n+2}(\lambda\zeta_{nl})K_n(\zeta_{nl})-I_n(\lambda\zeta_{nl})K_{n+2}(\zeta_{nl})}\right] \tag{7.22}$$

and the summation over l in (7.15) will be up to l =[number of zeros for each n]/2. From (7.11)–(7.18), we finally obtain

$$E_z(r,\phi,t) = -\frac{\eta_0}{2\pi a}\sum_{n=0}^{\infty}\varepsilon_n \cos n\phi\,[(-1)^n B_n(\tau) + \sum_l R_{nl}] \quad \text{for } \tau > (r_0' - 1) + \lambda(1 - r') \tag{7.23}$$

with $B_n(\tau)$ and R_{nl} given by (7.19) and (7.22), respectively. By following the same procedure, we can obtain the time domain solution of the scattered electric field outside the cylinder as

$$E_z^s(r,\phi,t) = -\frac{\eta_0}{2\pi a}\sum_{n=0}^{\infty}\varepsilon_n \cos n\phi\,[(-1)^n B_n^s(\tau) + \sum_l R_{nl}^s] \quad \text{for } \tau > r_0' + r' \tag{7.24}$$

where

$$R_{nl}^s = -2\mathrm{Re}\left[\frac{\lambda e^{\zeta_{nl}\tau}}{\zeta_{nl}}\,\frac{I_n(\lambda\zeta_{nl})}{K_{n+1}(\zeta_{nl})}\,\frac{K_n(r'\zeta_{nl})K_n(r_0'\zeta_{nl})}{\lambda^2 I_{n+2}(\lambda\zeta_{nl})K_n(\zeta_{nl}) - I_n(\lambda\zeta_{nl})K_{n+2}(\zeta_{nl})}\right] \tag{7.25}$$

and

$$B_n^s(\tau) = \frac{1}{2}\int_0^{\infty}\frac{B\,[2AD + BC]}{A^2 + \pi^2 B^2}\,e^{-z\tau}\,dz \tag{7.26}$$

in which

$$C = K_n(zr')\,K_n(zr_0') - \pi^2\,I_n(zr')\,I_n(zr_0') \tag{7.27}$$

and

$$D = I_n(zr')\,K_n(zr_0') + I_n(zr_0')\,K_n(zr') \ . \tag{7.28}$$

7.3 Discussion

It should be noted that for any ϕ, the expression of the total electric field inside the

cylinder is valid for all the time ranges while that of the scattered field outside the cylinder is valid only after the initial incident wave front has passed a distance of $r_0 + r$. This phenomenon is similar to that discussed in Section 4.3.

As for the numerical calculation of (7.23) and (7.24), there is no difficulty in computing the integral terms. In order to calculate the residue contributions, one should be able to calculate the zeros of $f_n(\zeta)$ in the left half ζ-plane and to find out the number of zeros of $f_n(\zeta)$ for each n. This will be part of our future work.

CHAPTER 8

CONCLUSIONS AND SUGGESTIONS FOR FUTURE RESEARCH

8.1 Conclusions

Analytical expressions for both the early- and late-time response of the currents induced on a perfectly conducting circular cylinder illuminated by a cylindrical electromagnetic wave have been derived and numerical results have been presented. The early-time results obtained by using different methods are in good agreement within their range of validity for both the shadow and illuminated regions. The late-time results are obtained with different formulations and the range of validity of the expressions has been discussed. A single expression for the current density response has been derived, which is valid and numerically useful for all the time ranges in the shadow region, for late time range in the illuminated region, and also for part of the early and intermediate time ranges at large angles in the illuminated region. Even though the results have been given explicitly for the case when the line current is a unit-step function, the response for the case of a general variation of the line current may be determined by superposition. From the treatment of the more general case of a cylindrical wave excitation, the current response to TM polarized plane electromagnetic waves has been obtained as a special case, the new expressions derived having a substantially larger range of validity than the previously known results. The early-time field response of a conducting cylinder to a cylindrical electromagnetic wave and the transient current response to an electromagnetic pulse of a double exponential type are also analyzed and numerical results are presented. Finally, the analysis of transient

field response of a dielectric cylinder to a cylindrical electromagnetic wave has also been carried out theoretically.

8.2 Future Research

One extension of this work would be to study the transient response of a coated conducting cylinder to electromagnetic waves.

Another problem is the analytical treatment of the transient response of elliptic cylinders, with the inherent complications introduced by the presence of Mathieu functions.

A more practical problem is that of the analysis of electromagnetic interference between pipelines and parallel transmission lines when a fault occurs on the latter. The pipeline can be modelled as a long, coated conducting cylinder, buried in a half space lossy medium (soil). While numerical methods have to be employed for practical configurations, the results obtained in this thesis can be used to validate the computer programs employed.

A mathematical problem arises in Chapter 7 which relates to the computation of the residue contributions in the case of transient scattering by a dielectric cylinder. The calculation of the zeros of $f_n(\zeta)$ is not difficult. But in order to calculate the residue contributions one has to know the number of zeros of $f_n(\zeta)$ for each n. This mathematical problem can be stated as follows: Find the number of zeros of $f_n(\zeta)$, as a function of n, where $f_n(\zeta)=I_n(\zeta\lambda)K_{n+1}(\zeta)+\lambda K_n(\zeta)I_{n+1}(\zeta\lambda)$, with I_n and K_n being the modified Bessel functions of the first and second kind, respectively, and $\lambda>1$, $\mathrm{Re}[\zeta]<0$.

APPENDIX A

DERIVATION OF EQUATION (2.1)

First we derive the expression of the electric field generated by the line source without the presence of the cylinder. The current density of the line source located at $(r_0,0)$ is

$$J_z = -\delta(x-r_0)\,\delta(y)u(t)\ . \tag{A.1}$$

The wave equation for the vector potential $\mathbf{A}=A_z(r,\phi,t)\mathbf{a}_z$ due to the line current is

$$\nabla^2 A_z - \frac{1}{c^2}\frac{\partial^2 A_z}{\partial t^2} = -\mu_0\,\delta(x-r_0)\,\delta(y)\,u(t)\ . \tag{A.2}$$

Taking the Laplace transform with respect to t, we have

$$\nabla^2 \tilde{A}_z - (\frac{s}{c})^2 \tilde{A}_z = -\frac{\mu_0}{s}\delta(x-r_0)\delta(y)\ . \tag{A.3}$$

Equation (A.3) is a Helmholtz equation whose solution in unbounded region is

$$\tilde{A}_z = \frac{j\mu_0}{4s} H_0^{(1)}(\frac{js}{c}\,|\mathbf{r}-\mathbf{r}_0|)\ . \tag{A.4}$$

Note that the appropriate initial and boundary conditions have been used in obtaining (A.4). The Laplace transform of the electric field intensity is given by

$$E_z^i(r,\phi,s) = -s\tilde{A}_z(r,\phi,s)\ . \tag{A.5}$$

We write the electric field as E_z^i because it will be the incident electric field when the

cylinder is present. From (A.4) and (A.5), we have

$$E_z^i = -\frac{j\mu_0}{4} H_0^{(1)}\left(\frac{js}{c}|\mathbf{r}-\mathbf{r}_0|\right) . \tag{A.6}$$

When $r < r_0$, by using the addition theorem of the Hankel functions, E_z can be expressed as

$$E_z^i = -\frac{j\mu_0}{4} \sum_{n=-\infty}^{\infty} H_n^{(1)}\left(\frac{jsr_0}{c}\right) J_n\left(\frac{jsr}{c}\right) e^{jn\phi} . \tag{A.7}$$

For $r < r_0$, the scattered electric field can be assumed in a form

$$E_z^s = -\frac{j\mu_0}{4} \sum_{n=-\infty}^{\infty} C_n H_n^{(1)}\left(\frac{jsr_0}{c}\right) H_n\left(\frac{jsr}{c}\right) e^{jn\phi} . \tag{A.8}$$

From the boundary condition

$$[E_z^i + E_z^s]_{r=a} = 0 \tag{A.9}$$

we have

$$C_n = -\frac{J_n\left(\frac{jsa}{c}\right)}{H_n^{(1)}\left(\frac{jsa}{c}\right)} . \tag{A.10}$$

Hence for $r < r_0$ we obtain the total electric field as

$$E_z = -\frac{j\mu_0}{4} \sum_{n=-\infty}^{\infty} H_n^{(1)}\left(\frac{jsr_0}{c}\right)\left[J_n\left(\frac{jsr}{c}\right) - \frac{J_n\left(\frac{jsa}{c}\right)}{H_n^{(1)}\left(\frac{jsa}{c}\right)} H_n^{(1)}\left(\frac{jsr}{c}\right)\right] e^{jn\phi} . \tag{A.11}$$

The Laplace transform of the induced current density on the surface of the cylinder is

$$J_z(\phi,s)=\frac{1}{\mu_0 s}\frac{\partial E_z}{\partial r}|_{r=a} \ . \tag{A.12}$$

From (A.11) and (A.12) and using the Wronskian of the Hankel functions

$$J_n'(z)H_n^{(1)}(z)-J_n(z)H_n^{(1)\prime}(z)=-\frac{2j}{z} \tag{A.13}$$

we obtain finally

$$J_z(\phi,s)=-\frac{1}{2\pi as}\sum_{n=-\infty}^{\infty}\frac{H_n^{(1)}(\frac{jsr_0}{c})}{H_n^{(1)}(\frac{jsa}{c})}e^{jn\phi} \ . \tag{A.14}$$

APPENDIX B

DERIVATION OF EQUATIONS (2.9) AND (2.10)

The expression related to $\frac{\partial H_\nu^{(1)}(z)}{\partial \nu}|_{\nu=\nu_n}$ is given by Franz [25]

$$\frac{\partial H_\nu^{(1)}(z)}{\partial \nu}|_{\nu=\nu_n} = \frac{2}{\pi} e^{-j2\pi/3} (\frac{6}{z})^{2/3} A'(q_n)$$

$$\cdot \left[1 - \frac{e^{j\pi/3}}{z^{2/3}} \frac{s_n}{5} - \frac{e^{-j\pi/3}}{z^{4/3}} \frac{37 s_n^2}{630} + \frac{1}{z^2} (-\frac{37}{3150} + \frac{563 s_n^3}{28350}) + \cdots \right] \tag{B.1}$$

where $A(q)$ is a kind of Airy function defined as

$$A(q) = \frac{\pi}{3} (\frac{q}{3})^{1/2} \left\{ J_{-1/3}[2(\frac{q}{3})^{3/2}] + J_{1/3}[2(\frac{q}{3})^{3/2}] \right\} \tag{B.2}$$

which satisfies the equation

$$\frac{d^2 w(z)}{d^2 z} + \frac{z}{3} w(z) = 0 \ . \tag{B.3}$$

s_n in (B.1) is given by

$$s_n = 6^{-1/3} q_n \tag{B.4}$$

and q_n is the $n-th$ zero of $A(q)$. A more commonly used Airy function Ai is defined as

$$Ai(-\alpha) = \frac{1}{3} \alpha^{1/2} [J_{-1/3}(\frac{2}{3}\alpha^{3/2}) + J_{1/3}(\frac{2}{3}\alpha^{3/2})] \tag{B.5}$$

which satisfies the equation

$$\frac{d^2w(z)}{d^2z} - zw(z) = 0 \ . \tag{B.6}$$

Letting α_n be the $n-th$ zero of $Ai(-\alpha)$, then q_n can be expressed in terms of α_n as

$$q_n = 3^{1/3}\alpha_n \ . \tag{B.7}$$

$Ai'(-\alpha_n)$ and $A'(q_n)$ can be derived from (B.2) and (B.5) as

$$A'(q_n) = \frac{\pi q_n}{9}\left\{ J_{-2/3}[2(\frac{q_n}{3})^{3/2}] - J_{1/3}[2(\frac{q_n}{3})^{3/2}] \right\} \tag{B.8}$$

$$Ai'(-\alpha_n) = -\frac{1}{3}\alpha_n[J_{-2/3}(\frac{2}{3}\alpha_n^{3/2}) - J_{2/3}(\frac{2}{3}\alpha_n^{3/2})] \ . \tag{B.9}$$

It can be seen from (B.7), (B.8) and (B.9) that

$$A'(q_n) = -3^{-2/3}\pi Ai'(-\alpha_n) \ . \tag{B.10}$$

Using (B.4), (B.7) and (B.9) in (B.1) and noting that $z = jsa/c$, we obtain

$$\dot{H}^{(1)}_{\nu_n}(\frac{jsa}{c}) = 2Ai'(-\alpha_n)(\frac{sa}{2c})^{-2/3}[1 - \frac{\alpha_n}{10}(\frac{sa}{2c})^{-2/3} + \frac{37}{2520}\alpha_n^2(\frac{sa}{2c})^{-4/3} + \cdots] \ . \tag{B.11}$$

The expression for ν_n is

$$\nu_n = z + e^{j\pi/3}z^{1/3}s_n - e^{-j\pi/3}z^{-1/3}\frac{s_n^2}{30} - \frac{1}{70z}(1 - \frac{s_n^3}{5}) + \cdots \ . \tag{B.12}$$

From (B.4), (B.7) and (B.12) and noting again that $z = jsa/c$, we have

$$\nu_n = j\,[\frac{sa}{c} + \alpha_n(\frac{sa}{2c})^{1/3} + \frac{\alpha_n^2}{60}(\frac{sa}{2c})^{-1/3} + \frac{1}{140}(1 - \frac{\alpha_n^3}{10})(\frac{sa}{2c})^{-1} + \cdots] \ . \tag{B.13}$$

APPENDIX C

DERIVATION OF EQUATION (2.16)

An outline of the derivation of (2.16) is given in this appendix. Since we can not obtain an analytical solution of the inverse Laplace transform of (2.11), we have to make further approximation to obtain a form which is suitable for performing the inverse Laplace transform analytically. Such an approximation is possible since we are only considering the case of $s \to \infty$. Using the relation (2.15), the factors in (2.13) can be written as

$$\nu \tanh\gamma = jz[1-(\frac{\nu}{z})^2]^{1/2} \tag{C.1}$$

$$(-\frac{1}{2}\nu\pi j\tanh\gamma)^{1/2} = (\frac{\pi}{2})^{1/2} z^{1/2}\,[1-(\frac{\nu}{z})^2]^{1/4} \tag{C.2}$$

$$\coth\gamma = -j\frac{\nu}{z}\,[1-(\frac{\nu}{z})^2]^{-1/2} \tag{C.3}$$

and

$$\begin{aligned} A_0 &= 1 \\ A_1 &= \frac{1}{8} - \frac{5}{24}(\frac{\nu}{z})^2\,[1-(\frac{\nu}{z})^2]^{-1} \\ A_2 &= \frac{3}{128} - \frac{77}{576}(\frac{\nu}{z})^2\,[1-(\frac{\nu}{z})^2]^{-1} + \frac{385}{3456}(\frac{\nu}{z})^4\,[1-(\frac{\nu}{z})^2]^{-2} \\ &\cdots\cdots . \end{aligned} \tag{C.4}$$

Note that when (2.13) is used in in (2.11), z and ν should be replaced by jsr_0/c and ν_n,

respectively. For convenience we denote $sa/2c$ by S. Thus $z = j\frac{2r_0}{a}S$ and

$$v_n = j[2S + \alpha_n S^{1/3} + \alpha_n^2 + \frac{1}{140}(1 - \frac{\alpha_n^3}{10})S^{-1} + \cdots] \tag{C.5}$$

$$\frac{v_n}{z} = \frac{a}{r_0}[1 + \frac{\alpha_n}{2}S^{-2/3} + \frac{\alpha_n^2}{120}S^{-4/3} + \frac{1}{280}(1 - \frac{\alpha_n^3}{10})S^{-2} + \cdots] \tag{C.6}$$

$$1 - (\frac{v_n}{z})^2 = [1 - (\frac{a}{r_0})^2][1 - \alpha_n \cos^2\phi_b S^{-2/3} - \frac{4}{15}\alpha_n^2 \cos^2\phi_b S^{-4/3} - (\frac{1}{140} + \frac{4}{525}\alpha_n^3)\cos^2\phi_b S^{-2} + \cdots] \tag{C.7}$$

$$[1 - (\frac{v_n}{z})^2]^{1/2} = [1 - (\frac{a}{r_0})^2]^{1/2}[1 - \frac{1}{2}PS^{-2/3} - \frac{1}{2}(Q + \frac{1}{4}P^2)S^{-4/3} - \frac{1}{2}(T + \frac{1}{2}PQ + \frac{1}{8}P^3)S^{-2} - \cdots] \tag{C.8}$$

$$[1 - (\frac{v_n}{z})^2]^{-1/2} = [1 - (\frac{a}{r_0})^2]^{-1/2}[1 + \frac{1}{2}PS^{-2/3} + \frac{1}{2}(Q + \frac{3}{4}P^2)S^{-4/3} + \frac{1}{2}(T + \frac{3}{2}PQ + \frac{5}{8}P^3)S^{-2} + \cdots] \tag{C.9}$$

$$[1 - (\frac{v_n}{z})^2]^{-1/4} = [1 - (\frac{a}{r_0})^2]^{-1/4}[1 + \frac{1}{4}PS^{-2/3} + \frac{1}{4}(Q + \frac{5}{8}P^2)S^{-4/3} + \frac{1}{4}(T + \frac{5}{4}PQ + \frac{15}{32}P^3)S^{-2} + \cdots] \tag{C.10}$$

$$[1 - (\frac{v_n}{z})^2]^{-1} = [1 - (\frac{a}{r_0})^2]^{-1}[1 + PS^{-2/3} + (Q + P^2)S^{-4/3} + (T + 2PQ + P^3)S^{-2} + \cdots] \tag{C.11}$$

$$[1 - (\frac{v_n}{z})^2]^{-3/2} = [1 - (\frac{a}{r_0})^2]^{-3/2}[1 + \frac{3}{2}PS^{-2/3} + \frac{3}{2}(Q + \frac{5}{4}P^2)S^{-4/3} + \frac{3}{2}(T + \frac{5}{2}PQ + \frac{35}{24}P^3)S^{-2} + \cdots] \tag{C.12}$$

where

$$P=\alpha_n\cot^2\phi_b$$

$$Q=\frac{4}{15}\alpha_n\cot^2\phi_b \tag{C.13}$$

$$T=(\frac{1}{140}+\frac{4}{525}\alpha_n^3)\cot^2\phi_b$$

and $\phi_b=\dfrac{a/r_0}{(1-a^2/r_0^2)^{1/2}}$ is the angular coordinate corresponding to the shadow boundary, as shown in Fig. 1.1. From (2.15) and (C.6), we have when $\nu=\nu_n$

$$\gamma=j\cos^{-1}\left\{\frac{a}{r_0}+\frac{a}{r_0}[\frac{\alpha_n}{2}S^{-2/3}+\frac{1}{280}(1-\frac{\alpha_n^3}{10})S^{-2}+\cdots]\right\}\ . \tag{C.14}$$

Expanding (C.14) at $\dfrac{a}{r_0}$, we obtain

$$\gamma=j[\phi_b-\frac{1}{2}\alpha_n\cos\phi_b S^{-2/3}-\alpha_n^2\cos\phi_b\,(\frac{1}{8}\cos^2\phi_b+\frac{1}{120})S^{-4/3}-\cdots]\ . \tag{C.15}$$

Equation (C.5) together with (C.15) gives

$$\nu_n\gamma=-2\phi_b S-\alpha_n(\phi_b-\cot\phi_b)S^{1/3}-US^{-1/3}-VS^{-1}+WS^{-5/3}+\cdots \tag{C.16}$$

where

$$U=\alpha_n^2(\frac{1}{60}\phi_b-\frac{31}{60}\cot\phi_b-\frac{1}{4}\cot^3\phi_b)$$

$$V=\frac{\phi_b}{140}(1-\frac{\alpha_n^3}{10})-\frac{1}{60}\alpha_n^3\cot\phi_b-\frac{1}{8}\alpha_n^3\cot^3\phi_b \tag{C.17}$$

$$W=\frac{1}{280}\alpha_n\cot\phi_b-\frac{11}{50400}\alpha_n^4\cot\phi_b+\frac{1}{480}\alpha_n^4\cot^3\phi_b\ .$$

From (C.2) and (C.8), we have

$$(-\frac{1}{2}\nu\pi j\tanh\gamma)^{1/2}=(\frac{\cot\phi_b}{\pi})^{1/2}e^{-j\pi/4}s^{-1/2}\,[1+\frac{1}{4}\alpha_n\cot^2 S^{-2/3}$$

$$+\frac{\alpha_n^2}{4}(\frac{4}{15}+\frac{5}{8}\cot^2\phi_b)\cot^2\phi_b S^{-4/3}+\cdots]\ . \qquad \text{(C.18)}$$

The summation in (2.13) can be written as

$$\sum_{m=0}^{\infty}\frac{\Gamma(m+\frac{1}{2})}{\Gamma(\frac{1}{2})}\frac{A_m}{(\frac{1}{2}\nu\tanh\gamma)^m}=1-\frac{1}{8}(\frac{a}{2r_0})S^{-1}[1-(\frac{\nu_n}{z})^2]^{-1/2}$$

$$-\frac{5}{24}(\frac{a}{2r_0})S^{-1}(\frac{\nu_n}{z})^2[1-(\frac{\nu_n}{z})^2]^{-3/2}-\frac{9}{128}(\frac{a}{2r_0})^2S^{-2}[1-(\frac{\nu_n}{z})^2]^{-1}$$

$$+\frac{77}{192}(\frac{a}{2r_0})^2S^{-2}(\frac{\nu_n}{z})^2[1-(\frac{\nu_n}{z})^2]^{-2}+\cdots\ . \qquad \text{(C.19)}$$

Using (C.9)-(C.12) in (C.19), we obtain

$$\sum_{m=0}^{\infty}\frac{\Gamma(m+\frac{1}{2})}{\Gamma(\frac{1}{2})}\frac{A_m}{(\frac{1}{2}\nu\tanh\gamma)^m}=1-\frac{1}{16}\cot\phi_b(1+\frac{5}{3}\cot^2\phi_b)S^{-1}$$

$$-\frac{1}{32}\alpha_n\cot^3\phi_b(\frac{13}{3}+5\cot^2\phi_b)S^{-5/3}+\cdots\ . \qquad \text{(C.20)}$$

By utilizing previous expressions, (2.13) can be approximated as

$$H_\nu^{(1)}(z)=-j(\frac{\cot\phi_b}{\pi})^{1/2}S^{-1/2}e^X\left\{1+(\frac{\alpha_n}{4}\cot^2\phi_b)S^{-2/3}-[\frac{1}{16}\cot\phi_b(1+\frac{5}{3}\cot^2\phi_b)]S^{-1}\right.$$

$$\left.+[\frac{\alpha_n^2}{4}(\frac{4}{15}+\frac{5}{8}\cot^2\phi_b)\cot^2\phi_b]S^{-4/3}-[\frac{1}{192}\alpha_n\cot^3\phi_b(29+35\cot^2\phi_b)]S^{-5/3}+\cdots\right\} \qquad \text{(C.21)}$$

where

$$X = 2(\phi_b - \tan\phi_b)S + \alpha_n\phi_b S^{1/3} + [U + \alpha_n^2\cos^2\phi_b(\frac{1}{4} + \frac{4}{15})]S^{-1/3}$$

$$+ [V + (\frac{1}{140} + \frac{4}{525}\alpha_n^3)\cos\phi_b + \frac{2}{15}\alpha_n^3\cot\phi_b + \frac{1}{8}\alpha_n^3\cot^5\phi_b]S^{-1} + \cdots \quad . \qquad \text{(C.22)}$$

Using (C.21) and (2.22) in (2.11) and retaining the first few terms, we can finally obtain (2.16) from which the time domain current density can be readily obtained by taking the inverse Laplace transform.

APPENDIX D

THE LAPLACIAN OPERATOR IN CAUSTIC COORDINATES

Consider

$$\nabla^2\Phi(x,y)=\frac{\partial^2\Phi(x,y)}{\partial x^2}+\frac{\partial^2\Phi(x,y)}{\partial y^2} \tag{D.1}$$

with

$$x=x(l,\psi)\,,\quad y=y(l,\psi) \tag{D.2}$$

and

$$l=l(x,y)\,,\quad \psi=\psi(x,y)\ . \tag{D.3}$$

Then

$$\frac{\partial\Phi}{\partial x}=\frac{\partial\Phi}{\partial l}\frac{\partial l}{\partial x}+\frac{\partial\Phi}{\partial\psi}\frac{\partial\psi}{\partial x} \tag{D.4}$$

$$\frac{\partial\Phi}{\partial y}=\frac{\partial\Phi}{\partial l}\frac{\partial l}{\partial y}+\frac{\partial\Phi}{\partial\psi}\frac{\partial\psi}{\partial y} \tag{D.5}$$

and

$$\frac{\partial^2\Phi}{\partial x^2}=\frac{\partial^2\Phi}{\partial l^2}(\frac{\partial l}{\partial x})^2+2\frac{\partial^2\Phi}{\partial l\partial\psi}\frac{\partial l}{\partial x}\frac{\partial\psi}{\partial x}+\frac{\partial^2\Phi}{\partial\psi^2}(\frac{\partial\psi}{\partial x})^2+\frac{\partial\Phi}{\partial l}\frac{\partial^2 l}{\partial x^2}+\frac{\partial\Phi}{\partial\psi}\frac{\partial^2\psi}{\partial x^2} \tag{D.6}$$

$$\frac{\partial^2\Phi}{\partial y^2}=\frac{\partial^2\Phi}{\partial l^2}(\frac{\partial l}{\partial y})^2+2\frac{\partial^2\Phi}{\partial l\partial\psi}\frac{\partial l}{\partial y}\frac{\partial\psi}{\partial y}+\frac{\partial^2\Phi}{\partial\psi^2}(\frac{\partial\psi}{\partial y})^2+\frac{\partial\Phi}{\partial l}\frac{\partial^2 l}{\partial y^2}+\frac{\partial\Phi}{\partial\psi}\frac{\partial^2\psi}{\partial y^2} \tag{D.7}$$

$$\nabla^2\Phi=[(\frac{\partial l}{\partial x})^2+(\frac{\partial l}{\partial y})^2]\frac{\partial^2\Phi}{\partial l^2}+2(\frac{\partial l}{\partial x}\frac{\partial \psi}{\partial x}+\frac{\partial l}{\partial y}+\frac{\partial \psi}{\partial y})\frac{\partial^2\Phi}{\partial l\partial\psi}$$

$$+[(\frac{\partial \psi}{\partial x})^2+(\frac{\partial \psi}{\partial y})^2]\frac{\partial^2\Phi}{\partial \psi^2}+(\frac{\partial^2 l}{\partial x^2}+\frac{\partial^2 l}{\partial y^2})\frac{\partial\Phi}{\partial l}+(\frac{\partial^2\psi}{\partial x^2}+\frac{\partial^2\psi}{\partial y^2})\frac{\partial\Phi}{\partial\psi}\ . \qquad \text{(D.8)}$$

The transformation equations between the Cartesian and the caustic coordinate systems are

$$x=\xi(\psi)+l\cos\psi \qquad \text{(D.9)}$$

$$y=\eta(\psi)+l\sin\psi \qquad \text{(D.10)}$$

where

$$\xi(\psi)=a(\cos\phi-\frac{1}{2}\cos\alpha\cos\psi) \qquad \text{(D.11)}$$

$$\eta(\psi)=a(\sin\phi-\frac{1}{2}\cos\alpha\sin\psi)\ . \qquad \text{(D.12)}$$

Rewriting (D.9) and (D.10) as

$$u(x,y,l,\psi)=x-\xi(\psi)-l\cos\psi=0 \qquad \text{(D.13)}$$

$$v(x,y,l,\psi)=y-\eta(\psi)-l\sin\psi=0 \qquad \text{(D.14)}$$

we have

$$\Delta=\frac{\partial(u,v)}{\partial(l,\psi)}=l\ . \qquad \text{(D.15)}$$

The following derivatives can be obtained directly through calculus

$$\frac{\partial l}{\partial x}=-\frac{1}{\Delta}\frac{\partial(u,v)}{\partial(x,\psi)}=\frac{1}{l}(\frac{d\eta}{d\psi}+l\cos\psi) \qquad \text{(D.16)}$$

$$\frac{\partial\psi}{\partial x}=-\frac{1}{\Delta}\frac{\partial(u,v)}{\partial(l,x)}=-\frac{1}{l}\sin\psi \qquad \text{(D.17)}$$

$$\frac{\partial l}{\partial y}=-\frac{1}{\Delta}\frac{\partial(u,v)}{\partial(y,\psi)}=-\frac{1}{l}(\frac{d\xi}{d\psi}-l\sin\psi) \tag{D.18}$$

$$\frac{\partial l}{\partial y}=-\frac{1}{\Delta}\frac{\partial(u,v)}{\partial(l,y)}=-\frac{1}{l}\cos\psi \tag{D.19}$$

$$\frac{\partial^2 l}{\partial x^2}=-\frac{1}{l^3}(\frac{d\eta}{d\psi}+l\cos\psi)^2+\frac{1}{l^2}(l-\frac{d\eta}{d\psi}\cos\psi+\frac{d^2\eta}{d\psi^2}\sin\psi) \tag{D.20}$$

$$\frac{\partial^2 l}{\partial y^2}=\frac{1}{l^3}(\frac{d\xi}{d\psi}-l\sin\psi)^2+\frac{1}{l^2}(l-\frac{d\xi}{d\psi}\sin\psi-\frac{d^2\xi}{d\psi^2}\cos\psi) \tag{D.21}$$

$$\frac{\partial^2\psi}{\partial x^2}=\frac{1}{l^3}\frac{d\eta}{d\psi}\sin\psi+\frac{1}{l^2}\sin 2\psi \tag{D.22}$$

$$\frac{\partial^2\psi}{\partial y^2}=\frac{1}{l^3}\frac{d\xi}{d\psi}\cos\psi-\frac{1}{l^2}\sin 2\psi \tag{D.23}$$

$$(\frac{\partial l}{\partial x})^2+(\frac{\partial l}{\partial y})^2=1+\frac{A}{l^2} \tag{D.24}$$

$$A=(\frac{d\eta}{d\psi})^2+(\frac{d\xi}{d\psi})^2 \tag{D.25}$$

$$\frac{\partial l}{\partial x}\frac{\partial\psi}{\partial x}+\frac{\partial l}{\partial y}\frac{\partial\psi}{\partial y}=-\frac{1}{l^2}B \tag{D.26}$$

$$B=\frac{d\xi}{d\psi}\cos\psi+\frac{d\eta}{d\psi}\sin\psi \tag{D.27}$$

$$(\frac{\partial\psi}{\partial x})^2+(\frac{\partial\psi}{\partial y})^2=\frac{1}{l^2} \tag{D.28}$$

$$\frac{\partial^2 l}{\partial x^2}+\frac{\partial^2 l}{\partial y^2}=\frac{1}{l}-\frac{C}{l^2}-\frac{A}{l^3} \tag{D.29}$$

$$C=\frac{d^2\eta}{d\psi^2}\sin\psi+\frac{d^2\xi}{d\psi^2}\cos\psi \tag{D.30}$$

$$\frac{\partial^2\psi}{\partial x^2}+\frac{\partial^2\psi}{\partial y^2}=\frac{B}{l^3}\ . \tag{D.31}$$

Using (D.16)-(D.31) in (D.8), we obtain

$$\nabla^2\Phi=(1+\frac{A}{l^2})\frac{\partial^2\Phi}{\partial l^2}+\frac{1}{l^2}\frac{\partial^2\Phi}{\partial\psi^2}+\frac{2B}{l^2}\frac{\partial^2\Phi}{\partial l\partial\psi}+(\frac{1}{l}-\frac{C}{l^2}-\frac{A}{l^3})\frac{\partial\Phi}{\partial l}+\frac{B}{l^3}\frac{\partial\Phi}{\partial\psi}\ . \tag{D.32}$$

Hence

$$\nabla^2=(1+\frac{A}{l^2})\frac{\partial^2}{\partial l^2}+\frac{1}{l^2}\frac{\partial^2}{\partial\psi^2}+\frac{2B}{l^2}\frac{\partial^2}{\partial l\partial\psi}+(\frac{1}{l}-\frac{C}{l^2}-\frac{A}{l^3})\frac{\partial}{\partial l}+\frac{B}{l^3}\frac{\partial}{\partial\psi}\ . \tag{D.33}$$

Where A, B and C are given by (D.25), (D.27) and (D.30). Note that A, B and C are in a different forms from those given by (3.27). From (D.11) and (D.12), we have

$$\frac{d\xi}{d\psi}=a[\frac{1}{2}\sin(\alpha+\psi)-(\sin\phi+\frac{1}{2}\sin\alpha\cos\psi)\frac{d\phi}{d\psi}] \tag{D.34}$$

$$\frac{d\eta}{d\psi}=a[-\frac{1}{2}\cos(\alpha+\psi)+(\cos\phi-\frac{1}{2}\sin\alpha\sin\psi)\frac{d\phi}{d\psi}] \tag{D.35}$$

$$\frac{d^2\xi}{d\psi^2}=a[(\frac{1}{2}\cos\alpha\cos\psi-\cos\phi)(\frac{d\phi}{d\psi})^2+\cos(\psi+\alpha)(1-\frac{d\phi}{d\psi})-(\sin\phi+\frac{1}{2}\sin\alpha\cos\psi)\frac{d^2\phi}{d^2\psi}] \tag{D.36}$$

$$\frac{d^2\eta}{d\psi^2}=a[(\frac{1}{2}\cos\alpha\sin\psi-\sin\phi)(\frac{d\phi}{d\psi})^2+\sin(\psi+\alpha)(1-\frac{d\phi}{d\psi})+(\cos\phi-\frac{1}{2}\sin\alpha\sin\psi)\frac{d^2\phi}{d^2\psi}]\ . \tag{D.37}$$

Using (D.34) and (D.35) in (D.25) and (D.27), (D36) and (D.37) in (D.30), respectively, we have

$$A=\frac{a^2}{4}\sin^2\alpha\,(1+\frac{d\phi}{d\psi})^2 \tag{D.38}$$

$$B = \frac{a}{2}\sin\alpha\left(1 + \frac{d\phi}{d\psi}\right) \tag{D.39}$$

$$C = a\left[-\frac{1}{2}\cos\alpha\left(\frac{d\phi}{d\psi}\right)^2 + \cos\alpha\left(1 - \frac{d\phi}{d\psi}\right) + \frac{1}{2}\sin\alpha\frac{d^2\phi}{d\psi^2}\right] . \tag{D.40}$$

APPENDIX E

DERIVATION OF EQUATION (3.30)

An outline of the derivation of (3.30) is given in this appendix. From $J_z(\phi, s)=\frac{1}{\mu_0 s}\frac{\partial E_z}{\partial r}\Big|_{r=a}$ and (3.29), we can write

$$J_z(\phi, s)=-\frac{1}{2kc}\frac{1}{\sqrt{2\pi k}}\frac{\partial E}{\partial r}\Big|_{r=a} \tag{E.1}$$

where E is given by

$$E=[\frac{1}{R^{1/2}}e^{-kR}-\frac{1}{R_0^{1/2}}(\frac{l_0}{l})^{1/2}e^{-k(R_0+l-\frac{a}{2}\cos\alpha)}]$$

$$+\frac{1}{k}[-\frac{1}{8}\frac{1}{R^{3/2}}e^{-kR}+\frac{1}{8}\frac{1}{R_0^{3/2}}(\frac{l_0}{l})^{1/2}e^{-k(R_0+l-\frac{a}{2}\cos\alpha)}]+\frac{1}{k}\frac{1}{2l^{1/2}}e^{-k(R_0+l-\frac{a}{2}\cos\alpha)}$$

$$\cdot\left\{[\frac{1}{4}(\frac{l_0}{R_0})^{1/2}\frac{\partial^2}{\partial\psi^2}(\frac{l_0}{R_0})^{1/2}]\frac{1}{l}+[\frac{1}{4}(\frac{l_0}{R_0})^{1/2}C+B\frac{\partial}{\partial\psi}(\frac{l_0}{R_0})^{1/2}]\frac{1}{l^2}+\frac{5}{12}A(\frac{l_0}{R_0})^{1/2}\frac{1}{l^3}\right\}_{l_0}^{l}$$

$$+\frac{1}{k^2}[\frac{9}{128}\frac{1}{R^{5/2}}e^{-kR}-\frac{9}{128}\frac{1}{R_0^{5/2}}(\frac{l_0}{l})^{1/2}e^{-k(R_0+l-\frac{a}{2}\cos\alpha)}]+\cdots . \tag{E.2}$$

The partial derivative of E with respect to r at $r=a$ is

$$\frac{\partial E}{\partial r}\Big|_{r=a}=\Bigg[[\frac{1}{R^{1/2}}\frac{\partial}{\partial r}e^{-kR}-\frac{1}{R_0^{1/2}}(\frac{l_0}{l})^{1/2}\frac{\partial}{\partial r}e^{-k(R_0+l-\frac{a}{2}\cos\alpha)}]$$

$$+[e^{-kR_0}\frac{\partial}{\partial r}R^{-1/2}-e^{-k(R_0+l-\frac{a}{2}\cos\alpha)}\frac{\partial}{\partial r}(\frac{l_0}{R_0 l})^{1/2}]$$

$$+\frac{1}{k}[-\frac{1}{8}\frac{1}{R^{3/2}}\frac{\partial}{\partial r}e^{-kR}+\frac{1}{8}\frac{1}{R_0^{3/2}}(\frac{l_0}{l})^{1/2}\frac{\partial}{\partial r}e^{-k(R_0+l-\frac{a}{2}\cos\alpha)}]$$

$$+\frac{1}{k}[-\frac{1}{8}e^{-kR}\frac{\partial}{\partial r}R^{-3/2}+\frac{1}{8}e^{-k(R_0+l-\frac{a}{2}\cos\alpha)}\frac{\partial}{\partial r}(\frac{l_0}{R^3 l})^{1/2}]+\frac{1}{k}\frac{1}{2l^{1/2}}e^{-k(R_0+l-\frac{a}{2}\cos\alpha)}$$

$$\cdot\frac{\partial}{\partial r}\Bigg[[\frac{1}{4}(\frac{l_0}{R_0})^{1/2}\frac{\partial^2}{\partial\psi^2}(\frac{l_0}{R_0})^{1/2}]\frac{1}{l}+[\frac{1}{4}(\frac{l_0}{R_0})^{1/2}C+B\frac{\partial}{\partial\psi}(\frac{l_0}{R_0})^{1/2}]\frac{1}{l^2}+\frac{5}{12}A(\frac{l_0}{R_0})^{1/2}\frac{1}{l^3}\Bigg]_{l_0}^{l}$$

$$+\frac{1}{k^2}[\frac{9}{128}\frac{1}{R^{5/2}}\frac{\partial}{\partial r}e^{-kR}-\frac{9}{128}\frac{1}{R_0^{5/2}}(\frac{l_0}{l})^{1/2}\frac{\partial}{\partial r}e^{-k(R_0+l-\frac{a}{2}\cos\alpha)}+\cdots\Bigg]_{r=a} \qquad \text{(E.3)}$$

where A, B and C are given by (3.27). In order to calculate the derivatives in (E.3) we have to derive $\frac{\partial l}{\partial r}|_{r=a}$ and $\frac{\partial\psi}{\partial r}|_{r=a}$ first. Replacing x and y in (D.13) and (D.14) by $r\cos\theta$ and $r\sin\theta$, respectively, we have

$$F(l,\psi,r,\theta)=l\cos\psi+a(\cos\phi-\frac{1}{2}\cos\alpha\cos\psi)-r\cos\theta=0 \qquad \text{(E.4)}$$

$$G(l,\psi,r,\theta)=l\sin\psi+a(\sin\phi-\frac{1}{2}\cos\alpha\sin\psi)-r\sin\theta=0 \qquad \text{(E.5)}$$

Then

$$\frac{\partial l}{\partial r}=\frac{\partial(F,G)/\partial(r,\psi)}{\partial(F,G)/\partial(l,\psi)} \qquad \text{(E.6)}$$

$$\frac{\partial \psi}{\partial r} = \frac{\partial(F,G)/\partial(l,r)}{\partial(F,G)/\partial(l,\psi)} \tag{E.7}$$

From (E.4) and (E.5), we have

$$\frac{\partial F}{\partial l} = \cos\psi \ , \quad \frac{\partial G}{\partial l} = \sin\psi \tag{E.8}$$

$$\frac{\partial F}{\partial \psi} = -l\sin\psi + a[-(\sin\phi + \frac{1}{2}\sin\alpha\cos\psi)\frac{d\phi}{d\psi} + \frac{1}{2}\sin(\alpha+\psi) \tag{E.9}$$

$$\frac{\partial G}{\partial \psi} = l\cos\psi + a[(\cos\phi - \frac{1}{2}\sin\alpha\sin\psi)\frac{d\phi}{d\psi} + \frac{1}{2}\cos(\alpha+\psi) \tag{E.10}$$

$$\frac{\partial F}{\partial r} = \cos\theta \ , \quad \frac{\partial G}{\partial r} = \sin\theta \tag{E.11}$$

From (E.8)-(E.11), we obtain

$$\frac{\partial(F,G)}{\partial(l,\psi)} = a\cos\alpha\frac{d\phi}{d\psi} \tag{E.12}$$

$$\frac{\partial(F,G)}{\partial(r,\psi)} = -a(1-\frac{1}{2}\sin^2\alpha)\frac{d\phi}{d\psi} - \frac{a}{2}\sin^2\alpha \tag{E.13}$$

and

$$\frac{\partial(F,G)}{\partial(l,r)} = \sin\alpha \tag{E.14}$$

Using (E.12)-(E.14) and noting that $l=l_0$ when $r=r_0$, we have

$$\frac{\partial l}{\partial r}\Big|_{r=a} = \frac{(1-\frac{1}{2}\sin^2\alpha)\frac{d\phi}{d\psi}\Big|_{l=l_0} + \frac{1}{2}\sin^2\alpha}{\cos\alpha\frac{d\phi}{d\psi}\Big|_{l=l_0}} \tag{E.15}$$

$$\frac{\partial \psi}{\partial r}\Big|_{r=a} = \frac{\sin\alpha}{\cos\alpha\frac{d\phi}{d\psi}\Big|_{l=l_0}} \ . \tag{E.16}$$

By using (E.15) and (E.16), the following derivatives can be derived

$$\frac{\partial}{\partial r}e^{-kR}\Big|_{r=a}=k\cos\alpha\, e^{-kR_0} \tag{E.17}$$

$$\frac{\partial}{\partial r}e^{-k(R_0+l-\frac{a}{2}\cos\alpha)}\Big|_{r=a}=-k\cos\alpha\, e^{-kR_0} \tag{E.18}$$

$$\frac{\partial}{\partial r}R^{-1/2}\Big|_{r=a}=\frac{1}{2}R_0^{-3/2}\cos\alpha \tag{E.19}$$

$$\frac{\partial}{\partial r}\left(\frac{l_0}{R_0 l}\right)^{1/2}\Big|_{r=a}=\frac{1}{2\cos\alpha}(R_0^{-3/2}\sin^2\alpha-l_0^{-1}R_0^{-1/2}) \tag{E.20}$$

$$\frac{\partial}{\partial r}R^{-3/2}\Big|_{r=a}=\frac{3}{2}R_0^{-5/2}\cos\alpha \tag{E.21}$$

$$\frac{\partial}{\partial r}\left(\frac{l_0}{R^3 l}\right)^{1/2}\Big|_{r=a}=\frac{1}{\cos\alpha}\left(\frac{3}{2}R_0^{-5/2}\sin^2\alpha-\frac{1}{2}l_0^{-1}R_0^{-3/2}\right)\ . \tag{E.22}$$

Denoting

$$V=\left[\left[\frac{1}{4}\left(\frac{l_0}{R_0}\right)^{1/2}\frac{\partial^2}{\partial\psi^2}\left(\frac{l_0}{R_0}\right)^{1/2}\right]\frac{1}{l}+\left[\frac{1}{4}\left(\frac{l_0}{R_0}\right)^{1/2}C+B\frac{\partial}{\partial\psi}\left(\frac{l_0}{R_0}\right)^{1/2}\right]\frac{1}{l^2}+\frac{5}{12}A\left(\frac{l_0}{R_0}\right)^{1/2}\frac{1}{l^3}\right]_{l_0}^{l} \tag{E.23}$$

since V is a function of l and ψ, and l and ψ are functions of r, we have

$$\frac{\partial V}{\partial r}\Big|_{r=a}=\left[\frac{\partial V}{\partial l}\frac{\partial l}{\partial r}+\frac{\partial V}{\partial\psi}\frac{\partial\psi}{\partial r}\right]_{l=l_0}\ . \tag{E.24}$$

$\frac{\partial V}{\partial l}\Big|_{l=l_0}$ and $\frac{\partial V}{\partial \psi}\Big|_{l=l_0}$ can be derived as

$$\frac{\partial V}{\partial l}\Big|_{l=l_0} = -U \tag{E.25}$$

$$\frac{\partial V}{\partial \psi}\Big|_{l=l_0} = \frac{a}{2}\sin\alpha \frac{d\alpha}{d\psi}\Big|_{l=l_0} U \tag{E.26}$$

where U is given by

$$U=[\frac{1}{4}(\frac{l_0}{R_0})^{1/2}+\frac{\partial^2}{\partial\psi^2}(\frac{l_0}{R_0})^{1/2}]\frac{1}{l^2}+2[\frac{C}{4}(\frac{l_0}{R_0})^{1/2}+B\frac{\partial}{\partial\psi}(\frac{l_0}{R_0})^{1/2}]\frac{1}{l^3}+\frac{5}{4}A(\frac{l_0}{R_0})^{1/2}\frac{1}{l^4}. \tag{E.27}$$

Using (E.15), (E.16), (E.25) and (E.26) in (E.24), we have

$$\frac{\partial V}{\partial r}\Big|_{r=a} = -\frac{1}{\cos\alpha}U \ . \tag{E.28}$$

We now derive the explicit expression for U. Since

$$\frac{\partial}{\partial r}(\frac{l_0}{R_0})^{1/2}\Big|_{r=a} = -\frac{a}{4}\sin\alpha[\frac{1}{l_0R_0}(1-\frac{d\phi}{d\psi})+2(\frac{1}{l_0R_0^3})^{1/2}\frac{d\phi}{d\psi}] \tag{E.29}$$

$$\frac{\partial^2}{\partial\psi^2}(\frac{l_0}{R_0})^{1/2} = \frac{a}{4}[-2(\frac{l_0}{R_0^3})^{1/2}\frac{\cos2\alpha}{\cos\alpha}\frac{d\phi}{d\psi}(1-\frac{d\phi}{d\psi})-\frac{1}{2}(\frac{1}{l_0R_0})^{1/2}\frac{1+\cos\alpha}{\cos\alpha}(1-\frac{d\phi}{d\psi})^2$$

$$+3a(\frac{l_0}{R_0^5})^{1/2}\sin^2\alpha(\frac{d\phi}{d\psi})^2+(\frac{l_0}{R_0})^{1/2}(\frac{1}{l_0}-\frac{2}{R_0})\sin\alpha\frac{d^2\phi}{d^2\psi}] \tag{E.30}$$

by using the previous relevant expressions, U can be derived as

$$U=\frac{1}{l_0^2}(\frac{l_0}{R_0})^{1/2}\Big\{\frac{3}{4}-[\frac{1}{2}\frac{a}{R_0}\frac{1}{\cos\alpha}-\frac{3}{4}(\frac{a}{l_0})^2\sin^2\alpha]\frac{d\phi}{d\psi}$$

$$+[\frac{1}{4}(\frac{a}{l_0})^2(3\sin^2\alpha-1)+\frac{a^2}{R_0l_0}(\frac{1}{4}-\sin^2\alpha)+\frac{3}{4}(\frac{a}{R_0})^2\sin^2\alpha](\frac{d\phi}{d\psi})^2$$

$$+\frac{1}{2}a\sin\alpha\left(\frac{1}{l_0}-\frac{1}{R_0}\right)\frac{d^2\phi}{d^2\psi}\Bigg\}. \tag{E.31}$$

From Fig. (3.1), we have

$$\begin{aligned}\psi&=\alpha+\phi\\ \psi&=2\alpha-\beta\\ r_0\sin\beta&=a\sin\alpha\end{aligned} \tag{E.32}$$

and from which we obtain

$$\frac{d\alpha}{d\psi}\Big|_{l=l_0}=-\frac{R_0+2l_0}{2(R_0+l_0)}\ . \tag{E.33}$$

Note that $l_0=\frac{a}{2}\cos\alpha$ and $R_0=(r_0^2+a^2-2r_0a\cos\phi)^{1/2}$ has been used in deriving (E.33).

From (E.32) and (E.33), we have

$$\frac{d\phi}{d\psi}=\frac{R_0}{2(R_0+l_0)} \tag{E.34}$$

$$\frac{d^2\phi}{d^2\psi}=\frac{1}{8}aR_0\sin\alpha\frac{R_0+4l_0}{(l_0+R_0)^3}\ . \tag{E.35}$$

U can now be derived through use of (E.34), (E.35) and (E.31), as

$$\begin{aligned}U=\frac{1}{16}\left(\frac{l_0}{R_0}\right)^{1/2}\frac{a^2}{(l_0+R_0)^3}&[(4\cos^2\alpha-3)\frac{1}{l_0}+R_0(\cos^2\alpha+5)\frac{1}{l_0^2}\\ &+R_0^2(10-3\cos^2\alpha)\frac{1}{l_0^3}+2R_0^3(4-3\cos^2\alpha)\frac{1}{l_0^4}]\end{aligned} \tag{E.36}$$

and finally

$$\frac{\partial V}{\partial r}\Big|_{r=a} = -\frac{1}{16}\frac{1}{\cos\alpha}\left(\frac{l_0}{R_0}\right)^{1/2}\frac{a^2}{(l_0+R_0)^3}\left[(4\cos^2\alpha-3)\frac{1}{l_0}+R_0(\cos^2\alpha+5)\frac{1}{l_0^2}\right.$$

$$\left.+R_0^2(10-3\cos^2\alpha)\frac{1}{l_0^3}+2R_0^3(4-3\cos^2\alpha)\frac{1}{l_0^4}\right] . \qquad \text{(E.37)}$$

Using (E.17)-(E.22) and (E.37) in (E.3), we can obtain $\frac{\partial E}{\partial r}\Big|_{r=a}$ and therefore from (E.1) we can finally obtain $J_z(\phi, s)$ as in (3.30).

APPENDIX F

EVALUATION OF THE INTEGRALS ALONG C_ε AND C_∞ IN (4.9) AND (4.10)

First consider the integral

$$\int_{C_\varepsilon} H_n(\zeta,\tau)\,d\zeta = \int_{C_\varepsilon} \frac{K_n(\zeta r_0')}{K_n(\zeta)}\,\frac{e^{\zeta\tau}}{\zeta}\,d\zeta \ . \tag{F.1}$$

The small argument approximations of $K_n(z)$ are [35]

$$K_0(z) \sim -\ln z \ , \quad K_n(z) \sim \frac{2^{n-1}(n-1)!}{z^n} \quad n = 1, 2, 3, \cdots \ . \tag{F.2}$$

substituting in (F.1) yields for small ζ

$$\int_{C_\varepsilon} H_n(\zeta,\tau)\,d\zeta \sim \frac{1}{r_0'^n}\int_{C_\varepsilon} \frac{e^{\zeta\tau}}{\zeta}d\zeta \quad n = 0, 1, 2, \cdots \ . \tag{F.3}$$

With

$$\frac{e^{\zeta\tau}}{\zeta} = \frac{1}{\zeta}[1 + \frac{\zeta\tau}{1!}\,\frac{(\zeta\tau)^2}{2!}\,\frac{(\zeta\tau)^3}{3!} + \cdots] = \frac{1}{\zeta} + P(\zeta) \tag{F.4}$$

where $P(\zeta)$ is an analytic function and is thus bounded over C_ε. Therefore

$$\lim_{\varepsilon\to 0} \left| \int_{C_\varepsilon} P(\zeta)\,d\zeta \right| \le 2\pi\varepsilon\,\mathrm{Max}\left|P(\zeta)\right| = 0 \tag{F.5}$$

which implies that

$$\lim_{\varepsilon\to 0} \int_{C_\varepsilon} P(\zeta)\,d\zeta = 0 \ . \tag{F.6}$$

On the other hand, elementary calculation gives

$$\lim_{\varepsilon\to 0}\int_{C_\varepsilon}\frac{1}{\zeta}\,d\zeta=-2\pi j\ . \tag{F.7}$$

Hence

$$\lim_{\varepsilon\to 0}\int_{C_\varepsilon}H_n(\zeta,\tau)\,d\zeta=\ =-2\pi j\,\frac{1}{r_0'^n} \tag{F.8}$$

Consider now the integral along C_∞. The asymptotic expression of $K_n(z)$ for large z is [35]

$$K_n(z)\ \sim(\frac{\pi}{2z})^{1/2}\,e^{-z}\ . \tag{F.9}$$

Thus, for large ζ, $H_n(\zeta,\tau)$ becomes

$$H_n(\zeta,\tau)\ \sim\frac{1}{r_0'^{1/2}}\,\frac{1}{\zeta}\,e^{\zeta[\tau-(r_0'-1)]}\ . \tag{F.10}$$

Therefore by theorem 25.1 in [9], when $\tau > r_0'-1$,

$$\lim_{\zeta\to\infty}\int_{C_\infty}H_n(\zeta,\tau)\,d\zeta=0 \tag{F.11}$$

APPENDIX G

THE BRANCH CUT INTEGRALS IN (4.11)

The integrals in question are

$$\int_{L_1} H_n(\zeta,\tau)\,d\zeta = \lim_{\substack{\varepsilon\to 0\\ \delta\to 0\\ \delta<<\varepsilon}} \int_{-\infty+j\delta}^{-\varepsilon+j\delta} H_n(\zeta,\tau)\,d\zeta \tag{G.1}$$

$$\int_{L_2} H_n(\zeta,\tau)\,d\zeta = \lim_{\substack{\varepsilon\to 0\\ \delta\to 0\\ \delta<<\varepsilon}} \int_{-\varepsilon-j\delta}^{-\infty-j\delta} H_n(\zeta,\tau)\,d\zeta \tag{G.2}$$

where $H_n(\zeta,\tau)$ is given by (4.5). Changing the variables

$$\zeta = -y + j\delta \tag{G.3}$$

in (G.1) and

$$\zeta = -y - j\delta \tag{G.4}$$

in (G.2), and noting that when $\delta \to 0$, $\zeta = ye^{j\pi}$ along L_1 and $\zeta = ye^{-j\pi}$ along L_2, yields

$$\int_{L_1} H_n(\zeta,\tau)\,d\zeta = -\int_0^{\infty} \frac{K_n(yr_0' e^{j\pi})}{K_n(ye^{j\pi})}\,\frac{e^{-y\tau}}{y}\,dy \tag{G.5}$$

$$\int_{L_2} H_n(\zeta,\tau)\,d\zeta = \int_0^{\infty} \frac{K_n(yr_0' e^{-j\pi})}{K_n(ye^{-j\pi})}\,\frac{e^{-y\tau}}{y}\,dy\ . \tag{G.6}$$

Using the relationship [27]

$$K_\nu(ze^{jm\pi}) = e^{-jm\nu\pi} K_\nu(z) - j\pi \frac{\sin m\nu\pi}{\sin \nu\pi} I_\nu(z) \tag{G.7}$$

we obtain in the limit when $\nu \to n$

$$K_n(ze^{jm\pi}) = (-1)^{mn} K_n(z) - j(-1)^m m\pi I_n(z) \ . \tag{G.8}$$

With (G.8) in (G.5) and (G.6) for $m = -1$ and 1, respectively,

$$\int_{L_1} H_n(\zeta,\tau)\, d\zeta = -\int_0^\infty \frac{(-1)^n K_n(yr_0') - j\pi I_n(yr_0')}{(-1)^n K_n(y) - j\pi I_n(y)} \frac{e^{-y\tau}}{y} dy \tag{G.9}$$

and

$$\int_{L_2} H_n(\zeta,\tau)\, d\zeta = \int_0^\infty \frac{(-1)^n K_n(yr_0') + j\pi I_n(yr_0')}{(-1)^n K_n(y) + j\pi I_n(y)} \frac{e^{-y\tau}}{y} dy \ . \tag{G.10}$$

From (G.9) and (G.10) we finally obtain

$$\int_{L_1} H_n(\zeta,\tau)\, d\zeta + \int_{L_2} H_n(\zeta,\tau)\, d\zeta = (-1)^n 2\pi j \int_0^\infty \frac{I_n(yr_0') K_n(y) - I_n(y) K_n(yr_0')}{K_n^2(y) + \pi^2 I_n^2(y)} \frac{e^{-y\tau}}{y} dy \ . \tag{G.11}$$

APPENDIX H

ZEROS OF $K_n(\zeta)$ IN THE SECOND QUADRANT OF THE ζ-PLANE

n = 2

$-0.12813737976561E+01 + j\ 0.42948496520872E+00$

n = 3

$-0.16817888047458E+01 + j\ 0.13080120322739E+01$

n = 4

$-0.19781618634659E+01 + j\ 0.22043719815469E+01$
$-0.26286711679571E+01 + j\ 0.43269664862178E+00$

n = 5

$-0.22186262746399E+01 + j\ 0.31130829449859E+01$
$-0.31351328447046E+01 + j\ 0.13038823977137E+01$

n = 6

$-0.24234043880011E+01 + j\ 0.40309615812693E+01$
$-0.35510979040001E+01 + j\ 0.21834951775779E+01$
$-0.39615580702543E+01 + j\ 0.43334540861474E+00$

n = 7

$-0.26031262658682E+01 + j\ 0.49559696065385E+01$
$-0.39081257398032E+01 + j\ 0.30708717702489E+01$
$-0.45126267774997E+01 + j\ 0.13027788416203E+00$

n = 8

$-0.27641429773113E+01 + j\ 0.58867128822557E+01$
$-0.42231522789550E+01 + j\ 0.39650659693875E+01$
$-0.49882787925533E+01 + j\ 0.21770827464791E+01$
$-0.52907612925994E+01 + j\ 0.43357769522400E+00$

n = 9

$-0.29105824231362E+01 + j\ 0.68221903314330E+01$
$-0.45064659455202E+01 + j\ 0.48652071432639E+01$
$-0.54097474475403E+01 + j\ 0.30565442393434E+01$
$-0.58665514666859E+01 + j\ 0.13023283269978E+01$

n = 10

$-0.30452934989589E+01 + j\ 0.77616556708745E+01$
$-0.47648453733731E+01 + j\ 0.57705555987101E+01$
$-0.57900271641805E+01 + j\ 0.39409726157695E+01$
$-0.63783949707942E+01 + j\ 0.21742485862010E+01$
$-0.66184818847101E+01 + j\ 0.43368620578616E+00$

n = 11

$-0.31703330955843E+01 + j\ 0.87045357352456E+01$
$-0.50030218041036E+01 + j\ 0.66804942939420E+01$
$-0.61377357070270E+01 + j\ 0.48300352803536E+01$
$-0.68414139615362E+01 + j\ 0.30498227248773E+01$
$-0.72100091440928E+01 + j\ 0.13021010316334E+01$

n = 12

$-0.32872394892778E+01 + j\ 0.96503795038428E+01$
$-0.52244433975899E+01 + j\ 0.75945087721483E+01$
$-0.64589235753598E+01 + j\ 0.57233724928599E+01$
$-0.72656756432984E+01 + j\ 0.39291350063279E+01$
$-0.77462284482268E+01 + j\ 0.21727425332139E+01$
$-0.79454591993994E+01 + j\ 0.43374542348703E+00$

n = 13

$-0.33971960963740E+01 + j\ 0.10598824843836E+02$
$-0.54317093818593E+01 + j\ 0.85121677243875E+01$
$-0.67580240069318E+01 + j\ 0.66206385259781E+01$
$-0.76582726080369E+01 + j\ 0.48120995042878E+01$
$-0.82384224409621E+01 + j\ 0.30461032680704E+01$
$-0.85478913319293E+01 + j\ 0.13019705250871E+01$

n = 14

$-0.35011347262876E+01 + j\ 0.11549576004515E+02$
$-0.56268328477159E+01 + j\ 0.94331067978003E+01$
$-0.70383949514330E+01 + j\ 0.75215155427960E+01$
$-0.80244182717383E+01 + j\ 0.56985584632486E+01$
$-0.86945589683412E+01 + j\ 0.39223687201080E+01$
$-0.91016718958228E+01 + j\ 0.21718455019979E+01$
$-0.92720111977992E+01 + j\ 0.43378122436165E+00$

n = 15

$-0.35998034722711E+01 + j\ 0.12502387907733E+02$
$-0.58114080140945E+01 + j\ 0.10357015709528E+02$
$-0.73026485067633E+01 + j\ 0.84257167702271E+01$
$-0.83680733215064E+01 + j\ 0.65883273760437E+01$
$-0.91205074549937E+01 + j\ 0.48015702277034E+01$
$-0.96155300480819E+01 + j\ 0.30438214772420E+01$
$-0.98824480844330E+01 + j\ 0.13018887246109E+01$

n = 16

$-0.36938129233477E+01 + j\ 0.13457054893311E+02$
$-0.59867211327807E+01 + j\ 0.11283628123211E+02$
$-0.75528614587363E+01 + j\ 0.93329854541168E+01$
$-0.86923273258187E+01 + j\ 0.74812164157161E+01$
$-0.95207359274662E+01 + j\ 0.56836598038964E+01$
$-0.10095906631980E+02 + j\ 0.39181159907959E+01$

−0.10449492658285E+02 + j 0.21712676784609E+01
−0.10598297154675E+02 + j 0.43380449999224E+00

n = 17

−0.37836685593809E+01 + j 0.14413402470064E+02
−0.61538265491726E+01 + j 0.12212713704804E+02
−0.77907154205255E+01 + j 0.10243092269415E+02
−0.89996431149415E+01 + j 0.83770406772229E+01
−0.98987363098417E+01 + j 0.65685489408385E+01
−0.10547711998372E+02 + j 0.47948164630530E+01
−0.10980094719455E+02 + j 0.30423181213323E+01
−0.11214860908087E+02 + j 0.13018340932525E+01

n = 18

−0.38697940375335E+01 + j 0.15371281149564E+02
−0.63136003816884E+01 + j 0.13144071858237E+02
−0.80175933100746E+01 + j 0.11155832327085E+02
−0.92920197702870E+01 + j 0.92756248804027E+01
−0.10257297171215E+02 + j 0.74561295897907E+01
−0.10974789107528E+02 + j 0.56739357545240E+01
−0.11479559099245E+02 + j 0.39152606805057E+01
−0.11792282009812E+02 + j 0.21708734986443E+01
−0.11924405660266E+02 + j 0.43382047493863E+00

n = 19

−0.39525482997518E+01 + j 0.16330561756041E+02
−0.64667793424973E+01 + j 0.14077526751410E+02
−0.82346476826133E+01 + j 0.12071022249847E+02
−0.95711050511953E+01 + j 0.10176805254940E+02
−0.10598685864886E+02 + j 0.83462858007171E+01
−0.11380210892584E+02 + j 0.65554434866061E+01
−0.11952042089367E+02 + j 0.47902083557596E+01
−0.12336222554043E+02 + j 0.30412741190005E+01
−0.12545810344020E+02 + j 0.13017958021530E+01

n = 20

−0.40322383826849E+01 + j 0.17291131803679E+02
−0.66139894136190E+01 + j 0.15012923335301E+02
−0.84428503184606E+01 + j 0.12988497501956E+02
−0.98382751768468E+01 + j 0.11080429978246E+02
−0.10924774316796E+02 + j 0.92389002618091E+01
−0.11766479051575E+02 + j 0.74392843593399E+01
−0.12400870595862E+02 + j 0.56672078736422E+01
−0.12851122931433E+02 + j 0.39132475161823E+01
−0.13131572947263E+02 + j 0.21705925222372E+01
−0.13250389904857E+02 + j 0.43383191067664E+00

APPENDIX I

EVALUATION OF THE INTEGRALS IN (4.47)-(4.49) FOR THE CASE OF A PLANE WAVE INCIDENCE

Consider first the integral

$$\int_{C_\varepsilon} H_n(\zeta,\tau)\,d\zeta = \int_{C_\varepsilon} \frac{e^{\zeta(\tau-1)}}{\zeta K_n(\zeta)} d\zeta \ . \tag{I.1}$$

Using the small argument approximations of $K_n(\zeta)$ in (I.1) yields for small ζ

$$\int_{C_\varepsilon} H_n(\zeta,\tau)\,d\zeta \sim \frac{1}{2^{n-1}(n-1)!} \int_{C_\varepsilon} \zeta^{n-1}\,d\zeta \qquad n=1, 2, 3\cdots . \tag{I.2}$$

It is obvious from (I.2) that $\lim_{\varepsilon\to 0} \int_{C_\varepsilon} H_n(\zeta,\tau)\,d\zeta = 0$ for $n=1, 2, 3\cdots$. For $n=0$, we have

$$\int_{C_\varepsilon} H_0(\zeta,\tau)\,d\zeta \sim -\int_{C_\varepsilon} \frac{1}{\zeta \ln\zeta} d\zeta \ . \tag{I.3}$$

Since along C_ε, $\zeta = \varepsilon e^{j\theta}$, we obtain

$$\lim_{\varepsilon\to 0} \left| \int_{C_\varepsilon} \frac{1}{\zeta\ln\zeta} d\zeta \right| \le \lim_{\varepsilon\to 0} 2\pi\varepsilon \,\mathrm{Max} \left| \frac{1}{\zeta\ln\zeta} \right| = \lim_{\varepsilon\to 0} 2\pi \left| \frac{1}{(\ln\varepsilon + j\theta)} \right| = 0 \ . \tag{I.4}$$

Hence

$$\int_{C_\varepsilon} H_0(\zeta,\tau)\,d\zeta = 0 \ . \tag{I.5}$$

Consider now the integral along C_∞. Using the asymptotic expression of $K_n(\zeta)$ for large ζ, $H_n(\zeta,\tau)$ becomes

$$H_n(\zeta,\tau) \sim 2^{1/2} \frac{e^{\zeta\tau}}{\zeta^{1/2}} \ . \tag{I.6}$$

Therefore by the theorem 25.1 in [9], when $\tau > 0$,

$$\lim_{R_\infty \to \infty} \int_{C_\infty} H_n(\zeta,\tau)\, d\zeta = 0 \ . \tag{I.7}$$

Let us consider now the branch cut integrals.

$$\int_{L_1} H_n(\zeta,\tau)\, d\zeta = \lim_{\substack{\varepsilon\to 0 \\ \delta\to 0 \\ \delta<<\varepsilon}} \int_{-\infty+j\delta}^{-\varepsilon+j\delta} H_n(\zeta,\tau)\, d\zeta \tag{I.8}$$

$$\int_{L_2} H_n(\zeta,\tau)\, d\zeta = \lim_{\substack{\varepsilon\to 0 \\ \delta\to 0 \\ \delta<<\varepsilon}} \int_{-\varepsilon-j\delta}^{-\infty-j\delta} H_n(\zeta,\tau)\, d\zeta \tag{I.9}$$

where $H_n(\zeta,\tau)$ is given in (4.45). By using the same change of variables as in Appendix G, the integrals along L_1 and L_2 can be expressed as

$$\int_{L_1} H_n(\zeta,\tau)\, d\zeta = -\int_0^\infty \frac{e^{-z(\tau-1)}}{z\, K_n(ze^{j\pi})}\, dz \tag{I.10}$$

$$\int_{L_2} H_n(\zeta,\tau)\, d\zeta = \int_0^\infty \frac{e^{-z(\tau-1)}}{z\, K_n(ze^{-j\pi})}\, dz \ . \tag{I.11}$$

Following the same procedure in Appendix G, we have

$$\int_{L_1} H_n(\zeta,\tau)\, d\zeta = -\int_0^\infty \frac{e^{-z(\tau-1)}}{z\,[(-1)^n K_n(z) - j\pi I_n(z)]}\, dz \tag{I.12}$$

and

$$\int_{L_2} H_n(\zeta,\tau)\, d\zeta = \int_0^\infty \frac{e^{-z(\tau-1)}}{z\,[(-1)^n K_n(z) + j\pi I_n(z)]}\, dz \ . \tag{I.13}$$

Finally

$$\left[\int_{L_1} + \int_{L_2}\right] H_n(\zeta,\tau)\, d\zeta = -2\pi j \int_0^\infty \frac{I_n(z) e^{-z(\tau-1)}}{z\,[K_n^2(z) + \pi^2 I_n^2(z)]}\, dz \ . \tag{I.14}$$

APPENDIX J

EVALUATION OF THE INTEGRALS IN (5.9)-(5.11) FOR THE CASE OF A PULSE INCIDENCE

First consider the integral

$$\int_{C_\varepsilon} H_n(\zeta,\tau)\,d\zeta = \int_{C_\varepsilon} \left(\frac{1}{\zeta+\gamma_1'} - \frac{1}{\zeta+\gamma_2'}\right) \frac{e^{\zeta(\tau-1)}}{\zeta K_n(\zeta)} d\zeta \ . \tag{J.1}$$

Using the small argument approximations of $K_n(\zeta)$ in (J.1) yields for small ζ

$$\int_{C_\varepsilon} H_n(\zeta,\tau)\,d\zeta \sim \left(\frac{1}{\gamma_1'} - \frac{1}{\gamma_2'}\right) \frac{1}{2^{n-1}(n-1)!} \int_{C_\varepsilon} \zeta^{n-1}\,d\zeta \qquad n=1, 2, 3\cdots . \tag{J.2}$$

It is obvious from (J.2) that $\lim\limits_{\varepsilon\to 0} \int\limits_{C_\varepsilon} H_n(\zeta,\tau)\,d\zeta = 0$. For $n=0$, we have

$$\int_{C_\varepsilon} H_0(\zeta,\tau)\,d\zeta \sim -\left(\frac{1}{\gamma_1'} - \frac{1}{\gamma_2'}\right) \int_{C_\varepsilon} \frac{1}{\zeta \ln\zeta}\, d\zeta \ . \tag{J.3}$$

Since along C_ε, $\zeta = \varepsilon e^{j\theta}$, we obtain

$$\lim_{\varepsilon\to 0} \left| \int_{C_\varepsilon} \frac{1}{\zeta\ln\zeta}\, d\zeta \right| \le \lim_{\varepsilon\to 0} 2\pi\varepsilon\, \mathrm{Max} \left| \frac{1}{\zeta\ln\zeta} \right| = \lim_{\varepsilon\to 0} 2\pi \left| \frac{1}{(\ln\varepsilon + j\theta)} \right| = 0 \ . \tag{J.4}$$

Hence

$$\int_{C_\varepsilon} H_0(\zeta,\tau)\,d\zeta = 0 \ . \tag{J.5}$$

Consider now the integral along C_∞. Using the asymptotic expression of $K_n(\zeta)$ for large ζ, $H_n(\zeta,\tau)$ becomes

$$H_n(\zeta,\tau) \sim 2^{1/2} \left(\frac{1}{\zeta+\gamma_1'} - \frac{1}{\zeta+\gamma_2'}\right) \frac{e^{\zeta\tau}}{\zeta^{1/2}} \ . \tag{J.6}$$

Therefore by the theorem 25.1 in [9], when $\tau > 0$,

$$\lim_{R_\infty \to \infty} \int_{C_\infty} H_n(\zeta,\tau)\, d\zeta = 0 \ . \tag{J.7}$$

Let us consider now the integrals along the branch cut and infinitesimal semicircles. The integrals $\int_{L_1}$ and $\int_{L_2}$ each consists of three parts, namely

$$\int_{L_1} H_n(\zeta,\tau)\, d\zeta = \lim_{\substack{\varepsilon\to 0 \\ \delta\to 0 \\ \delta<<\varepsilon}} \left[\int_{-\infty+j\delta}^{-(\gamma_2'+\varepsilon)+j\delta} + \int_{-(\gamma_2'-\varepsilon)+j\delta}^{-(\gamma_1'+\varepsilon)+j\delta} + \int_{-(\gamma_1'-\varepsilon)+j\delta}^{-\varepsilon+j\delta} \right] H_n(\zeta,\tau)\, d\zeta \tag{J.8}$$

$$\int_{L_2} H_n(\zeta,\tau)\, d\zeta = \lim_{\substack{\varepsilon\to 0 \\ \delta\to 0 \\ \delta<<\varepsilon}} \left[\int_{-\varepsilon-j\delta}^{-(\gamma_1'-\varepsilon)-j\delta} + \int_{-(\gamma_1'+\varepsilon)-j\delta}^{-(\gamma_2'-\varepsilon)-j\delta} + \int_{-(\gamma_2'+\varepsilon)-j\delta}^{-\infty-j\delta} \right] H_n(\zeta,\tau)\, d\zeta \tag{J.9}$$

where $H_n(\zeta,\tau)$ is given in (5.6). Changing the variables

$$\zeta = -z + j\delta \tag{J.10}$$

in (J.8) and

$$\zeta = -z - j\delta \tag{J.11}$$

in (J.9), and noting that when $\delta \to 0$, $\zeta = ze^{j\pi}$ along L_1 and $\zeta = ze^{-j\pi}$ along L_2, yields

$$\int_{L_1} H_n(\zeta,\tau)\, d\zeta = -\int_0^\infty \left(\frac{1}{\gamma_1' - z} - \frac{1}{\gamma_2' - z}\right) \frac{e^{-z(\tau-1)}}{z\, K_n(ze^{j\pi})}\, dz \tag{J.12}$$

$$\int_{L_2} H_n(\zeta,\tau)\, d\zeta = \int_0^\infty \left(\frac{1}{\gamma_1' - z} - \frac{1}{\gamma_2' - z}\right) \frac{e^{-z(\tau-1)}}{z\, K_n(ze^{-j\pi})}\, dz \ . \tag{J.13}$$

Now following the same procedure in Appendix G, we have

$$\int_{L_1} H_n(\zeta,\tau)\,d\zeta = -\int_0^{\infty} \left(\frac{1}{\gamma_1' - z} - \frac{1}{\gamma_2' - z}\right) \frac{e^{-z(\tau-1)}}{z\,[(-1)^n K_n(z) - j\pi I_n(z)]}\,dz \qquad \text{(J.14)}$$

and

$$\int_{L_2} H_n(\zeta,\tau)\,d\zeta = \int_0^{\infty} \left(\frac{1}{\gamma_1' - z} - \frac{1}{\gamma_2' - z}\right) \frac{e^{-z(\tau-1)}}{z\,[(-1)^n K_n(z) + j\pi I_n(z)]}\,dz\ . \qquad \text{(J.15)}$$

Finally

$$\left[\int_{L_1} + \int_{L_2}\right] H_n(\zeta,\tau)\,d\zeta = -2\pi j \int_0^{\infty} \left(\frac{1}{\gamma_1' - z} - \frac{1}{\gamma_2' - z}\right) \frac{I_n(z)e^{-z(\tau-1)}}{z\,[K_n^2(z) + \pi^2 I_n^2(z)]}\,dz\ . \qquad \text{(J.16)}$$

REFERENCES

[1] L. B. Felsen (Ed.), *Transient Electromagnetic Fields*, Berlin, Heidelberg, New York: Springer-Verlag, 1976.

[2] A. J. Poggio and E. K. Miller, "Computational Techniques for Electromagnetics," in *Computer Techniques for Electromagnetics*, R. Mittra, Ed., New York: Pergamon, 1973.

[3] C. E. Baum, "Emerging technology for transient and broad-band analysis and synthesis of antennas and scatterers," *Proc. IEEE*, vol. 64, pp. 1598-1616, 1976.

[4] C. L. Bennet and G. F. Ross, "Time-domain electromagnetics and its applications," *Proc. IEEE*, vol. 66, pp. 299-318, 1978.

[5] E. M. Kennaugh and D. L. Moffatt, "Transient and impulse response approximations," *Proc. IEEE*, vol. 53, pp. 893-901, 1965.

[6] C. E. Baum, "On the singularity expansion method for the solution of electromagnetic interaction problems," Interaction Notes 88, 1971.

[7] R. H. Schafer and R. G. Kouyoumjian, "Transient currents on a cylinder illuminated by an impulsive plane wave," *IEEE Trans. Antennas Propagat.*, vol. AP-23, pp. 627-638, 1975.

[8] J. R. Wait and A. M. Conda, "On diffraction of electromagnetic pulses by curved conducting surfaces," *Can. J. Phys.*, vol. 37, pp. 1384-1396, 1959.

[9] G. Doetsch, *Introduction to the Theory and Application of the Laplace Transformation*, New York: Springer-Verlag, 1974.

[10] J. R. Wait, "Transient response of the penumbral currents for plane wave diffraction by a cylinder," *Can. J. Phys.*, vol. 47, pp. 1307-1312, 1969.

[11] Y. M. Chen, "The transient behavior of diffraction of plane pulse by a circular cylinder," *Int. J. Eng. Sci.*, vol. 2, pp. 417-429, 1964.

[12] R. Barakat, "Diffraction of a plane step pulse by a perfectly conducting cylinder," *J. Opt. Soc. Amer.*, vol. 55, pp. 998-1002, 1965.

[13] H. Uberall, H. D. Doolittle and J. V. McNicholas, "Use of sound pulses for a study of circumferential waves," *J. Acoust. Soc. Amer.*, vol. 39, pp. 564-578, 1965.

[14] R. H. Schafer, "Transient currents on a perfectly-conducting cylinder illuminated by unit-step and impulsive plane waves," Ph.D. dissertation, Dept. of Elect. Eng., Ohio State Univ., Columbus, 1967.

[15] C. L. Bennet and W. L. Weeks, "Transient scattering from conducting cylinders," *IEEE Trans. Antennas Propagat.*, vol. AP-18, pp. 627-633, 1970.

[16] S. W. Lee, V. Jamnejad and R. Mittra, " An asymptotic series for early time response in transient problems," *IEEE Trans. Antennas Propagat.*, vol. AP-21, pp. 895-899, 1973.

[17] C. I. Chuang, D. P. Nyquist, K. M. Chen and B. C. Drachman, "Singularity Expansion Method formulation for impulse response of a perfectly conducting thick cylinder," *Radio Science*, vol. 20, pp. 1025-1030, 1985.

[18] A. G. Tijhuis, "Angularly propagating waves in a radially inhomogeneous, lossy dielectric cylinder and their connection with the natural modes," *IEEE Trans. Antennas Propagat.*, vol. AP-34, pp. 813-824, 1986.

[19] A. G. Tijhuis and R. M. Weiden, SEM approach to transient scattering by a lossy, radially inhomogeneous dielectric circular cylinder, *Wave Motion*, vol. 8, pp. 43-63, 1986.

[20] F. G. Friedlander, "Diffraction of pulses by a circular cylinder," *Comm. Pure Appl. Math.*, vol. 7, pp. 705-732, 1954.

[21] F. Gilbert and L. Knopoff, "Scattering of impulsive elastic waves by a rigid cylinder," *J. Acoust. Soc. Amer.*, vol. 31, pp. 1169-1175, 1959.

[22] E. Heyman and L. B. Felsen, "Creeping waves and resonances in transient scattering by smooth convex objects," *IEEE Trans. Antennas Propagat.*, vol. AP-31, pp. 426-437, 1983.

[23] E. Heyman and L. B. Felsen, "Traveling wave and SEM representations for transient scattering by a circular cylinder," *J. Acoust. Soc. Amer.*, vol. 79, pp. 230-238, 1986.

[24] G. N. Watson, "The diffraction of electric waves by the earth," *Proc. Roy. Soc.*, A95, pp. 83-89, 1918.

[25] W. Franz and R. Galle, "Semiasymptotishe Reihen fur die Beugung einer ebenen Welle am Zylinder," *Z. Naturforsch.*, vol. 10a, pp. 374-378, 1955.

[26] J. C. P. Miller, "The Airy Integral," *British Assoc. Adv. Sci. Math. Tables*, Part-vol. B, London: Cambridge University Press, 1946.

[27] G. N. Watson, *A Treatise on the Theory of Bessel Functions*, London: Cambridge University Press, 1962.

[28] F. G. Friedlander, *Sound Pulses*, London: Cambridge University Press, 1958.

[29] A. Erdelyi, W. Magnus, F. Oberhettinger and F. G. Tricomi, *Higher Transcendental Functions*, vol. 2, New York: McGraw-Hill, 1953.

[30] J. J. Bowman, T. B. A. Senior and P. L. E. Uslenghi, *Electromagnetic and Acoustic Scattering by Simple Shapes*, Amsterdam, The Netherlands: North-Holland Publ., 1969.

[31] E. T. Copson, *Asymptotic Expansions*, London: Cambridge University Press, 1965.

[32] J. B. Keller, R. M. Lewis and B. D. Seckler, "Asymptotic solution of some diffraction problems," *Commun. Pure Appl. Math.*, vol. 9, pp. 207-265, 1956.

[33] J. Ma and I. R. Ciric, "Transient response of conducting cylinders to cylindrical electromagnetic waves," in *Proceedings of IEEE AP-S International Symposium*, Syracuse, New York, June 26-30, 1988.

[34] J. Ma and I.R. Ciric, "Early-time currents induced on a cylinder by a cylindrical electromagnetic wave," *IEEE Trans. Antennas Propagat.*, vol. AP-39, pp. 455-463, 1991.

[35] M. Abramowitz and I. A. Stegun, *Handbook of mathematical functions*, Dover, New York, 1972.

[36] G. E. Roberts and H. Kaufman, *Table of Laplace Transform*, Philadelphia: W. B. Saunders, 1966.

[37] A. G. Tijhuis, Private communication, 1989.

[38] J. Ma and I. R. Ciric, "Early-time field response of a conducting cylinder excited by a line current," in *Proceedings of IEE Sixth International Conference on Antennas and Propagation*, London, England, April 4-7, 1989.